AD NUMBER

AD872159

LIMITATION CHANGES

TO:

Approved for public release; distribution is unlimited.

FROM:

Distribution authorized to U.S. Gov't. agencies and their contractors; Critical Technology; MAY 1970. Other requests shall be referred to U.S. Army Aviation Materiel Laboratories, Fort Eustis, VA 23604. This document contains export-controlled technical data.

AUTHORITY

USAAMRDL ltr, 23 Jun 1971

USAAVLABS TECHNICAL REPORT 70-27

CALCULATION AND DESIGN OF JOINTS MADE FROM COMPOSITE MATERIALS

By

Alberto Puppo
Harold Evensen

May 1970

U. S. ARMY AVIATION MATERIEL LABORATORIES
FORT EUSTIS, VIRGINIA

CONTRACT DAAJ02-69-C-0034
WHITTAKER CORPORATION
RESEARCH & DEVELOPMENT DIVISION
SAN DIEGO, CALIFORNIA

Disclaimers

The findings in this report are not to be construed as an official Department of the Army position unless so designated by other authorized documents.

When Government drawings, specifications, or other data are used for any purpose other than in connection with a definitely related Government procurement operation, the United States Government thereby incurs no responsibility nor any obligation whatsoever; and the fact that the Government may have formulated, furnished, or in any way supplied the said drawings, specifications, or other data is not to be regarded by implication or otherwise as in any manner licensing the holder or any other person or corporation, or conveying any rights or permission, to manufacture, use, or sell any patented invention that may in any way be related thereto.

Disposition Instructions

Destroy this report when no longer needed. Do not return it to the originator.

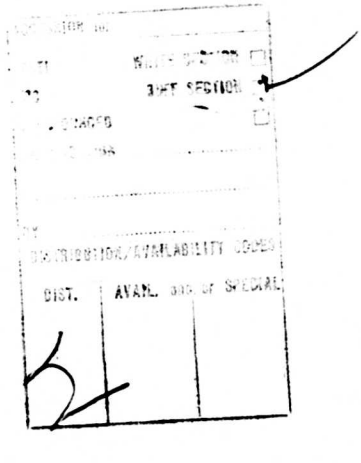

DEPARTMENT OF THE ARMY
HEADQUARTERS US ARMY AVIATION MATERIEL LABORATORIES
FORT EUSTIS, VIRGINIA 23604

The work reported herein was performed under Contract DAAJ02-69-C-0034 with Whittaker Corporation, Research and Development Division, San Diego, California.

The data contained in the report are the results of a study conducted of joints made from fiber composite material to develop a rational joint design. A finite-element computer program, used to obtain stress distributions in composite joints, is also presented.

The report has been reviewed by the U.S. Army Aviation Materiel Laboratories and is considered to be technically sound. It is published for the exchange of information and the stimulation of future research.

Task 1F162204A17001
Contract DAAJ02-69-C-0034
USAAVLABS Technical Report 70-27
May 1970

CALCULATION AND DESIGN OF JOINTS MADE FROM COMPOSITE MATERIALS

Final Report

By

Alberto Puppo
and
Harold Evensen

Prepared by

Whittaker Corporation
Research & Development Division
San Diego, California

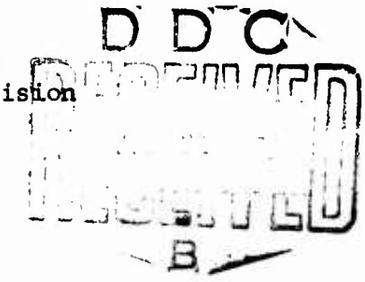

for

U. S. ARMY AVIATION MATERIEL LABORATORIES
FORT EUSTIS, VIRGINIA

ABSTRACT

This report contains a study of joints made from fiber composite materials. Several types of joints are considered, such as bolted and adhesive joints.

Elements for a rational joint design are presented, as well as test results. A finite element computer program, used to obtain stress distributions in composite joints, is included.

FOREWORD

This report was prepared by Whittaker Research & Development Division, San Diego, California, under Contract DAAJ02-69-C-0034, Task 1F162204A17001, for the U. S. Army Aviation Materiel Laboratories, Fort Eustis, Virginia. Work was accomplished under the direction of Mr. A. J. Gustafson, Army project officer. This final report covers the period November 1968 through December 1969. Mr. Alberto Puppo was the program manager and principal investigator. Dr. Juan Haener, senior scientist, contributed to the technical content.

The author acknowledges the assistance of Mr. Theodore Neff in the development of the computer program.

TABLE OF CONTENTS

LIST OF ILLUSTRATIONS (CONT.)

LIST OF ILLUSTRATIONS (CONT.)

LIST OF ILLUSTRATIONS (CONT.)

LIST OF SYMBOLS

PERTAINING TO BOLTED JOINTS:

a, h	bolt hole radius and through-depth
P, Q	axial and transverse applied forces
R,b	external radius at bolt section
t	wrap thickness at bolt section
$\sigma_\theta, \sigma_r, \tau_{r\theta}$	tangential, radial and shear stress components
$(\ )_f, (\ )_{ult}$	denotes ultimate values

PERTAINING TO BONDED LAP JOINTS:

$\bar{e}$	maximum allowable error
E	adherend modulus
G_o	adhesive shear modulus at zero strain
k, τ_ℓ	adhesive parameters
ℓ	lap length
P	applied or reaction load
P_{ult}, γ_{ult}	ultimate force and adhesive shear strain
t	thickness
u	adherend displacement
x	coordinate parallel to bond line
1,2,a	subscripts denoting doubler, mainplate and adhesive
γ, ε	shear strain and longitudinal strain
σ_n, τ	adhesive normal and shear stresses
$\Delta(\ )$	denote increments or corrections

LIST OF SYMBOLS (CONT.)

$( )'', ( )'$	primes denote second and first derivative with respect to x
$( )^{(1)}, ( )^{(2)}$	denote initial and improved estimated values
$( )_o, ( )_{\ell/2}, ( )_\ell$	denote values at x = 0, x = $\ell/2$, and x = ℓ
$( )_{o\gamma}, ( )_{\ell\gamma}$ $( )_{o\gamma'}, ( )_{\ell\gamma'}$	denote incremented values

PERTAINING TO FINITE ELEMENTS:

a,b,c	subscripts denoting vertices of the basic triangle
$\{a\}\{\varepsilon\}$	triangle displacement coefficient and strain vectors
[C],[C']	material local and transformed stiffness matrixes
E,G,ν	material tensile and shear modulus, poisson's ratio
[K],[K']	triangle local and transformed stiffness matrices
ℓ,m	trigonometric functions cosβ, sinβ
R_1, R_2, R_3	denotes edges of triangle
[T]	transformation matrix
T_1, T_2, T_3	triangle thickness coefficients
u,v	horizontal and vertical displacements
W	strain energy function
α, β, γ	subscripts denoting midpoints of sides of the basic triangle
β	fiber orientation angle, relative to local coordinate systems
$\gamma_o - \gamma_9$	integrals appearing in strain energy function

LIST OF SYMBOLS (CONT.)

$\{\delta\}\{P\}$	triangle vector displacement and force vectors
ξ,η	local horizontal and vertical coordinates
$[\ *],\{*\}$	denotes matrix and vector for entire structure

TECHNICAL DISCUSSION

BOLTED JOINTS: GENERAL CONSIDERATIONS

In this section, the fundamental problems of the design of bolted joints in composite materials (particularly, glass-epoxy) are considered.

A bolted joint, Figure 1, must withstand, in general, an axial force P and a transverse force Q. Other forces, out of the plane, can exist, but in most cases their magnitudes are negligible in comparison with P and Q.

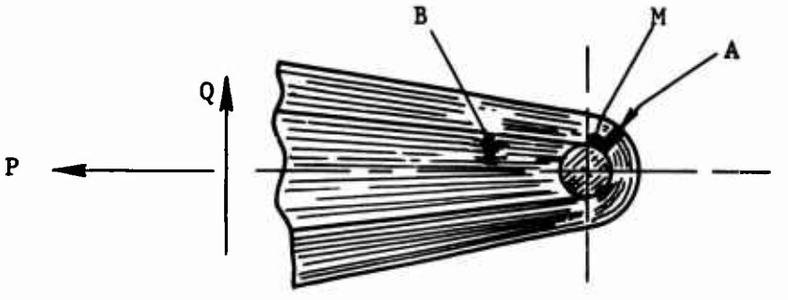

Figure 1. General Bolted Joint.

Because of its construction, the fiber orientation in a bolted joint is practically confined to the one shown in Figure 1. Fibers through cross-section A are continuous, while those through cross-section B are discontinuous due to the presence of the bolt hole. When the axial load P is tensile, as shown in Figure 1, the fibers A act in tension, but the fibers B, near the hole, are nearly free of stresses. Because of this stress difference, a shear stress is developed along the fiber direction starting at the point M. When the load P is increased, the shear stress at M produces the failure of the matrix of the composite. A crack is propagated, as shown in Figure 2, simultaneously with increasing P. Test results indicate that the magnitude of P sufficient to initiate the shear crack at M is only one-fourth to one-fifth of the value that produces the final failure. Once the shear crack is completely developed, the joint behaves as a simple loop joint for tensile load P, with the darkened fibers of Figure 3 in tension and the central region practically free of stresses.

If the joint of Figure 3 is unloaded and then reloaded up to the previous load level, no further changes in the stress distribution are observed. Thus, the shear crack has no further effect on the behavior of the joint once it is developed. In fact, the location of the shear crack can be controlled if the fibers A are not bonded to the fibers B during the fabrication process.

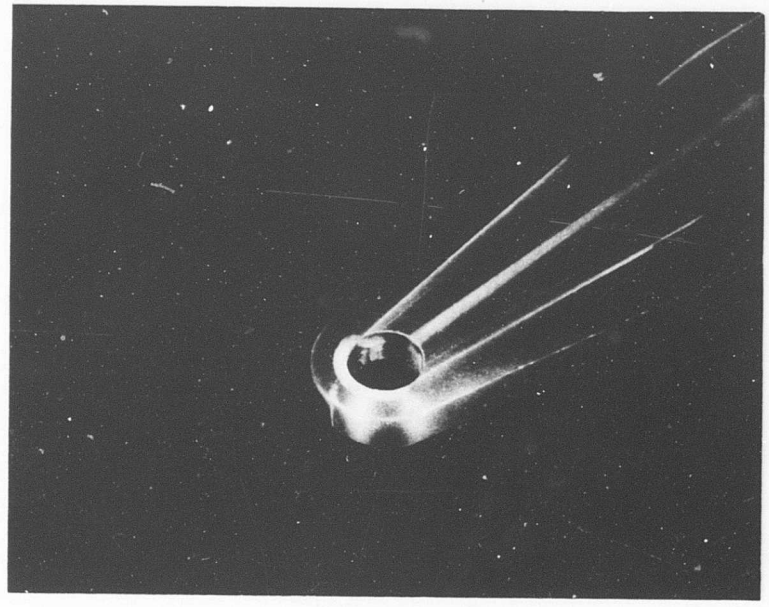

Figure 2. Shear Crack in Bolted Joint After First Loading in Tension.

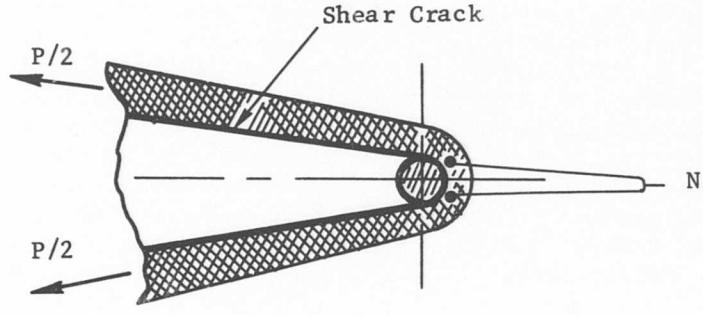

Figure 3. Joint in Tension After the Propagation of the Shear Crack.

If the tension load P is increased after the propagation of the shear crack, a final failure of the joint will appear in the neighborhood of the point N (Figure 3). The stresses at the point N are as shown in Figure 4: (a tangential tensile stress σ_θ acting along the fiber direction

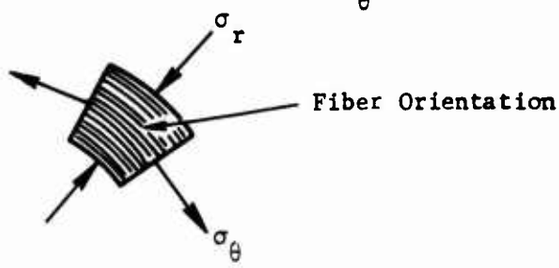

Figure 4. Stresses at the Points N (See Figure 3).

and a radial compressive stress σ_r, perpendicular to the fiber direction). Because the stresses σ_θ and σ_r act simultaneously, the failure of the joint is actually produced by combination of the effects of each stress. If the radius a of the hole is large in comparison with t (see Figure 5), the stress σ_θ is much larger than σ_r. In this case, the failure mode of

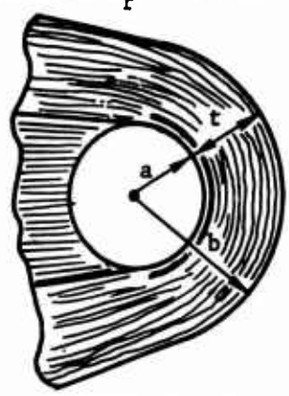

Figure 5. Nomenclature for the Bolted Joint.

the joint is a tensile failure of the fibers, as represented in Figure 6.

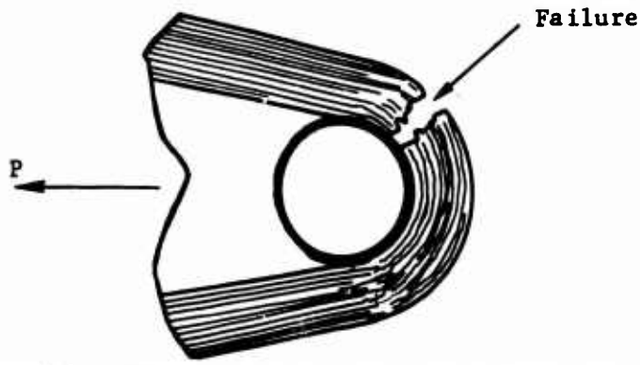

Figure 6. Typical Failure of a Joint With a>>t.

If, on the other hand, the radius a is much smaller than t , the radial stress σ_r is greater than σ_θ and the typical failure of the joint is as indicated in Figure 7. In this case,

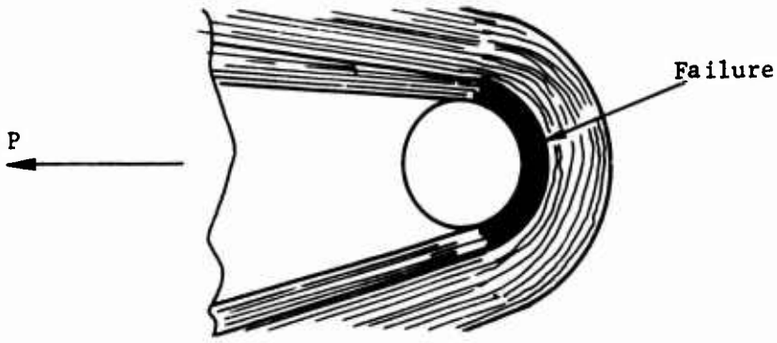

Figure 7. Typical Failure of a Joint With a$\ll$ t.

the failure is produced essentially by the compressive radial stress σ_θ. Only the region near the bolt is affected by this type of failure.

From the previous description it should be evident that, with fixed external radius b and joint thickness h , the tensile failure load P and the failure mode will depend upon the t/a ratio. Then, P will achieve a maximum for some optimum t/a ratio. By performing several tests on glass-epoxy bolted joints, it was determined that this optimum ratio is unity. A description of the specimens and the test results are given in the next section of this report.

Now, let us consider when the axial load P is compressive. Even for relatively small values of P, the failure mode depicted in Figure 8 was observed. This failure is due to a wedging effect produced by the bolt,

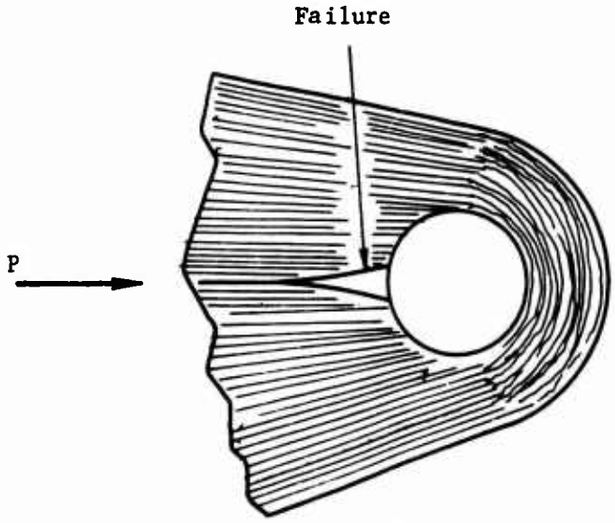

Figure 8. Failure Under Compressive Loading.

breaking the composite in the direction perpendicular to the fibers. In order to avoid this type of premature failure in compression, a specially shaped bushing, as represented in Figure 9, can be used.

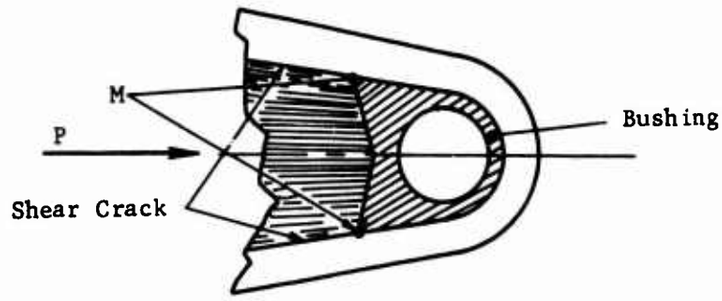

Figure 9. Joint With Special Bushing for Compressive Loading.

When the compressive load P is applied and its magnitude increased, a shear crack is initiated in the points M (see Figure 9) because of the stress difference between the compressed fibers of the central region, shown in the figure, and the practically stress-free fibers surrounding the bushing. After the completion of this shear crack (Figure 9), the fibers of the central region behave as simple compression members. The shape of the contact surface between the bushing and the compressed composite avoids any wedging effect that would tend to separate the fibers. This bushing design has proven, in compression tests, to be very effective. In fact, the compression ultimate loading in joints with this type of bushing is always greater than the ultimate tension load.

It must be pointed out that the radius a is the external radius of the bushing, when the tension design is employed.

The shear force Q is, in most cases, only a fraction of P . The joint design previously described has an ultimate shear force Q of about one-tenth of the ultimate P in tension. In special cases when Q is, for example, one half of P , either the joint design must be changed or the load transmission must be performed in another manner to avoid such high shear forces.

The ultimate tensile load of a joint with a ratio t/a = 1 has been found to correspond with the following expression:

$$P_{ult} = \sigma_{ult}\, t\, h \qquad (1)$$

where h is the joint thickness.

This formula is in good agreement with the test results. It should be emphasized that it is generally impossible to predict the ultimate load of a composite joint from a stress analysis based upon a linear behavior of the material. Such analysis must be used only as a guide to optimize the proportion of the dimensions.

The expression (1) can be interpreted as if a concentration factor of 2 is applied to uniformly distributed stress σ_θ in the tangential direction while ignoring the radial stress σ_r. (See Figure 10)

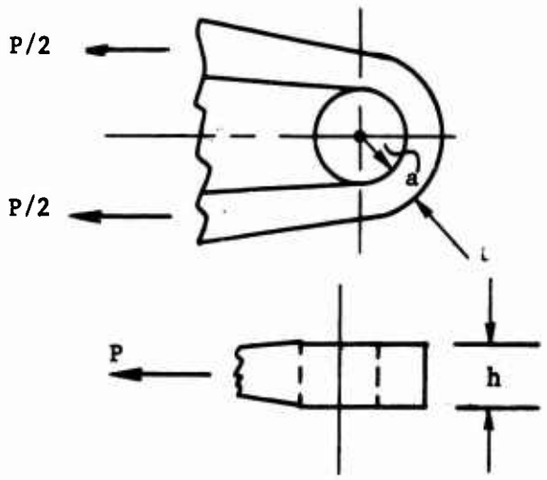

Figure 10. Joint Design Configuration After First Tensile Load.

In some cases, the design of the bolted joint is based upon not only ultimate loads but also maximum deflection. For a joint designed according to the expression (1) (t/a = 1), the hole elongation for glass-epoxy joints is found to be about a/2 in the instant previous to failure. For other load values, the deflection can be reasonably estimated by assuming a linear load-deflection curve.

RESULTS OF TESTS ON BOLTED JOINTS: OPTIMUM t/a RATIO

A series of tests were performed to determine the optimum t/a ratio. The bolted joint configuration used for this purpose is shown in Figure 11.

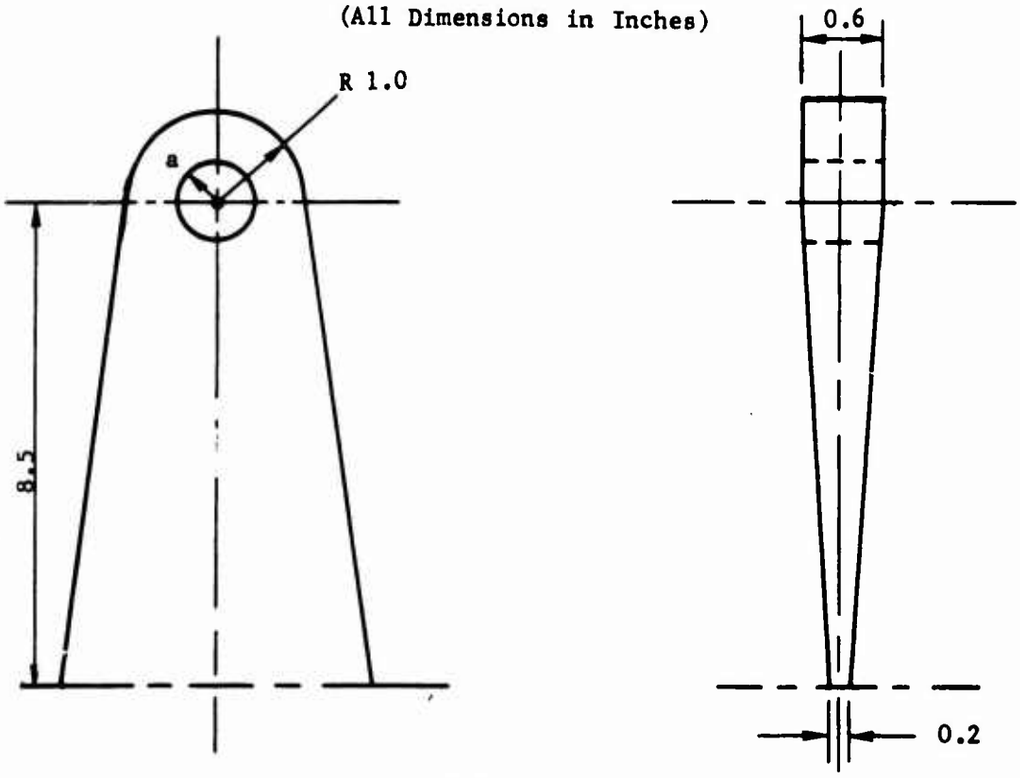

Figure 11. Joint Configuration.

The test results are summarized in Table I. From the values in this table, the ultimate failure load is plotted as a function of t/a in Figure 12. As this figure indicates, the optimum t/a ratio is approximately unity.

TABLE I

TENSILE TESTS

SPECIMEN	RADIUS a INCHES	RATIO t/a	ULTIMATE FAILURE LOAD 10^3 LB	AVERAGE OF ULTIMATE FAILURE LOAD 10^3 LB
1	0.375	1.67	38.6	
2	0.375	1.67	39.3	38.8
3	0.375	1.67	38.4	
4	0.437	1.29	43.5	45.1
5	0.437	1.29	46.7	
6	0.500	1.00	54.2	
7	0.500	1.00	55.0	54.3
8	0.500	1.00	53.6	
9	0.563	0.78	52.7	53.1
10	0.563	0.78	53.4	
11	0.625	0.60	50.8	
12	0.625	0.60	49.7	50.1
13	0.625	0.60	49.9	

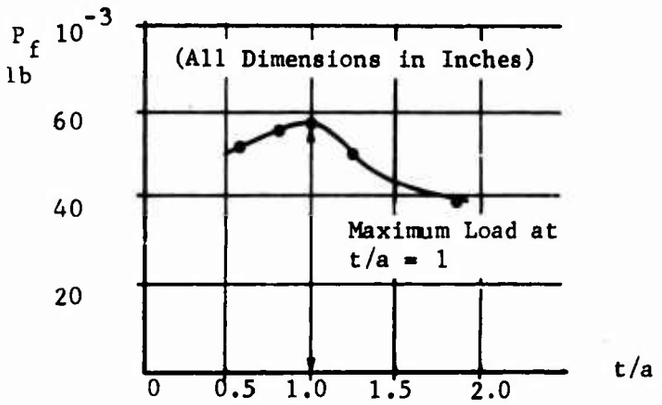

Figure 12. Ultimate Load as Function of t/a.

MULTIPLE-BOLTED JOINT

Many structures require the use of multiple-bolted joints, rather than joints for only one bolt. With the multiple joint, the force transmission occurs over a more extended region, thus avoiding the load concentration on a reduced area which occurs with the simple joint. However, in general, the specific strength of the simple joint is greater than that of the multiple joint when composite materials are employed.

The design of multiple joints is completely analogous to that of simple joints. All the considerations given in the first section of this report are applicable to these joints. The total tensile or compressive load must be divided in equal parts between the simple component joints, each of which can then be individually treated as the simple joint of the previous sections.

Figure 13 shows the multiple joint, fabricated and tested. For the fabrication of this joint, the joint of Figure 14 was made using the winding guide of Figure 15 and the press-mold of Figure 16. After molding, this joint was cut into three parts and bonded, as indicated in Figure 13, to obtain the multiple joint. The simple tape layers, with fibers oriented perpendicular to the loading direction, have no principal structural function, but they assist the bonding by holding the parts together. Multiple joints fabricated by this procedure are shown in Figure 18.

The fabricated multiple joints were tested in tension, using the attachments shown in Figure 19. Figure 20 shows the multiple joint mounted in the test machine. Two specimens were tested in tension. The ultimate failure loads were 23,800 and 24,800 lb, respectively. Figures 21 and 22 illustrate the failure mode.

The failure load for this type of joint is estimated using the expression (1), obtaining

$$P_{ult} = 180{,}000 \times 0.1 \times 0.25 \times 6 = 27{,}000 \text{ lb},$$

where $\sigma_{ult} = 180{,}000$ psi is assumed for the glass-epoxy composite and a perfect uniformity in the load distribution is assumed for each bolt. It must be noted that, for these joints, the t/a ratio is 0.5 instead of the optimum t/a = 1. These dimensions were adopted for construction reasons.

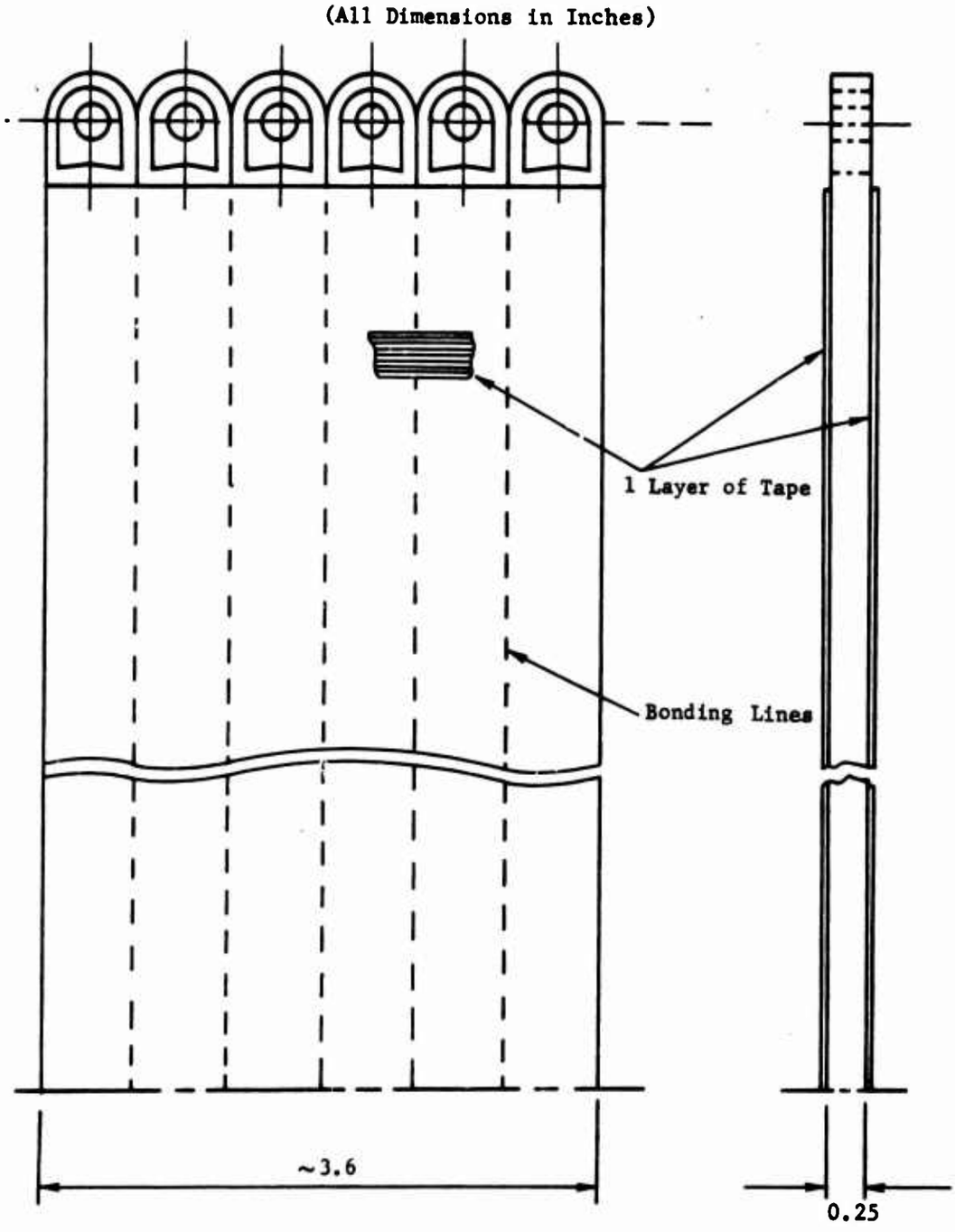

Figure 13. Multiple Joint, Final Configuration.

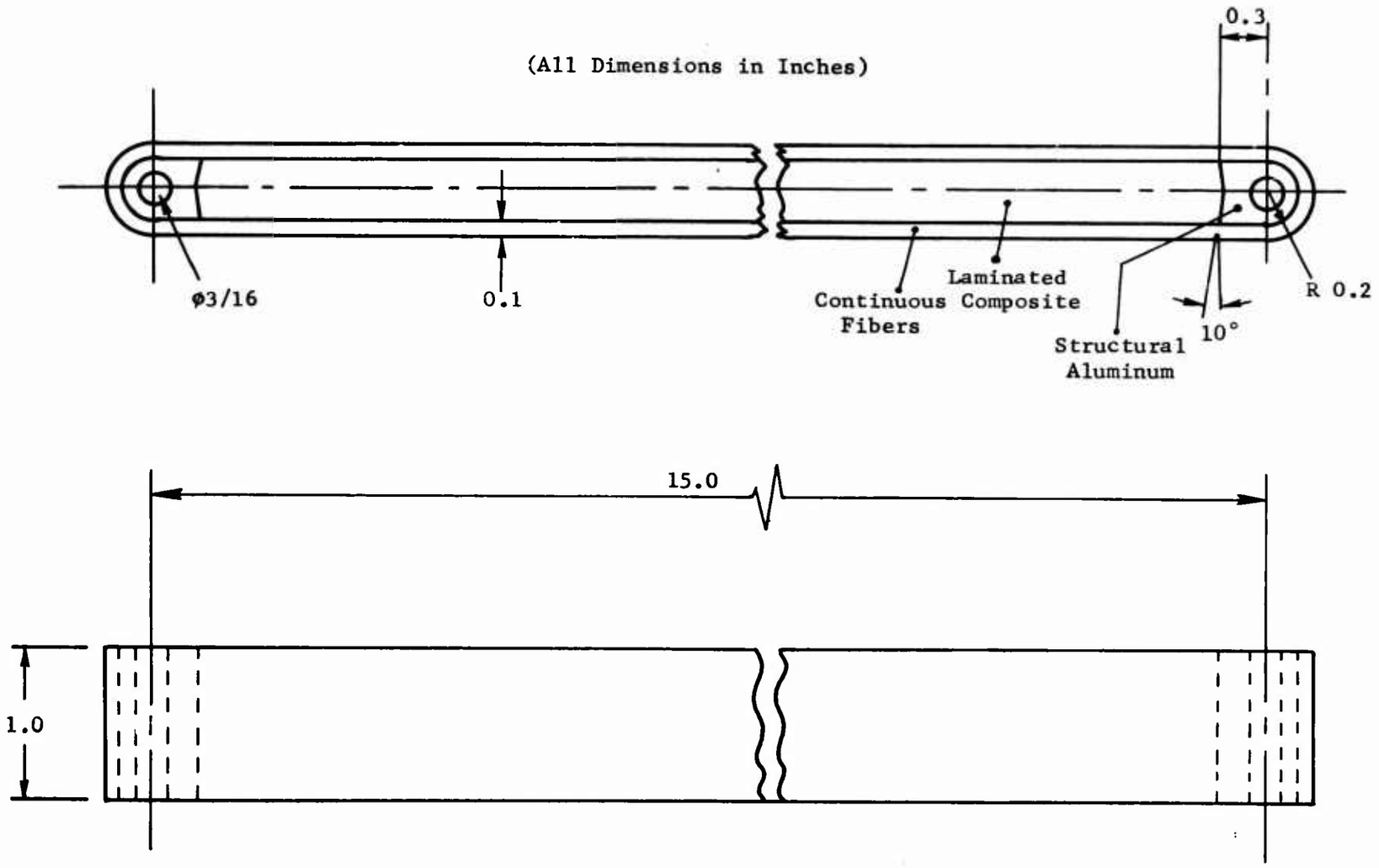

Figure 14. Multiple Joint, First Stage of Fabrication.

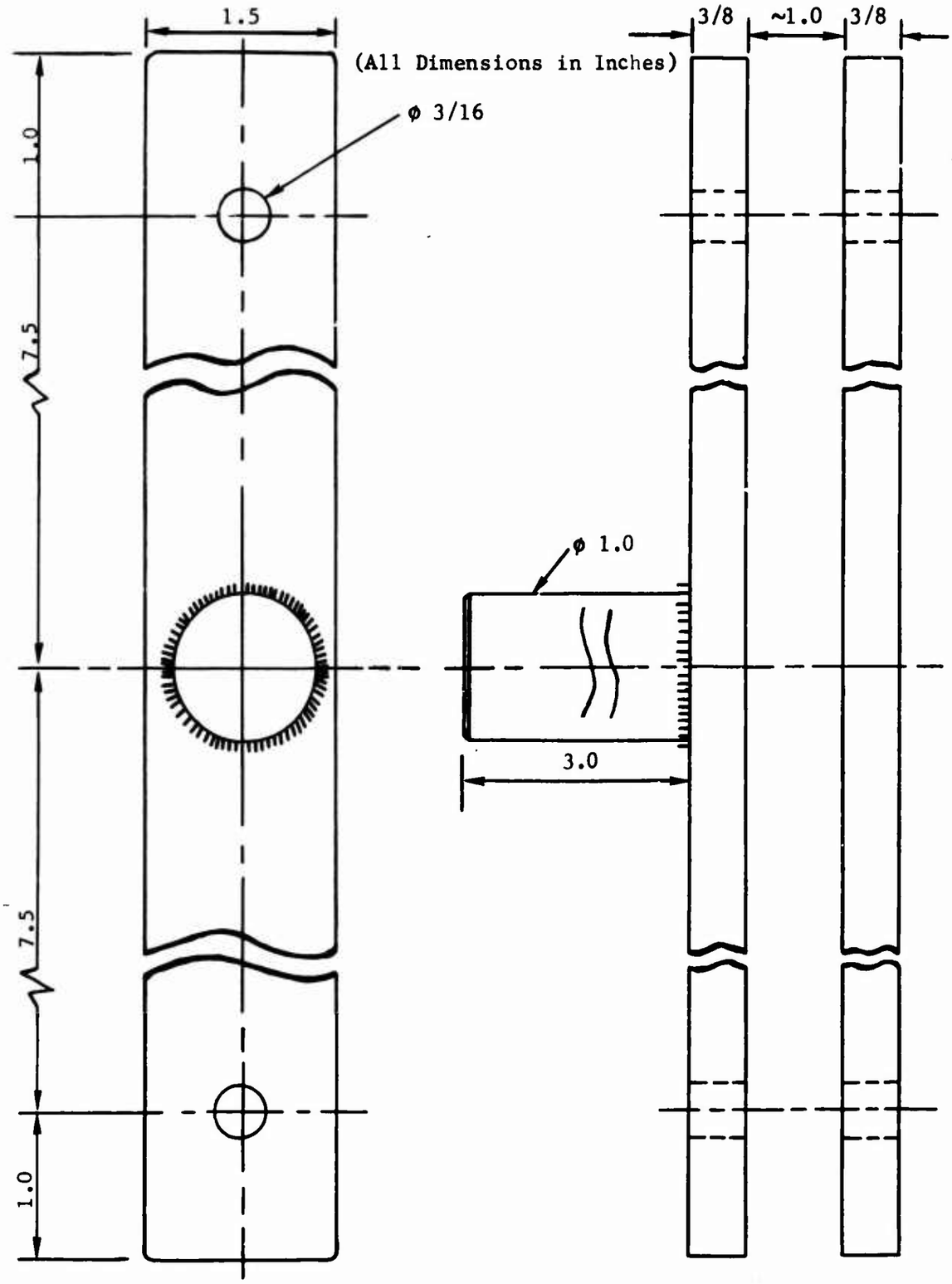

Figure 15. Winding Guide for Multiple Joint Fabrication.

(All Dimensions in Inches)

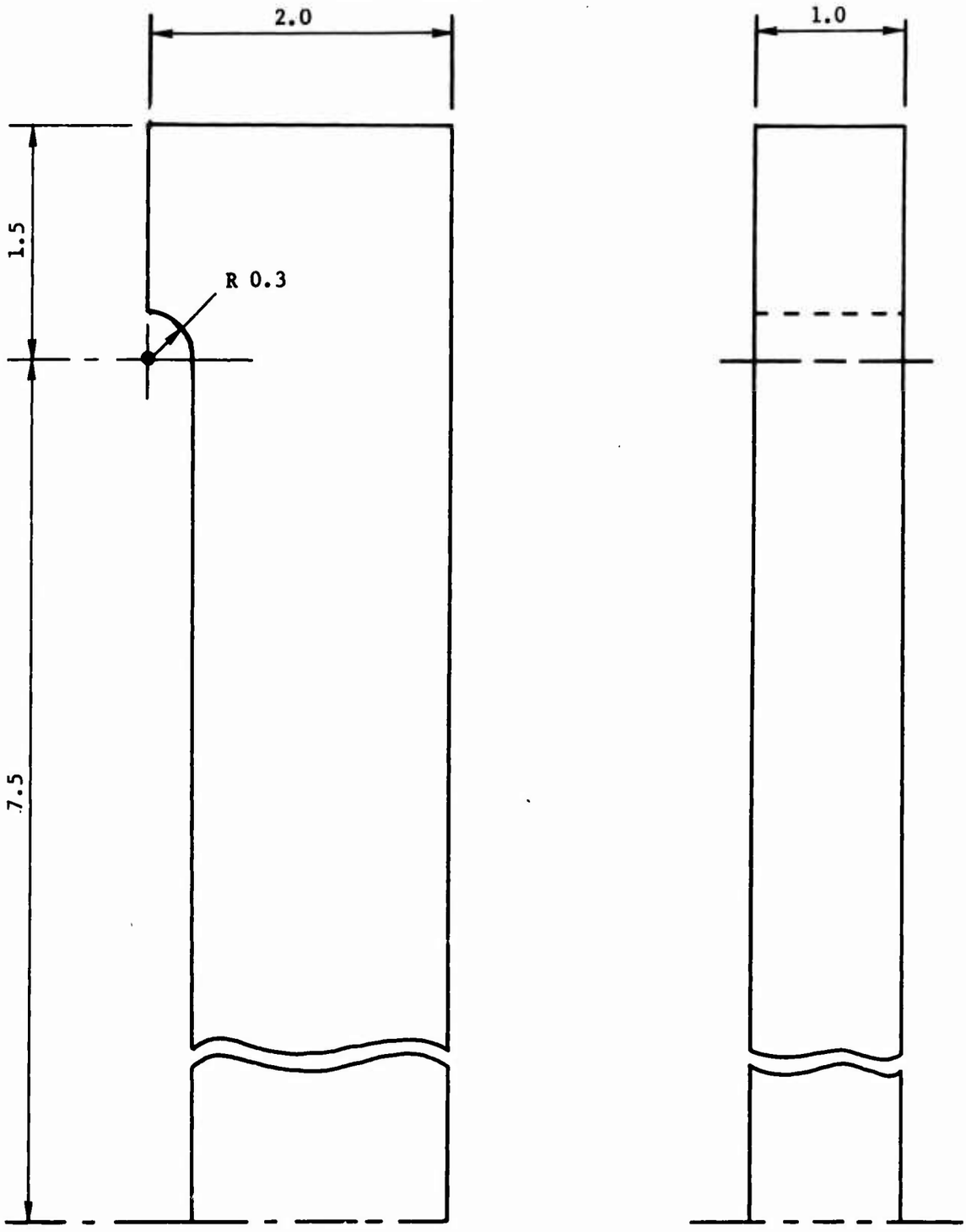

QUANTITY: 2

Figure 16. Press-Mold for Multiple Joint Fabrication.

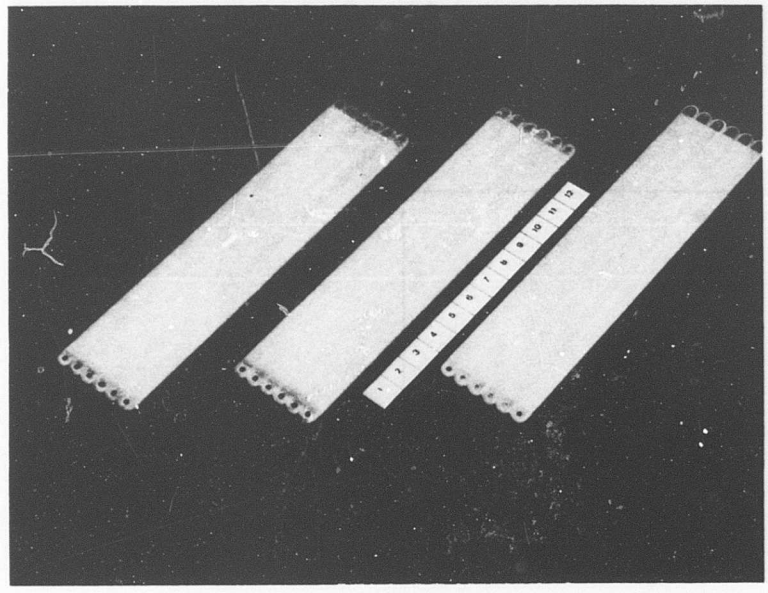

Figure 17. Multiple Joints.

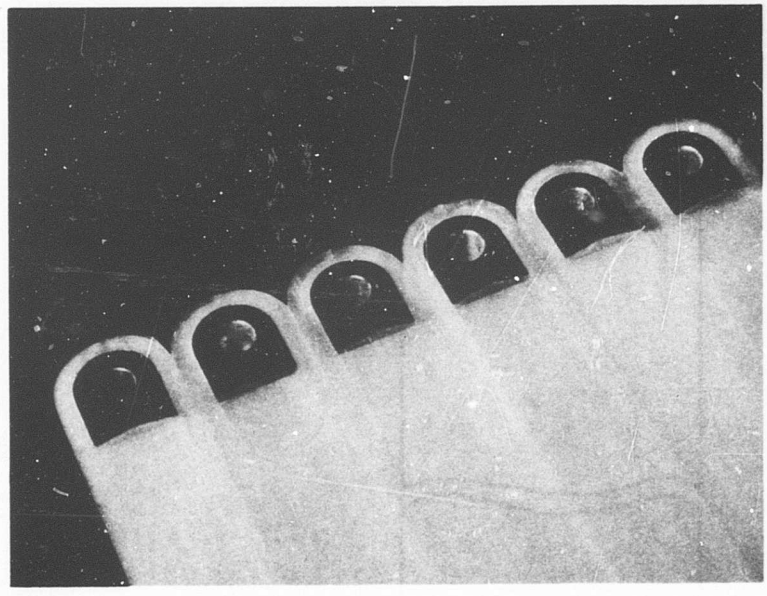

Figure 18. Multiple Joint, Detail of the Inserts.

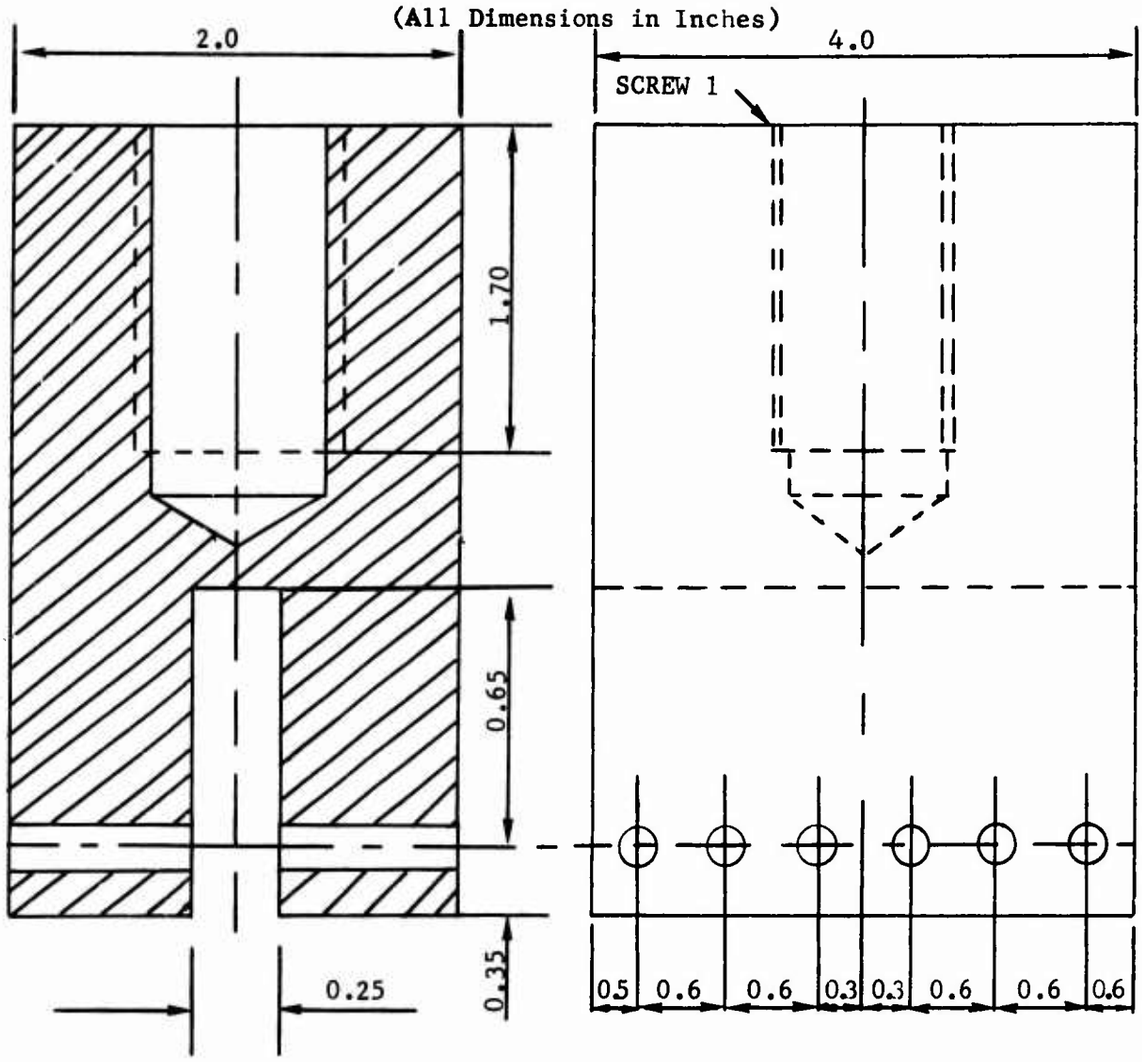

QUANTITY: 2 (STEEL)

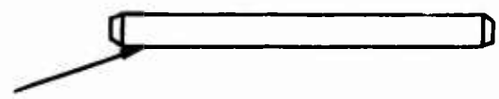

PIN 3/16, LENGTH 2.5, STEEL SAE 1050

QUANTITY: 14

Figure 19. Multiple Joint, Test Device.

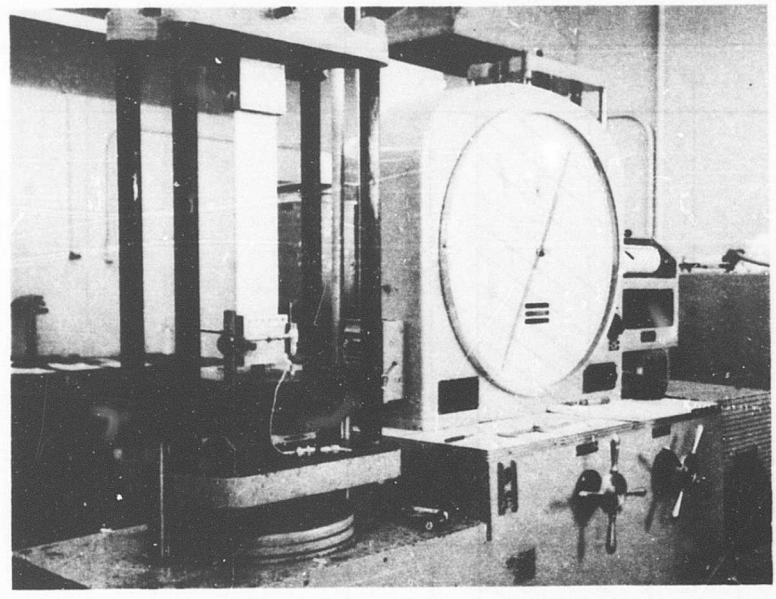

Figure 20. Tension Testing of a Multiple Joint.

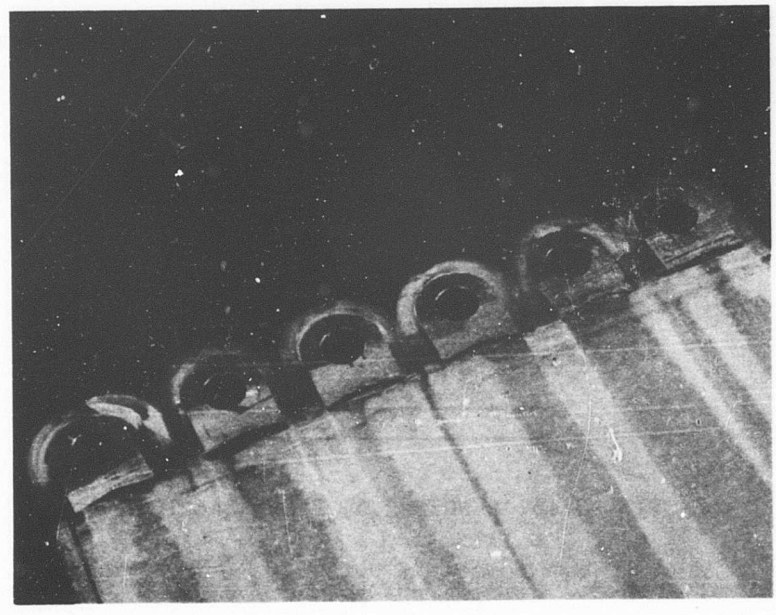

Figure 21. Tested Multiple Joint.

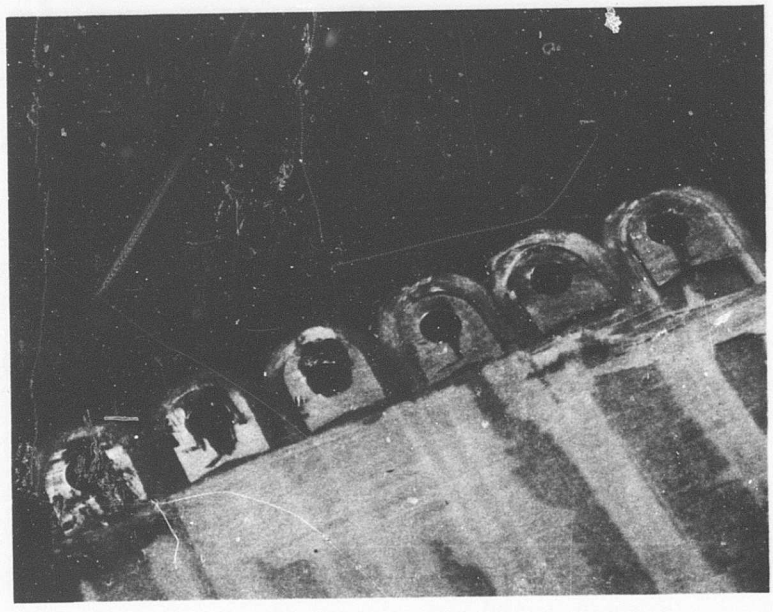

Figure 22. Tested Multiple Joint.

IN-PLANE BOLTED JOINT

This section considers a joint with the bolt in the loading plane. The configuration of this joint is shown in Figure 23, where only half of the fabricated joint is represented. Figures 24 and 25 are drawings of the winding device and the press-mold, respectively, utilized in the fabrication of the specimens.

Two different failure modes can be expected in this joint. Because the t/a ratio is only 0.333, a fiber failure of the type shown in Figure 6 is one of the possible modes of failure. Another is the transverse failure shown in Figure 26, where a debonding of the wound part occurs along line AB. The debonding is due to the tensile stresses acting perpendicularly to the loading direction. The stress analysis of the joint shows that this stress σ_n acting across AB is only

$$\sigma_n \simeq \frac{\sigma_\theta}{43}$$

where σ_θ is the tangential stress at CD. Thus, if σ_θ reaches the value 180,000 psi, σ_n is about 4,200 psi. Since the transverse tensile stress is smaller than the failure stress of the unidirectional composite in transverse tension, this joint would be expected to fail at CD rather than across AB. However, the failure occurred at AB in both joints tested. This can be explained if the degradation of the composite tensile strength in the fiber direction is considered. High tensile stresses in the fiber direction produce micro-cracks in the matrix. These cracks result in high stress concentrations in the material. Then, a crack propagation phenomenon is initiated along AB, and the failure mode will be that indicated in Figure 26, even when σ_n is, as an average stress (without considering the stress concentrations produced by the micromechanical cracks), very small.

Figure 27 shows the joint mounted in the testing machine for a tension test. Note the attachment used in the testing. Two joints were tested, both failing along AB (Figure 26) at loads of 22,000 and 24,800 lb., respectively. Figures 28 and 29 show a tested specimen.

(All Dimensions in Inches)

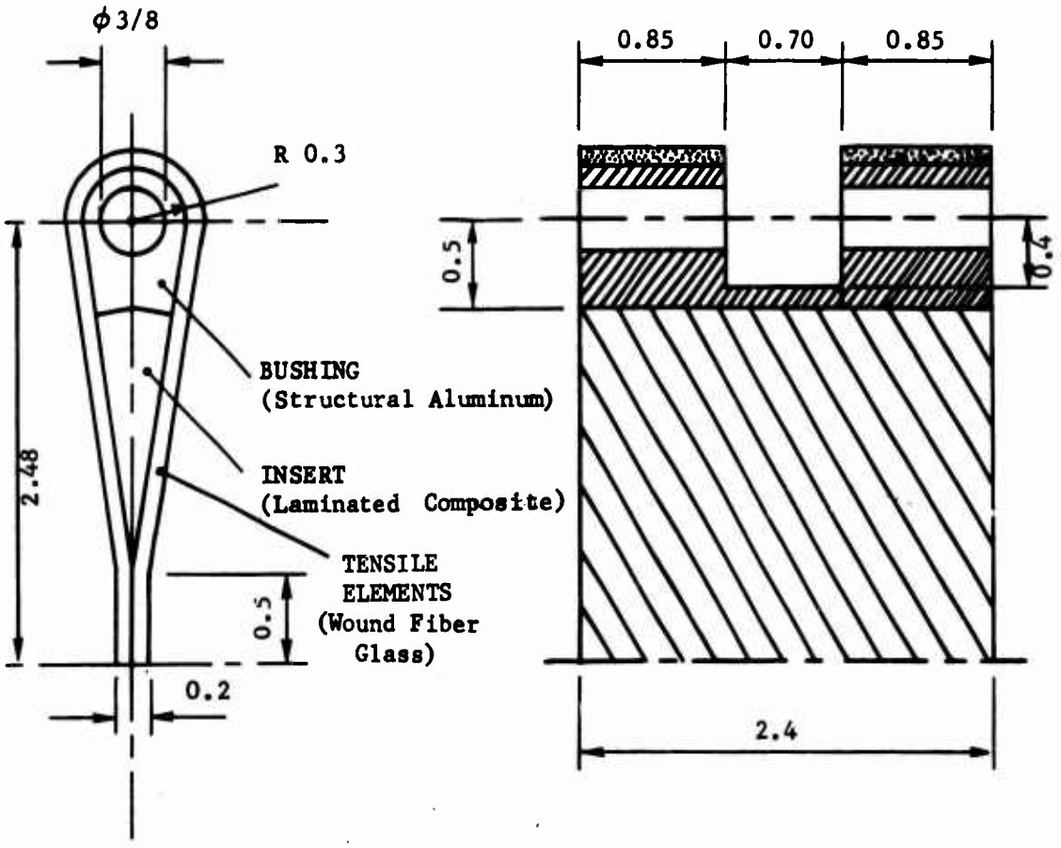

Figure 23. In-Plane Bolted Joint, General Configuration.

(All Dimensions in Inches)

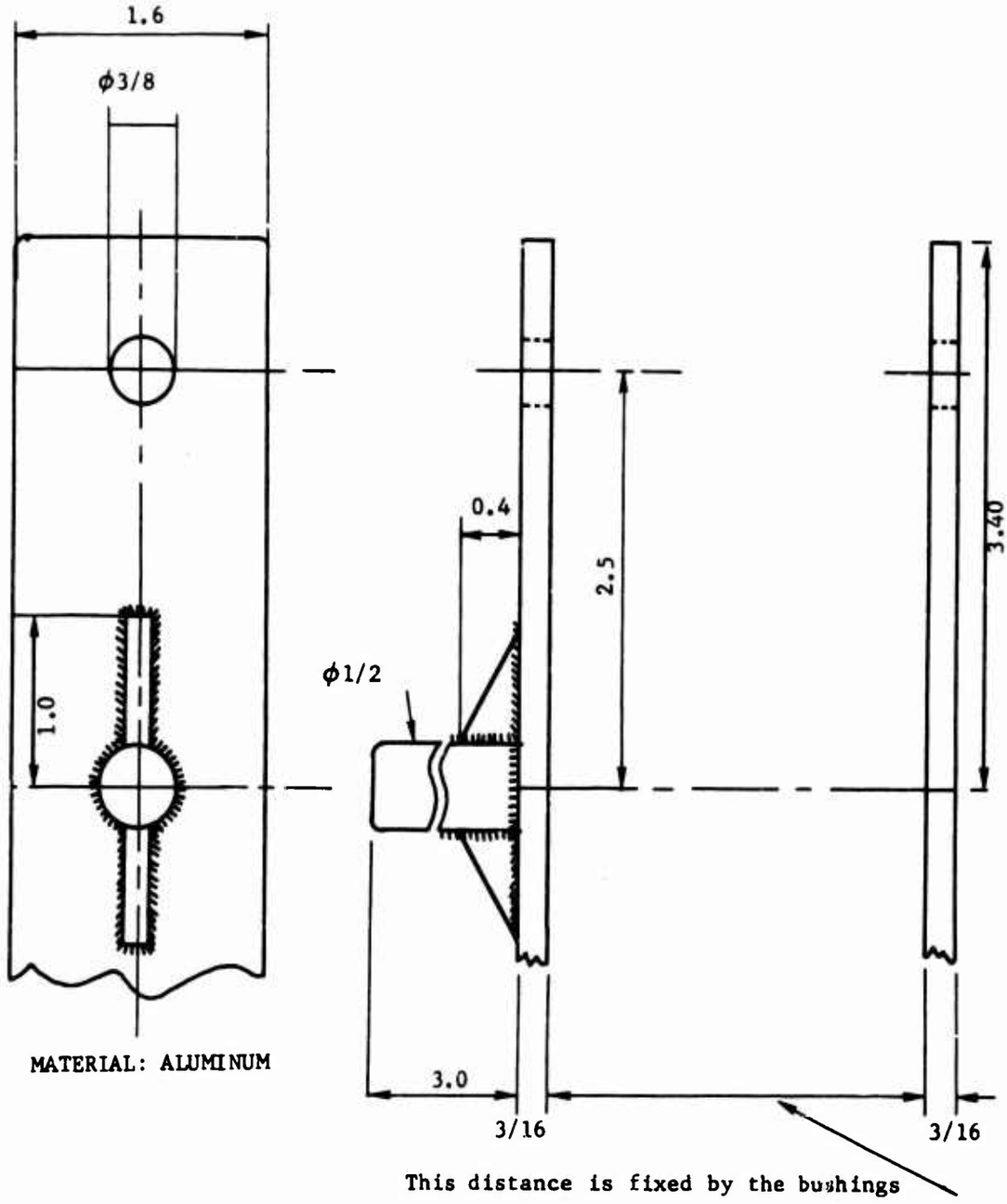

Figure 24. In-Plane Bolted Joint, Winding Device.

(All Dimensions in Inches)

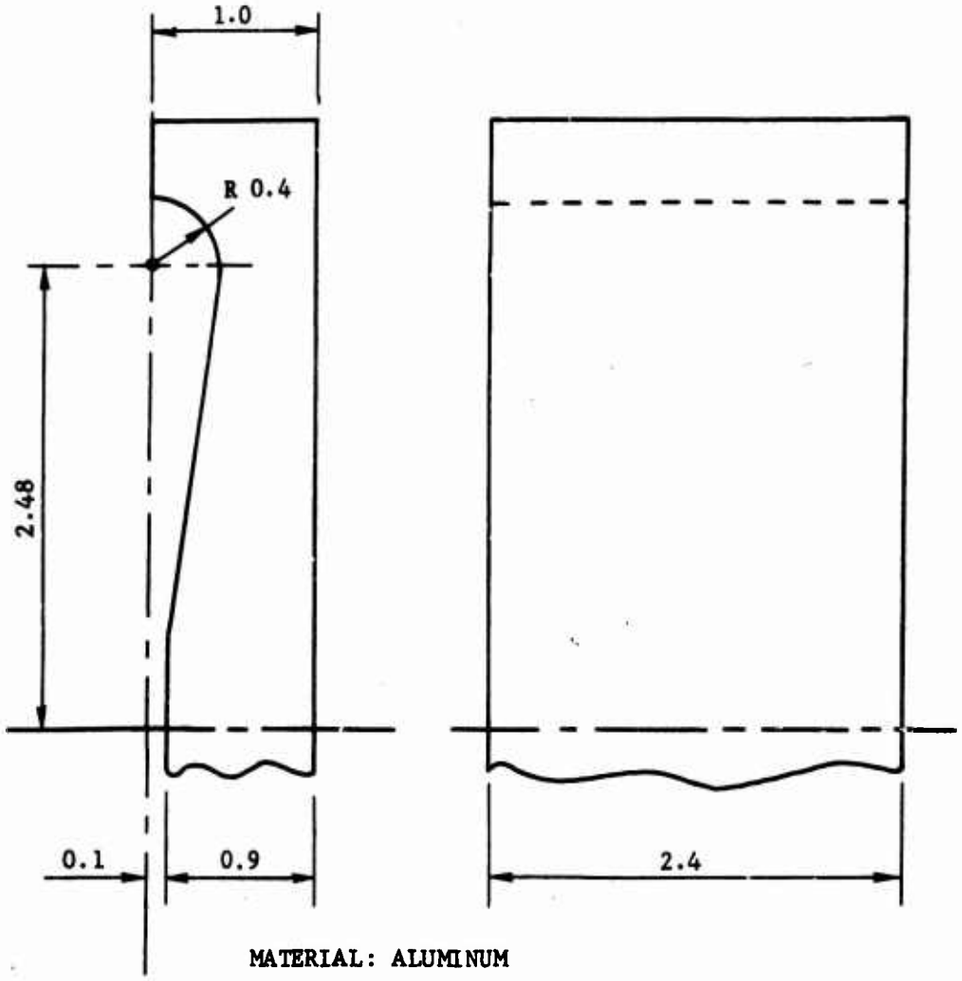

MATERIAL: ALUMINUM

QUANTITY: 2

Figure 25. In-Plane Bolted Joint, Press-Mold.

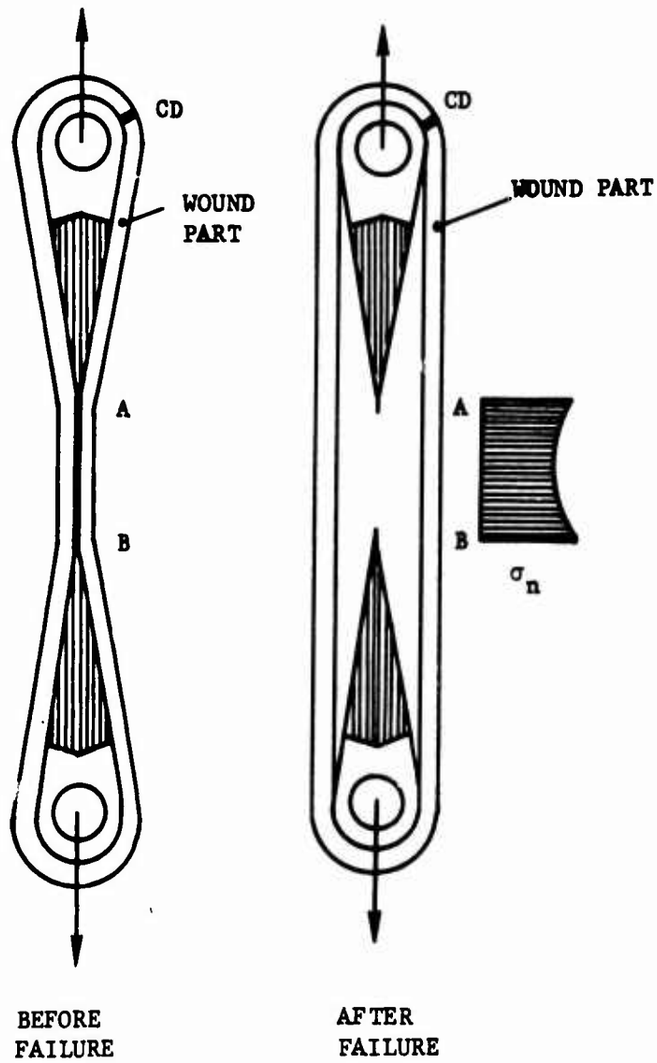

Figure 26. Failure Mode.

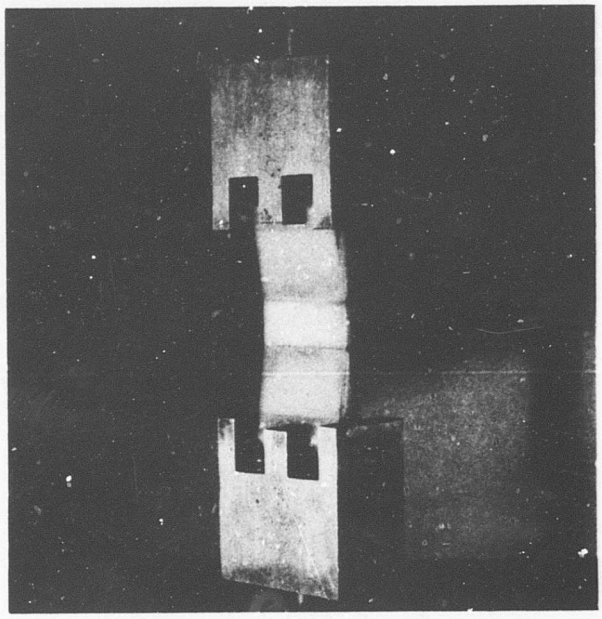

Figure 27. In-Plane Bolted Joint Mounted in the Testing Machine.

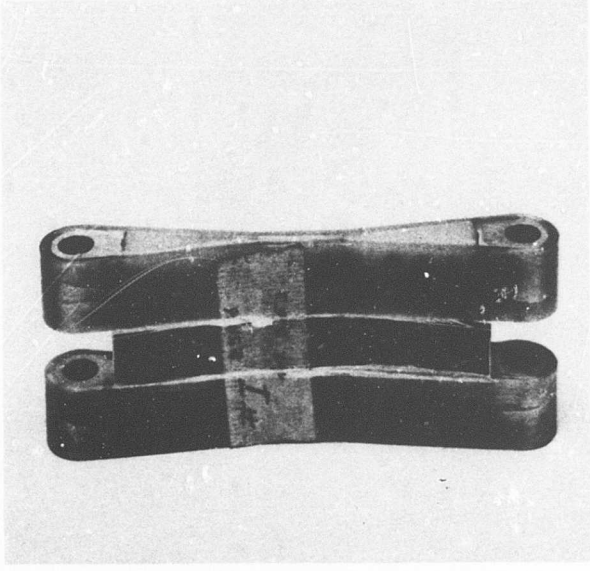

Figure 28. In-Plane Bolted Joint After Testing.

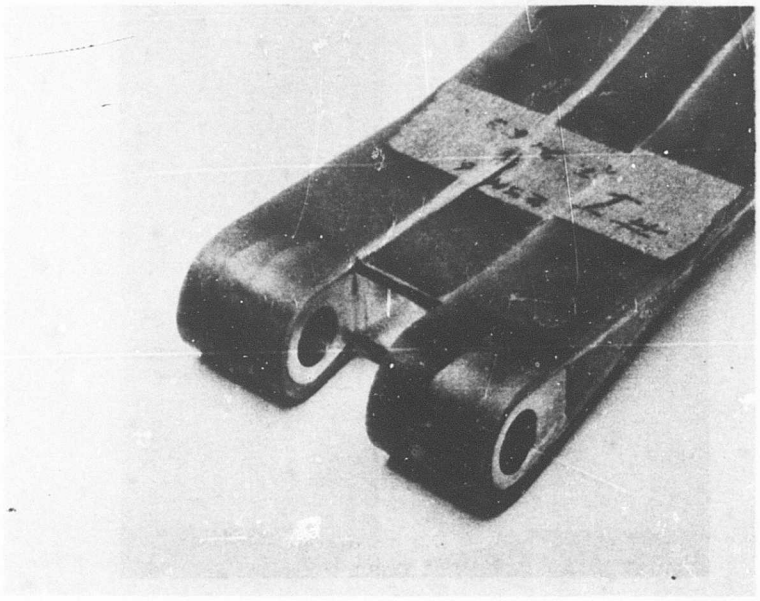

Figure 29. In-Plane Bolted Joint After Testing.

OFF-PLANE BOLTED JOINT

In this type of joint, the axis of the bolt is not on the plane of loading. This joint differs from the joints previously considered, in that it includes an adhesive surface which has a structural function to perform.

The off-plane joint is depicted in Figures 30, 31 and 32. In the fabrication of this type of joint, the winding guide of Figure 33 and the press-mold of Figure 34 were used. The fabricated specimens are shown in Figure 35.

Figure 36 shows the specimen mounted in the testing machine for a tension test. Figure 37 is the drawing of the attachment used for the testing.

Two specimens were tested, and failure loads of 2640 and 2915 lb., respectively, were obtained. The failure mode is shown in Figures 38 and 39. This failure mode is surprising, since shear failure along the entire adhesive layer (Figure 40) was expected. Instead, the failure occurs in a region of small tensile stress acting perpendicular to the plane of the adhesive. The failure shown in Figures 38 and 39 does not occur in the adhesive; rather, it is a transverse-tensile failure in the composite.

This failure can be interpreted using the arguments of the previous section; that is, it is related to the crack propagation phenomenon associated with the appearance of micro-cracks in the matrix.

From analysis of this joint and the analysis stated in the previous section, the following conclusion can be made: in joint design using composite materials, it is necessary to eliminate all regions in which the unidirectional composite is under transverse tensile stresses. Failure occurs even for very small values of these stresses, because of this crack propagation phenomenon.

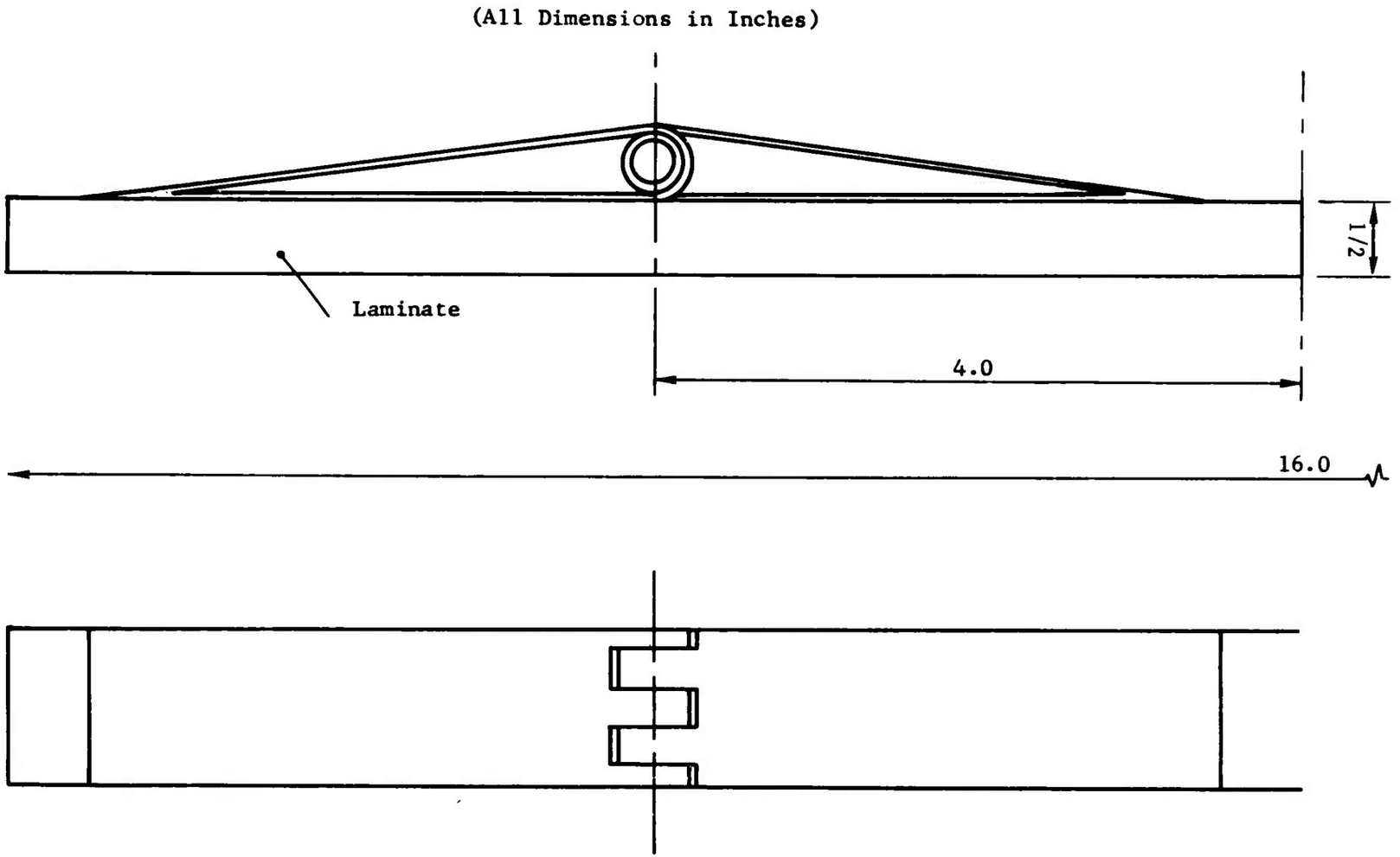

Figure 30. Off-Plane Joint, General Configuration.

(All Dimensions in Inches)

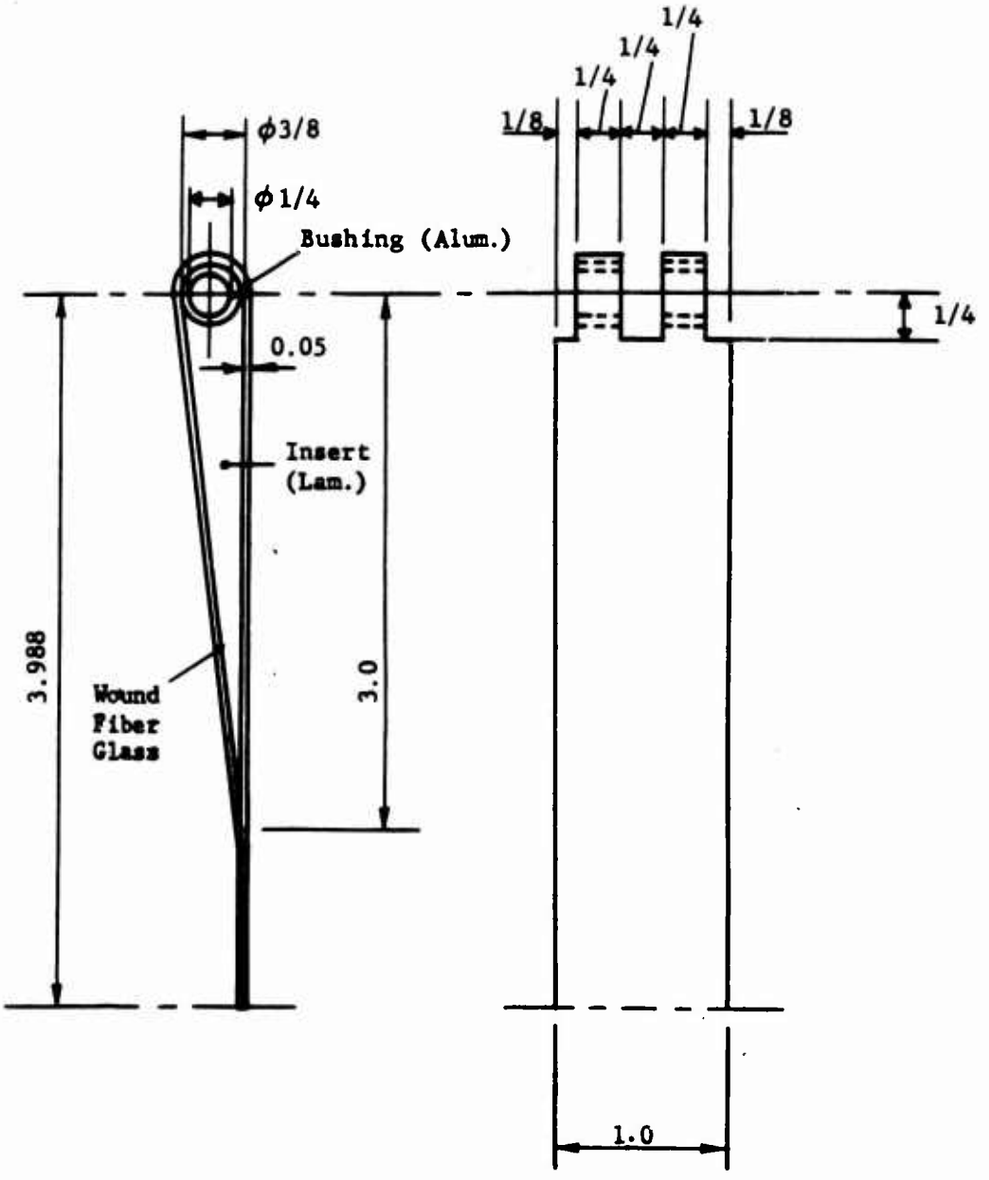

Figure 31. Off-Plane Joint, Parts.

(All Dimensions in Inches)

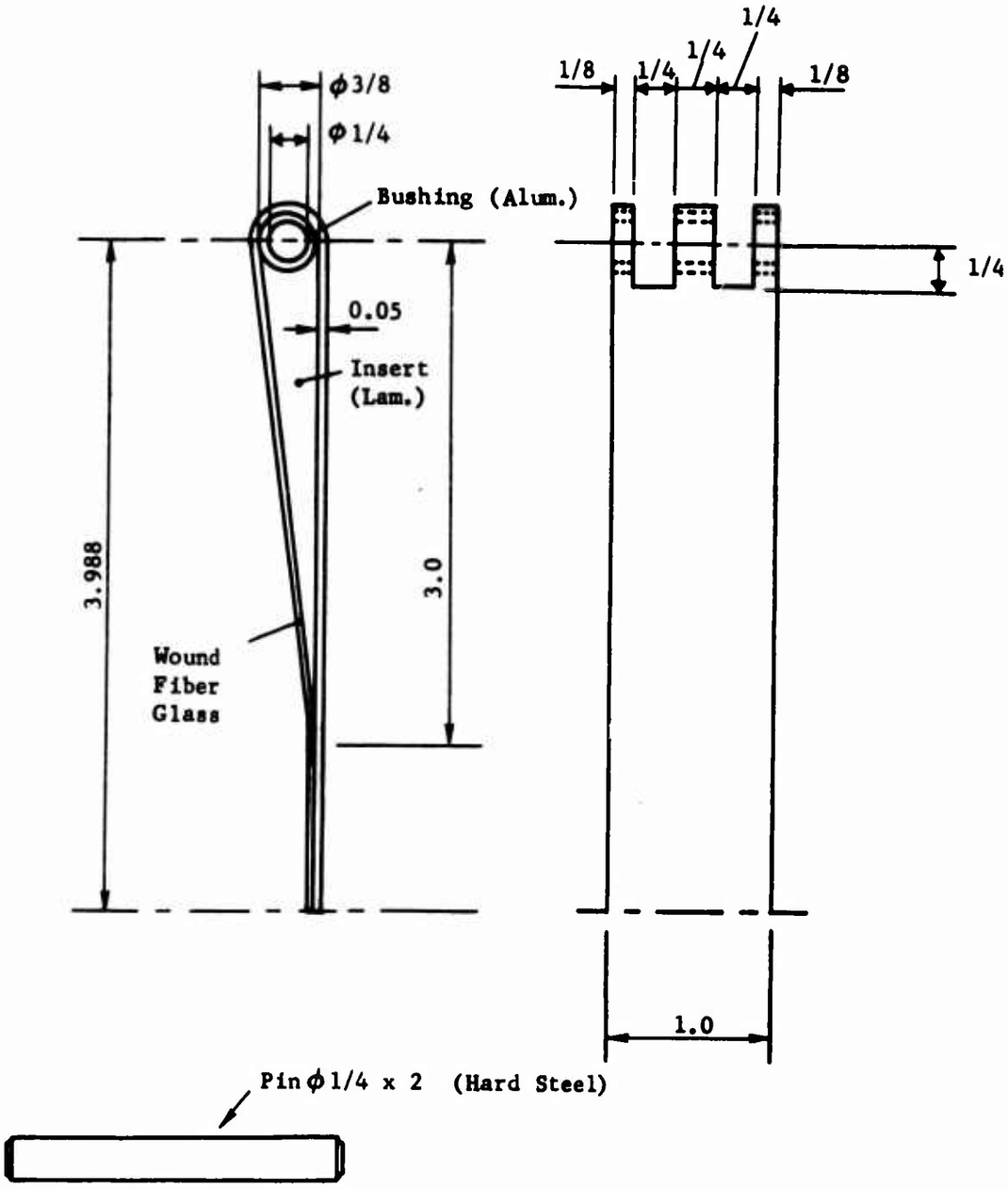

Figure 32. Off-Axis Joint, Parts.

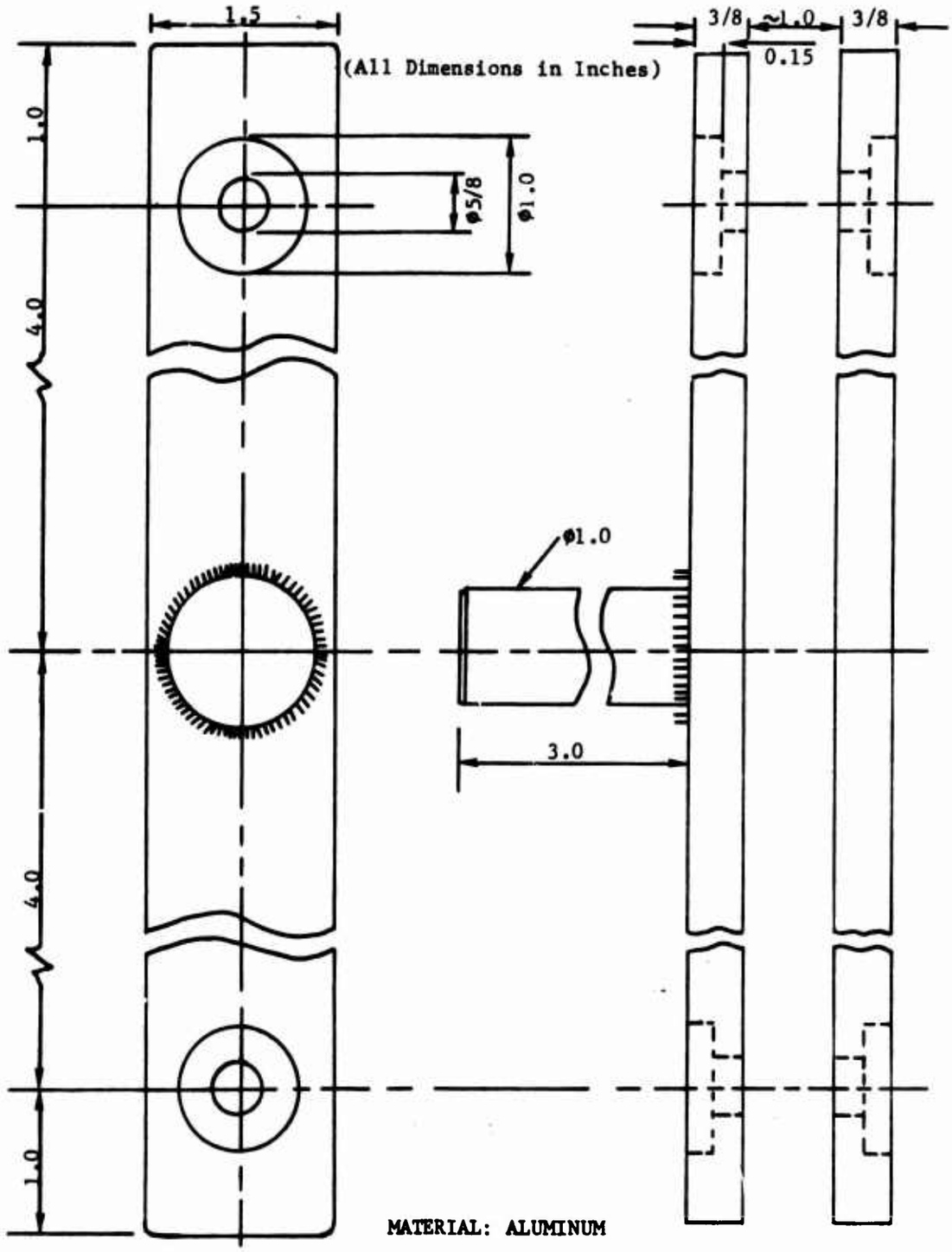

Figure 33. Off-Plane Joint, Winding Guide.

(All Dimensions in Inches)

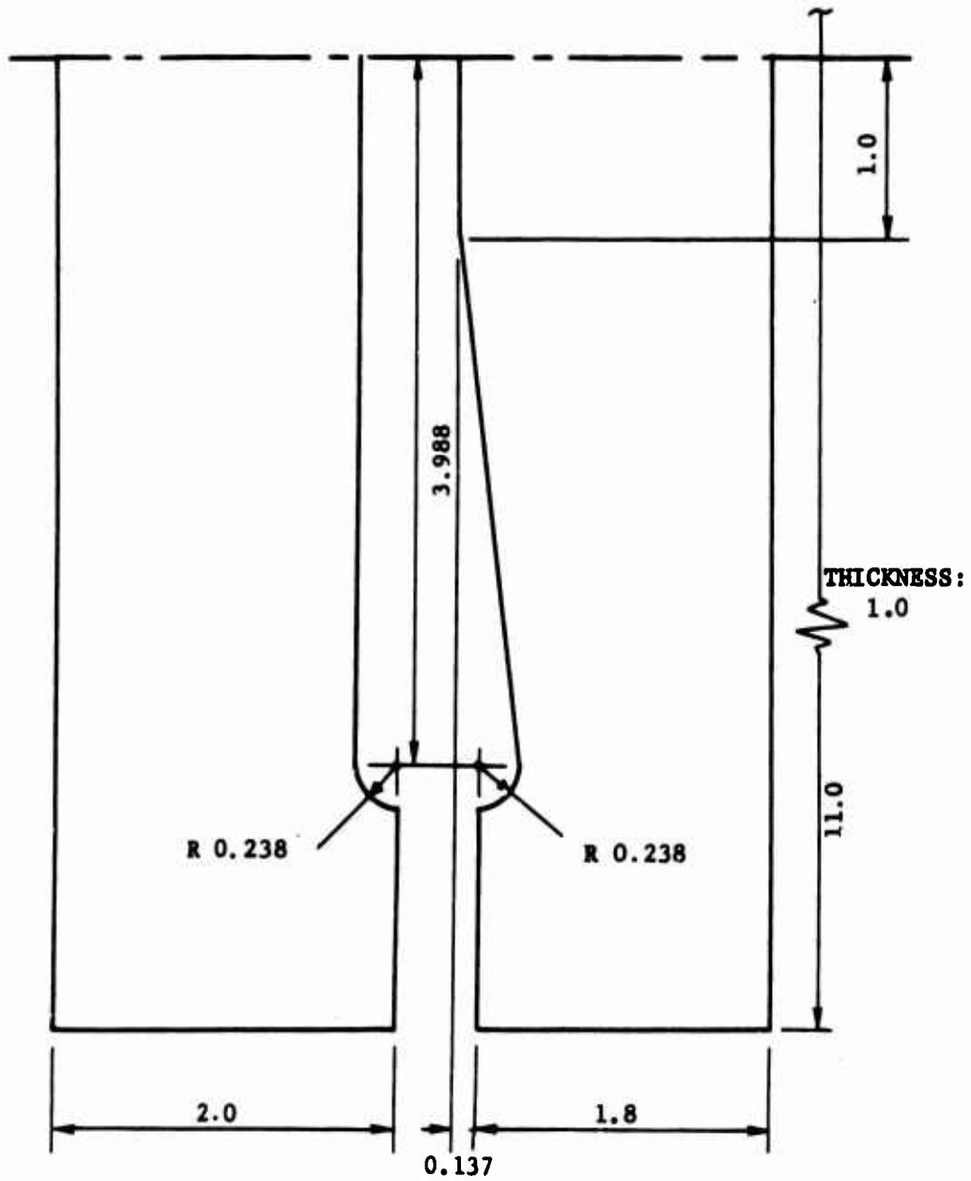

MATERIAL: ALUMINUM

Figure 34. Off-Plane Joint, Press-Mold.

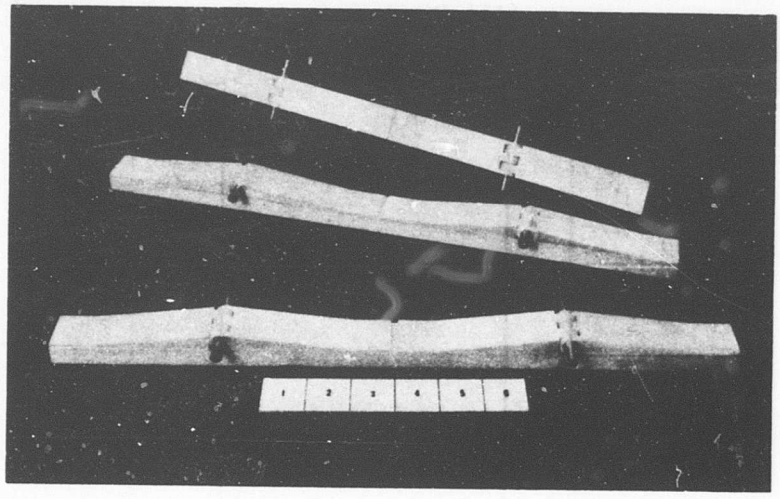

Figure 35. Off-Plane Joint Specimens.

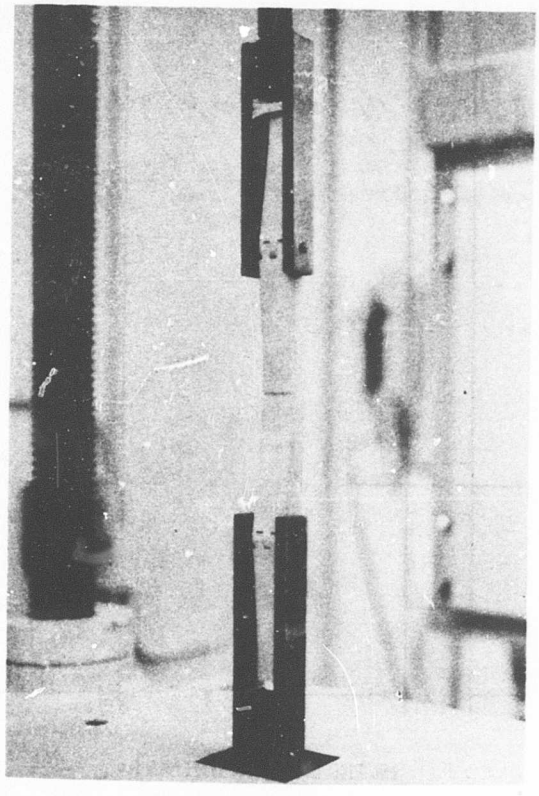

Figure 36. Off-Plane Joint Specimen Mounted for Testing.

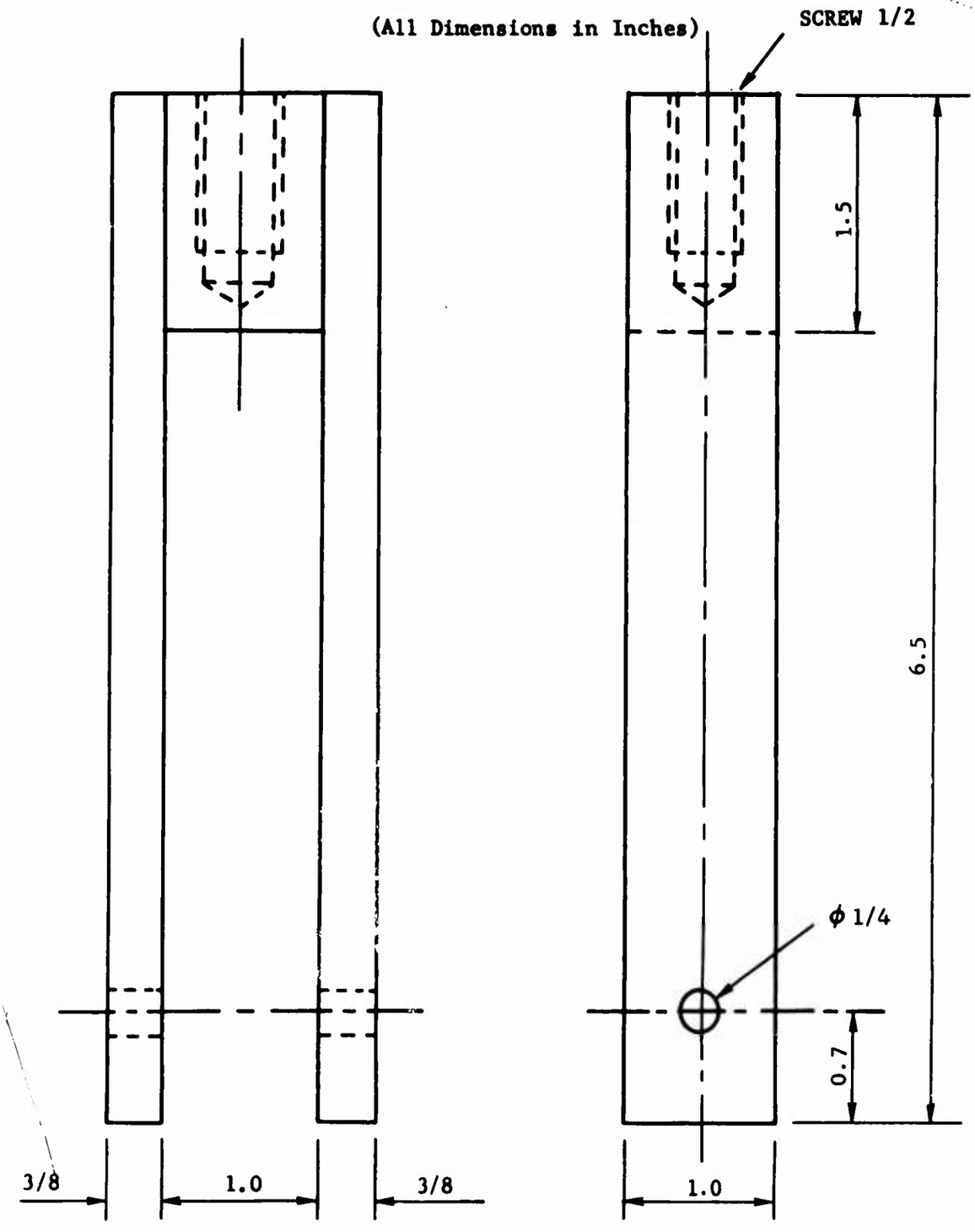

Figure 37. Off-Plane Joint, Attachment for Testing.

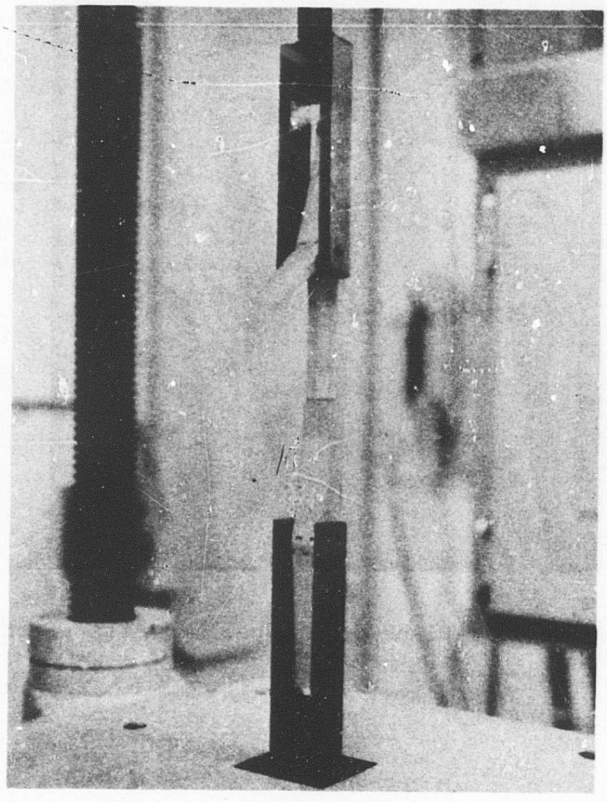

Figure 38. Off-Plane Joint Specimen After Testing.

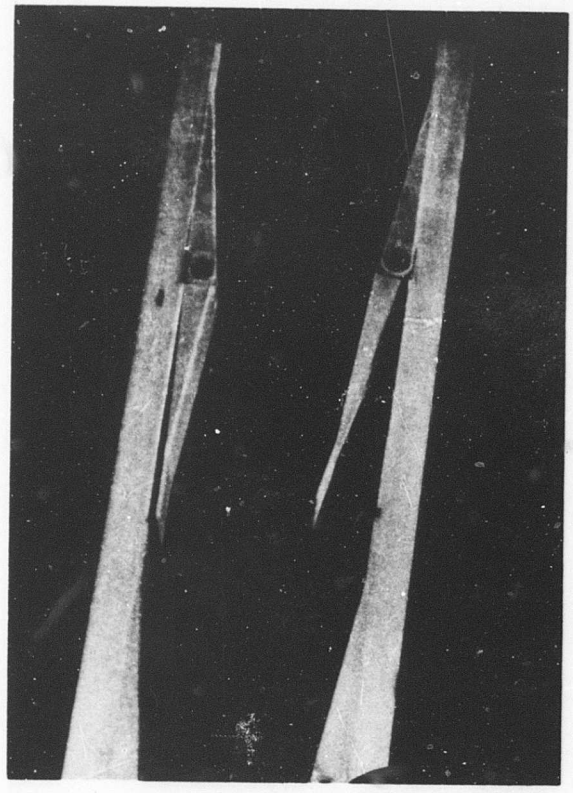

Figure 39. Off-Plane Joint Specimen After Testing.

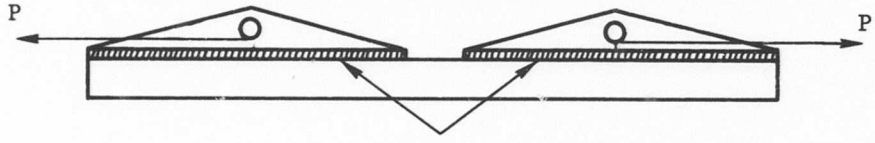

Figure 40. Adhesive Layers.

ORTHOGONAL JOINT

This type of joint, shown in Figure 41, is used to introduce small forces into a wall. It facilitates the application of handles or other devices. The drawing of the fabricated joints is shown in Figure 42, while Figure 43 shows the unidirectional composite ring from which parts of the joint are obtained. Figure 44 is the winding device utilized to fabricate the ring of Figure 43.

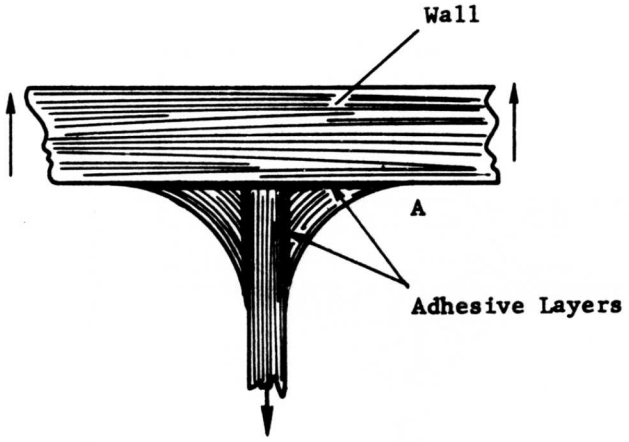

Figure 41. Orthogonal Joint.

Figure 45 shows three fabricated specimens. Four specimens were tested in the manner shown in Figure 46. Figure 47 is the drawing of the test support used in this test. The failure loads were 1845 and 1970 lb., respectively, in the first two specimens; while in the other two, failure loads of 2975 and 3005 lb., respectively, were obtained. The only difference between the two sets of specimens was the adhesive specification: for the first two, Narmco 227 adhesive was used; for the other two specimens, an epoxy-polyamide adhesive was used. The results obtained in the testing of the last two can be considered satisfactory. Figure 48 shows bonding failure in the first two specimens. Figure 49 shows the failure of a specimen fabricated with the epoxy-polyamide adhesive. In this case, the adhesive bond is improved and the failure occurs in the composite itself, as well as in the adhesive layer.

(All Dimensions in Inches)

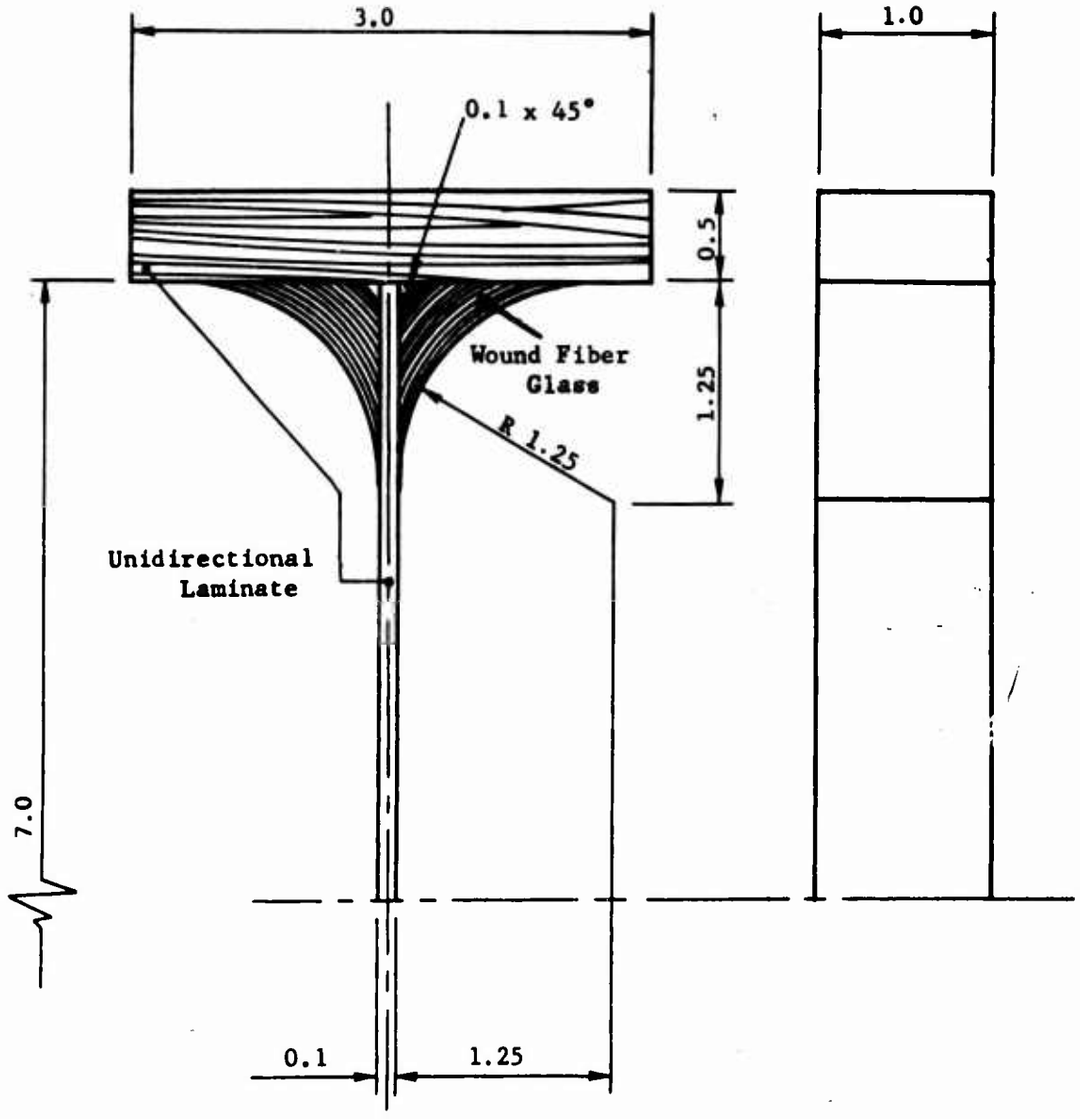

Figure 42. Orthogonal Joint, General Configuration

(All Dimensions in Inches)

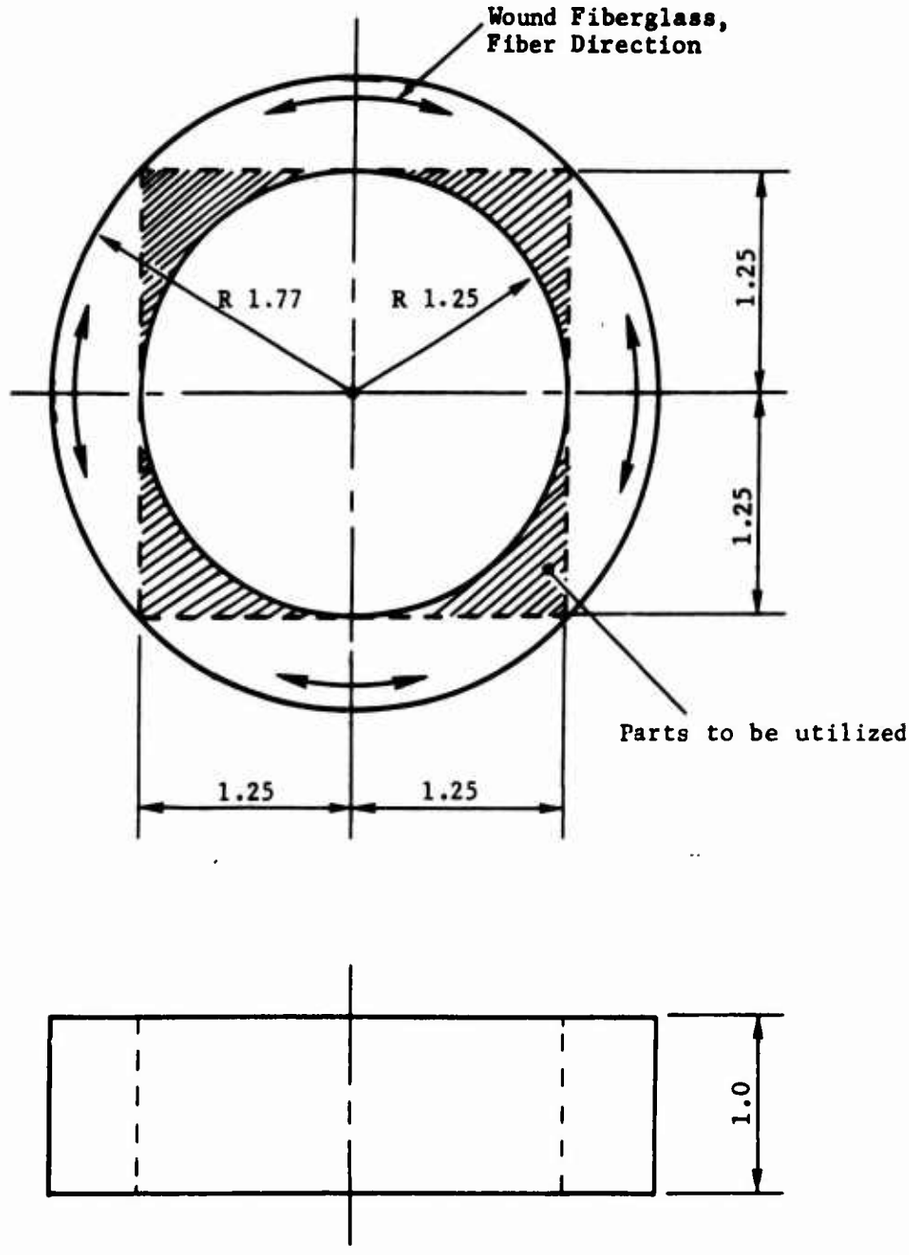

Figure 43. Orthogonal Joint, Fabrication of Parts.

(All Dimensions in Inches)

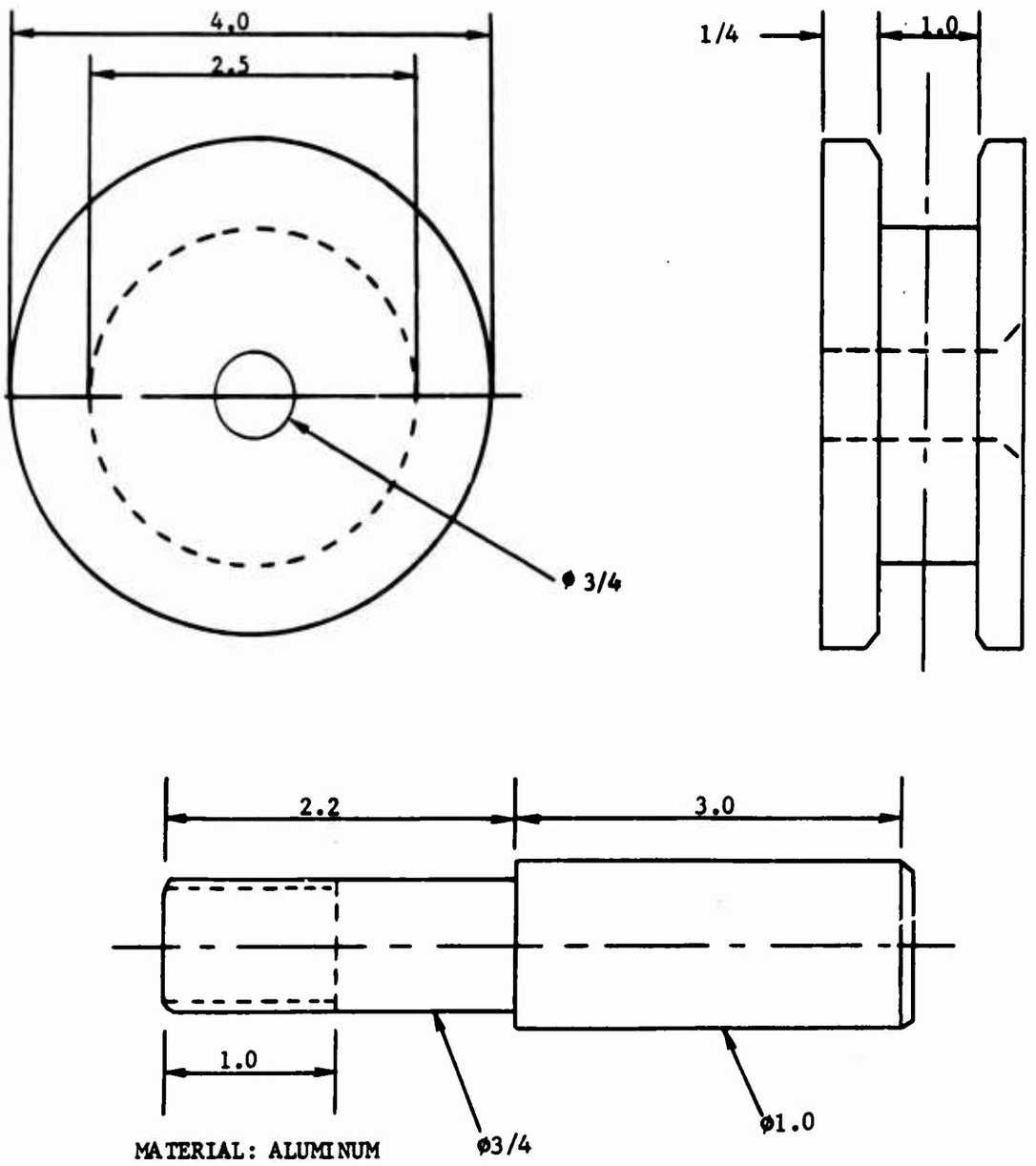

Figure 44. Orthogonal Joint, Winding Device.

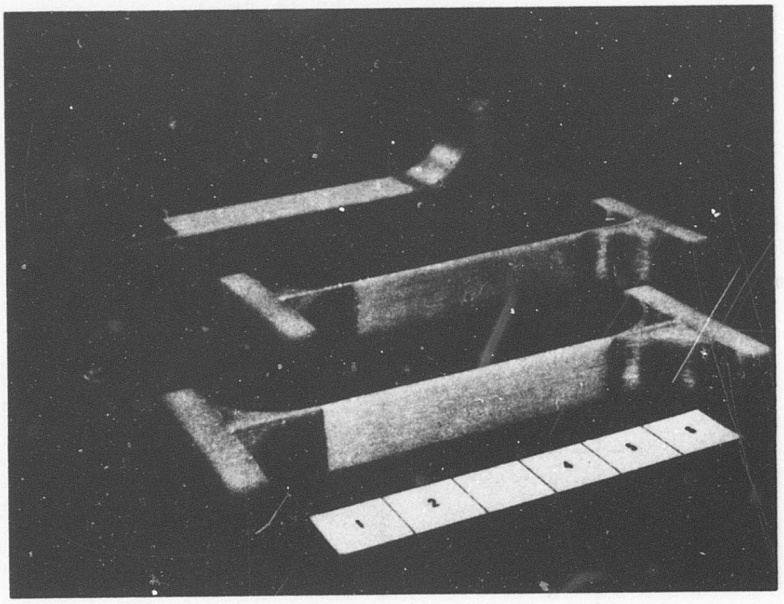

Figure 45. Orthogonal Joint Specimens.

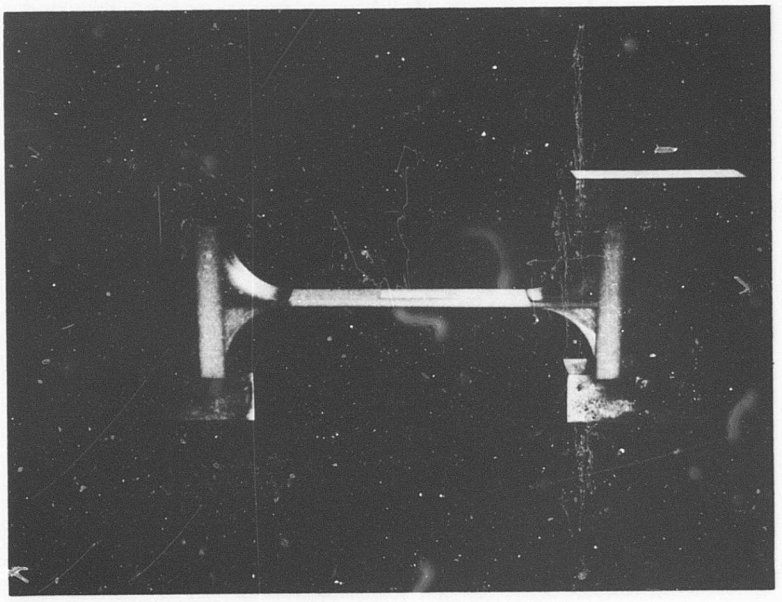

Figure 46. Orthogonal Joint Mounted in the Testing Machine.

(All Dimensions in Inches)

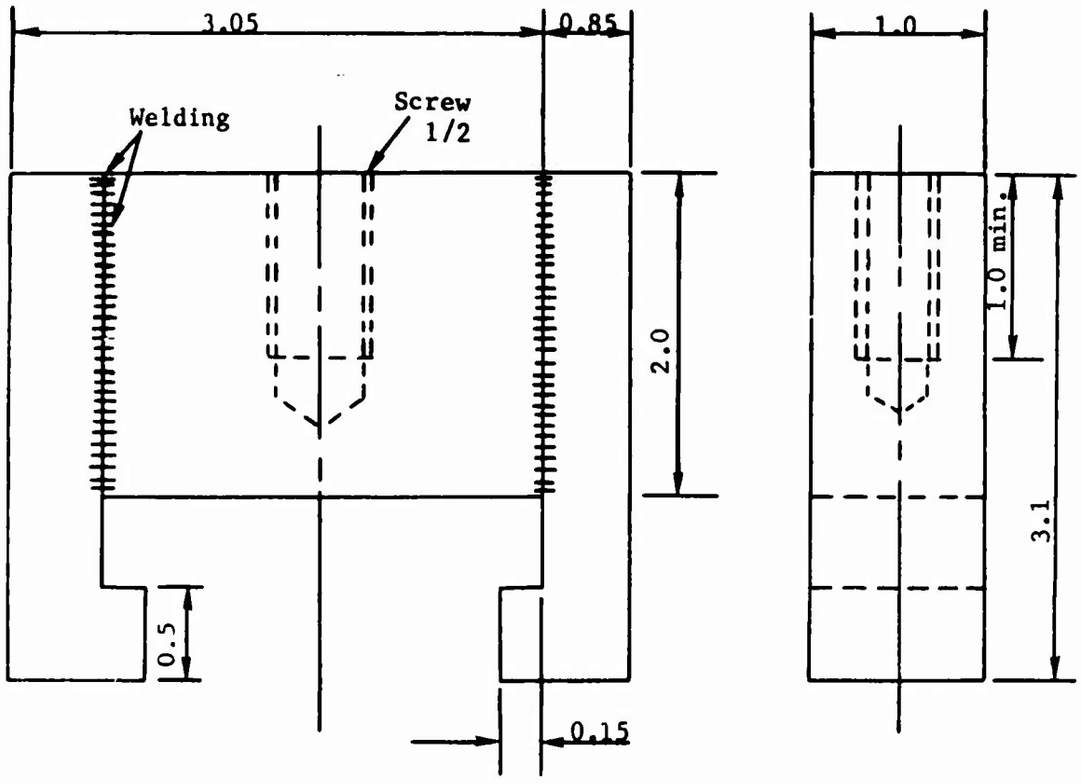

Figure 47. Orthogonal Joint Test Attachment.

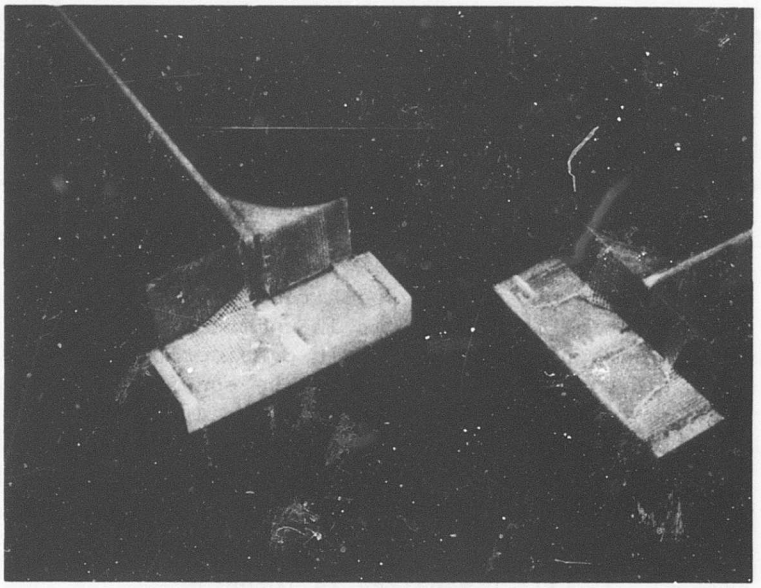

Figure 48. Orthogonal Joint With Narmco 227 Adhesive After Testing.

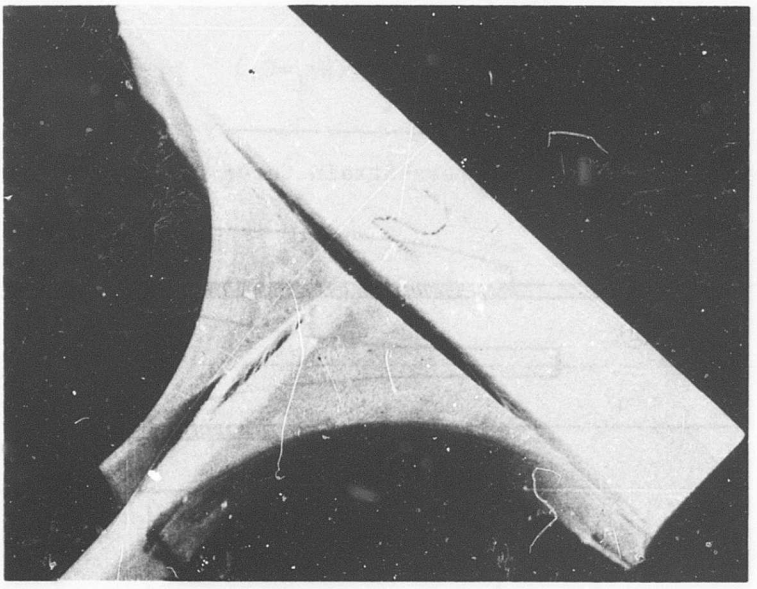

Figure 49. Orthogonal Joint With Epoxy-Polyamide Adhesive After Testing.

LAP JOINT

The lap joint is one of the most important types of joints, especially in structures of composite materials, where the use of rivets and bolts is not advisable.

The correct design of lap joints requires an understanding of the mechanism for load transfer from one part to the other through the adhesive. The shear stress distribution was analyzed in References 1 through 4 under the assumption of linear, perfectly elastic behavior of both adhesive and adherent. This study shows that the shear stress concentration is very high for the joint dimensions usually required by the technical applications. On the other hand, most of the adhesives in common use exhibit a nonlinear stress-strain relationship, and may sustain considerable strain before failure. The behavior of the adhesive can still be considered perfectly elastic, in the sense that no residual deformation remains after the unloading, even from stress levels approaching the failure stress. A typical stress-strain curve for an adhesive is shown in Figure 50. A convenient analytical expression for such curve is:

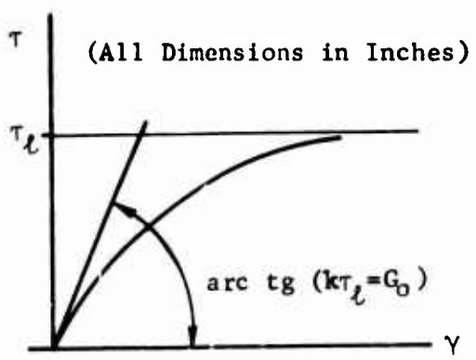

Figure 50. Typical Stress-Strain Curve for the Adhesive.

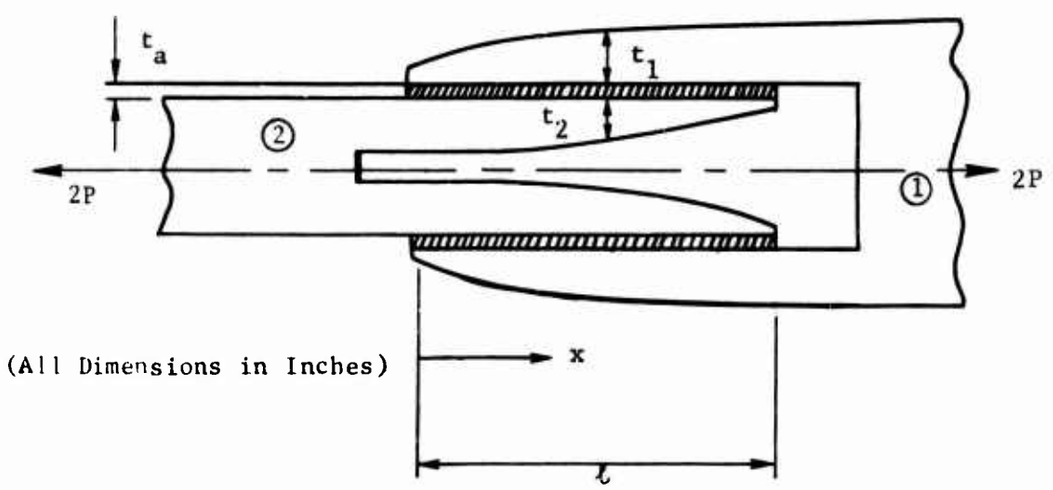

Figure 51. Lap Joint General Nomclature.

$$\tau = \tau_{\ell}\left(1-e^{-k\gamma}\right), \tag{2}$$

where τ_{ℓ} and k are constant. The initial shear modulus G_o is

$$G_o = \left(\frac{d\tau}{d\gamma}\right)_{\gamma = 0} = k\tau_{\ell} \tag{3}$$

Let us consider the lap joint shown in Figure 51. Applying the equilibrium condition to the section depicted in Figure 52,

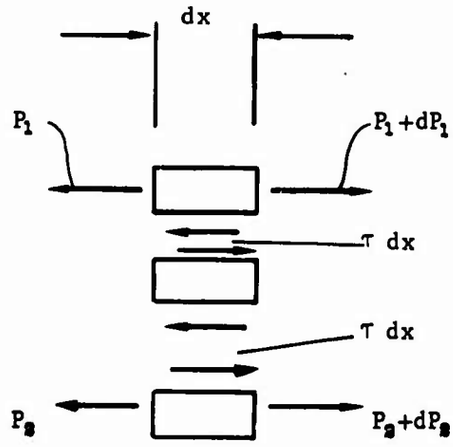

Figure 52. Infinitesimal Element.

the following equations are obtained:

$$\tau = \frac{dP_1}{dx}\ , \quad P_1+P_2 = P = \text{constant} \tag{4}$$

The shear deformation in the adhesive is

$$\gamma = \frac{u_1 - u_2}{t_a} \tag{5}$$

where u_1 and u_2 are displacements of the two adherends.

Differentiating γ of equation (5) with respect to x, the following relation is obtained.

$$\epsilon_1 - \epsilon_2 = t_a \frac{d\gamma}{dx} \tag{6}$$

Assuming Hooke's law to be valid in the adherend,

$$\varepsilon_1 = \frac{P_1}{E_1 t_1} , \quad \varepsilon_2 = \frac{P_2}{E_2 t_2} , \tag{7}$$

equation (6) can be rephrased

$$\frac{P_1}{E_1 t_1} - \frac{P_2}{E_2 t_2} = t_a \frac{d\gamma}{dx} \tag{8}$$

Differentiating (8) with respect to x and applying equations (4), we find

$$\tau(\gamma) = \frac{1}{\left(\frac{1}{t_1 E_1} + \frac{1}{t_2 E_2}\right)^2} \left[\left(\frac{1}{t_1 E_1} + \frac{1}{t_2 E_2}\right) \left(t_a \frac{d^2\gamma}{dx^2} + \frac{P}{E_2} \frac{d}{dx}\left(\frac{1}{t_2}\right) \right) \right.$$

$$\left. - \left(t_a \frac{d\gamma}{dx} + \frac{P}{t_2 E_2} \right) \frac{d}{dx} \left(\frac{1}{t_1 E_1} + \frac{1}{t_2 E_2} \right) \right] \tag{9}$$

If, in particular, t_1 and t_2 are constant, this equation becomes the familiar expression for the double straight-lap joint:

$$\tau(\gamma) = \frac{t_a}{\frac{1}{t_1 E_1} + \frac{1}{t_2 E_2}} \frac{d^2\gamma}{dx^2} \tag{10}$$

Finally, introducing the definition (2), a nonlinear differential equation in γ is obtained:

$$\frac{d^2\gamma}{dx^2} = \tau_\ell \left(1 - e^{-k\gamma}\right) \frac{\frac{1}{t_1 E_1} + \frac{1}{t_2 E_2}}{t_a} \tag{11}$$

Equation (11) is a nonlinear differential equation of the form

$$\gamma'' = f(\gamma)$$

and will be integrated numerically. The boundary conditions are

$$\left(P_1\right)_{x=0} = 0 \ , \left(P_1\right)_{x=\ell} = P$$

or, from equations (4) and (8),

$$\left(\frac{d\gamma}{dx}\right)_{x=o} = -\frac{P}{t_a t_a E}, \quad \left(\frac{d\gamma}{dx}\right)_{x=\ell} = \frac{P}{t_1 t_a E} \tag{12}$$

Therefore, the problem of finding the shear stress distribution in a lap joint with nonlinear adhesive requires the solution of the differential equation (11) with the boundary conditions (12).

The function that solves the differential equation (11) has the form shown in Figure 53. The values γ_o' and γ_ℓ' of the derivatives at the ends are known (equations (12)), but the values γ_o and γ_ℓ are not. This problem must be solved using a trial-and-error method.

Let us assume certain initial values $\gamma_{\ell/2}^{(1)}$ and $\gamma_{\ell/2}^{'(1)}$ for the function γ and its derivative in $x = \frac{\ell}{2}$. Applying the Runge-Kutta formulas to equations (11), the strains and their derivatives are found at the ends; i.e.,

$$\gamma_{\ell/2}^{(1)}, \gamma_{\ell/2}^{'(1)} \xrightarrow{\text{Runge-Kutta}} \gamma_o^{(1)}, \gamma_o^{'(1)}, \gamma_\ell^{(1)}, \gamma_\ell^{'(1)} \tag{13}$$

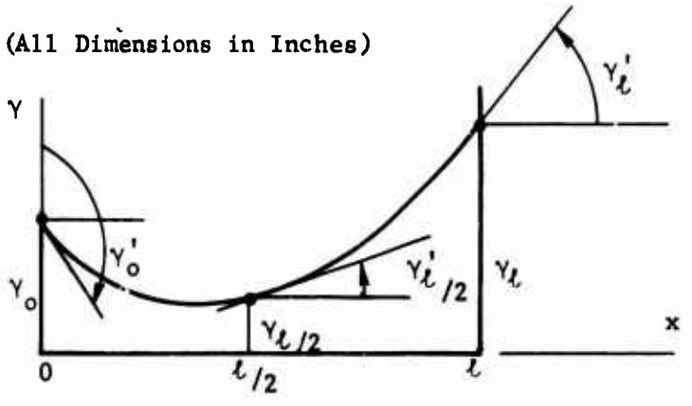

Figure 53. γ as Function of x.

Incrementing the values of $\gamma_{\ell/2}^{(1)}$ and $\gamma_{\ell/2}^{'(1)}$ by $\Delta\gamma_{\ell/2}^{(1)}$ and $\Delta\gamma_{\ell/2}^{'(1)}$, respectively, the effects of these increments on the end values can be determined:

$$\gamma_{\ell/2}^{(1)} + \Delta\gamma_{\ell/2}^{(1)} \;,\; \gamma_{\ell/2}^{'(1)} \xrightarrow{\text{Runge-Kutta}} \gamma_{o\gamma}^{'(1)} \;,\; \gamma_{o\gamma}^{(1)} \;,\; \gamma_{\ell\gamma}^{(1)} \;,\; \gamma_{\ell\gamma}^{'(1)}$$

$$\gamma_{\ell/2}^{(1)} \;,\; \gamma_{\ell/2}^{'(1)} + \Delta\gamma_{\ell/2}^{'(1)} \xrightarrow{\text{Runge-Kutta}} \gamma_{o\gamma}^{(1)} \;,\; \gamma_{o\gamma'}^{'(1)} \;,\; \gamma_{\ell\gamma'}^{(1)} \;,\; \gamma_{\ell\gamma'}^{'(1)} \tag{14}$$

With the results of equations (13) and (14), the following pa tial derivatives can be computed approximately:

$$\frac{\partial\gamma_o'}{\partial\gamma_{\ell/2}} \doteq \frac{\gamma_{o\gamma}^{'(1)} - \gamma_o^{'(1)}}{\Delta\gamma_{\ell/2}} \;,\; \frac{\partial\gamma_o'}{\partial\gamma_{\ell/2}'} \doteq \frac{\gamma_{o\gamma'}^{'(1)} - \gamma_o^{'(1)}}{\Delta\gamma_{\ell'/2}}$$

$$\frac{\partial\gamma_\ell'}{\partial\gamma_{\ell/2}} \doteq \frac{\gamma_{\ell\gamma}^{'(1)} - \gamma_\ell^{'(1)}}{\Delta\gamma_{\ell/2}} \frac{\partial\gamma_\ell'}{\partial\gamma_{\ell/2}'} \doteq \frac{\gamma_{\ell\gamma'}^{'(1)} - \gamma_\ell^{'(1)}}{\Delta\gamma_{\ell/2}'} \tag{15}$$

On the other hand, the increments of the end values γ_o' and γ_ℓ' are related to the increments of the starting values by the relations

$$\Delta\gamma_o' = \frac{\partial\gamma_o'}{\partial\gamma_{\ell/2}}\Delta\gamma_{\ell/2} + \frac{\partial\gamma_o'}{\partial\gamma_{\ell/2}'}\Delta\gamma_{\ell/2}'$$

$$\Delta\gamma_\ell' = \frac{\partial\gamma_\ell'}{\partial\gamma_{\ell/2}}\Delta\gamma_{\ell/2} + \frac{\partial\gamma_\ell'}{\partial\gamma_{\ell/2}'}\Delta\gamma_{\ell/2}' \tag{16}$$

By taking

$$\gamma_o' - \gamma_o^{'(1)} = \Delta\gamma_o^{'(1)} \;,\; \gamma_\ell' - \gamma_\ell^{'(1)} = \Delta\gamma_\ell^{'(1)} \tag{17}$$

and combining with equations (16), we have

$$\frac{\partial\gamma_o'}{\partial\gamma_{\ell/2}}\Delta\gamma_{\ell/2} + \frac{\partial\gamma_o'}{\partial\gamma_{\ell/2}'}\Delta\gamma_{\ell/2}' = \gamma_o^{'(1)} - \gamma_o'$$

$$\frac{\partial\gamma_\ell'}{\partial\gamma_{\ell/2}}\Delta\gamma_{\ell/2} + \frac{\partial\gamma_\ell'}{\partial\gamma_{\ell/2}'}\Delta\gamma_{\ell/2}' = \gamma_\ell^{'(1)} - \gamma_\ell' \tag{18}$$

Once the partial derivatives are computed using equations (15), the system (18) can be solved for the increments $\Delta\gamma_{\ell/2}$ and $\Delta\gamma'_{\ell/2}$. With these values, the improved starting values can be obtained:

$$\gamma^{(2)}_{\ell/2} = \gamma^{(1)}_{\ell/2} + \Delta\gamma_{\ell/2} \quad , \quad \gamma'^{(2)}_{\ell/2} = \gamma'^{(1)}_{\ell/2} + \Delta\gamma'_{\ell/2}$$

and the process is repeated. New increments $\Delta\gamma^{(2)}_{\ell/2}$ and $\Delta\gamma'^{(2)}_{\ell/2}$ are adopted, the partial derivatives (15) are computed and the system (18) is solved for $\Delta\gamma_{\ell/2}$ and $\Delta\gamma'_{\ell/2}$. The process is considered complete when the error in the satisfaction of the boundary conditions is smaller than some value $\bar{e}$. The function $\tau(x)$ is then obtained by substitution of $\gamma(x)$ into equation (2).

Figure 54 shows the stress diagrams corresponding to a lap joint with $t_1 = t_2 = 0.0625$ in., $t_a = 0.004$, $\ell = 1.0$ in. The adhesive stress-strain relationship is

$$\tau(\gamma) = 5000\ (1-e^{-36\gamma})\ \text{psi},$$

which corresponds to an initial modulus

$$(G)_{\gamma=0} = k\tau_{\ell} = 0.18 \times 10^{6}\ \text{psi}.$$

From inspection of the curves, it can be noted that the stress concentrations at the ends decrease when the load is increased. This is due to the non-linear behavior of the adhesive.

The ultimate load of the joint can be evaluated if a design ultimate distortion γ_{ult} of the adhesive is specified. For example, for $\gamma_{ult} = 0.04$, the ultimate load would be $P \cong 1000$ lb.

Figure 55 shows the stress diagrams corresponding to a joint with a double thickness of adhesive ($t_a = 0.008$ in.). It can be observed that the stress concentrations are decreased below those for the single-thickness adhesive.

Figures 56 and 57 show the stress diagrams corresponding to two lap-joint combinations. In both, one adherent is a glass-epoxy composite while the other is either aluminum or steel. In these cases, the stress diagrams are not symmetric with respect to $x = \frac{\ell}{2}$.

Four lap-joint specimens were fabricated and tested. Figure 58 shows these joints. Figure 59 shows one of them after testing. Table II indicates the test results:

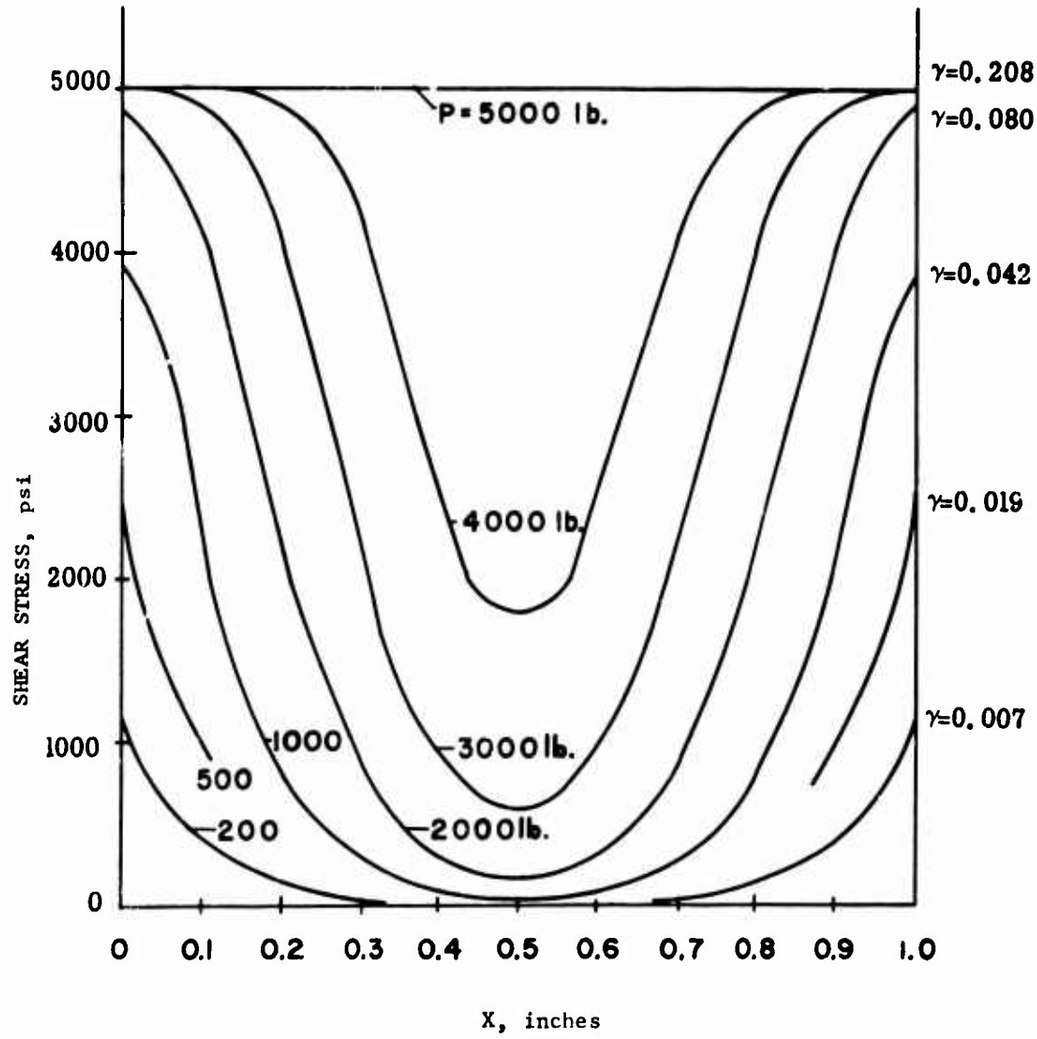

Figure 54. Effect of Bond-Line Thickness t_a on Adhesive Shear Stress Distributions, t_a = 0.004 inch, $E_1 = E_2 = 10 \times 10^6$ psi, $t_1 = t_2$ = 0.0625 inch, ℓ = 1.0 inch, τ_ℓ = 5,000 psi, k = 36.

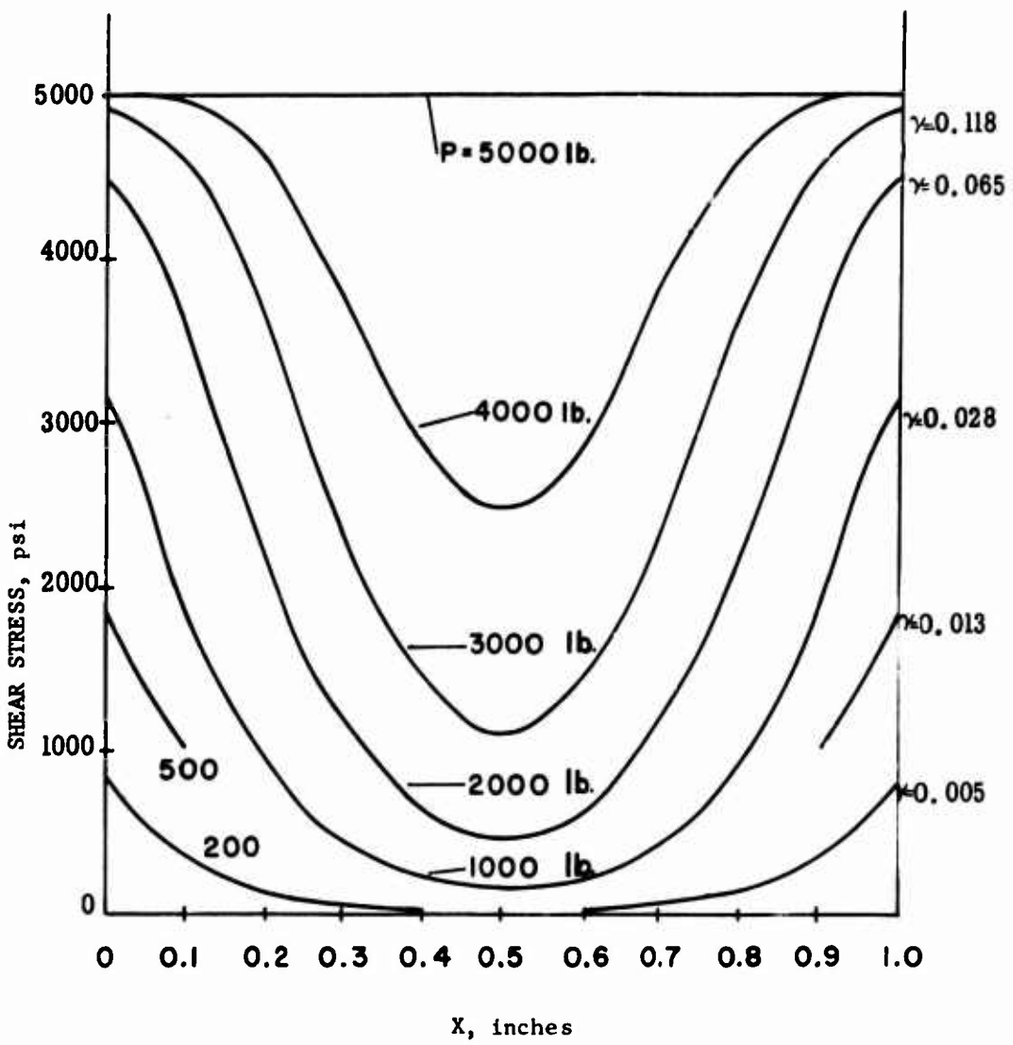

Figure 55. Effect of Bond-Line Thickness t_a on Adhesive Shear Stress Distributions, t_a = 0.008 inch, $E_1 = E_2 = 10 \times 10^6$ psi, $t_1 = t_2$ = 0.0625 inch, ℓ = 1.0 inch, τ_ℓ = 5,000 psi, k = 36.

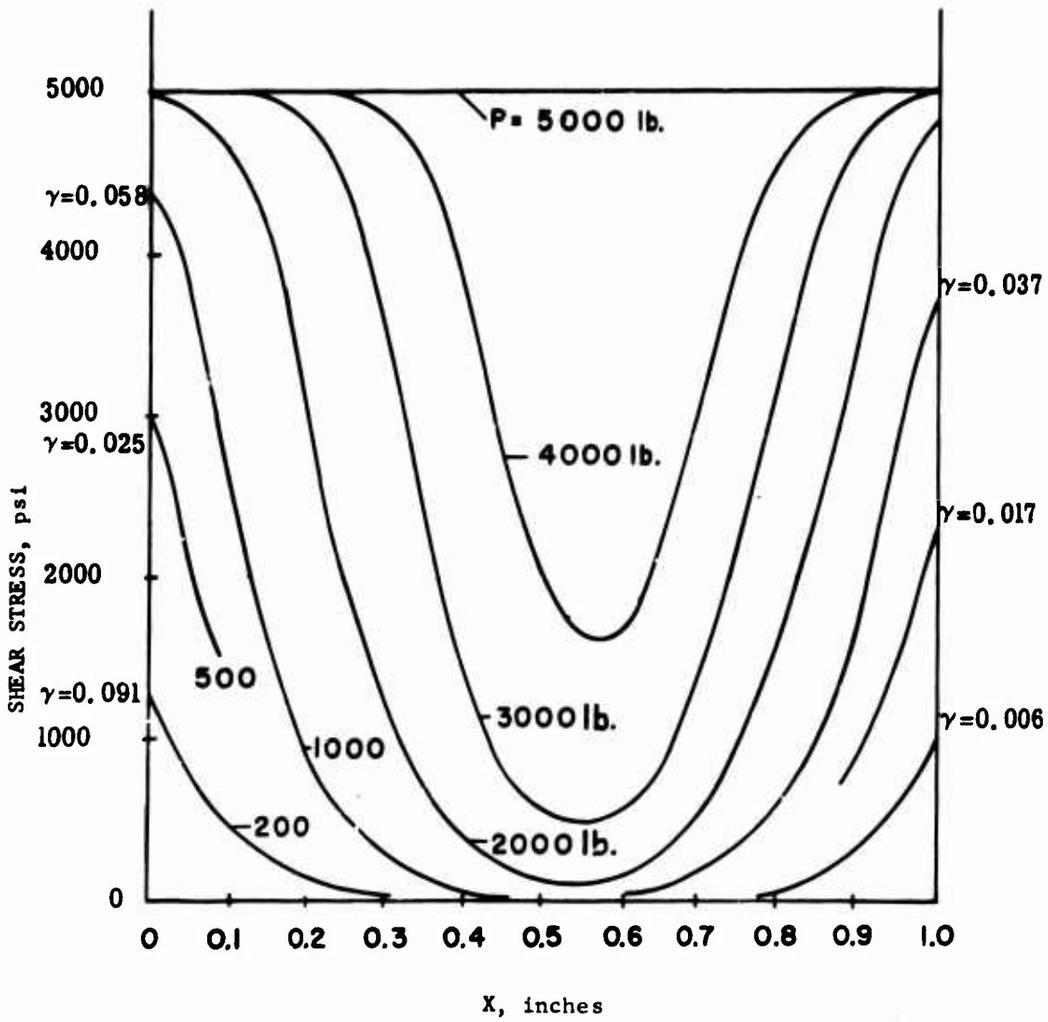

Figure 56. Effect of Doubler Modulus E_1 on Adhesive Shear Stress Distributions, E_1 = 10 x 10^6 psi (Aluminum), E_2 = 7 x 10^6 psi, $t_1 = t_2$ = 0.0625 inch, t_a = 0.004 inch, ℓ = 1.0 inch, τ_ℓ = 5,000 psi, k = 36.

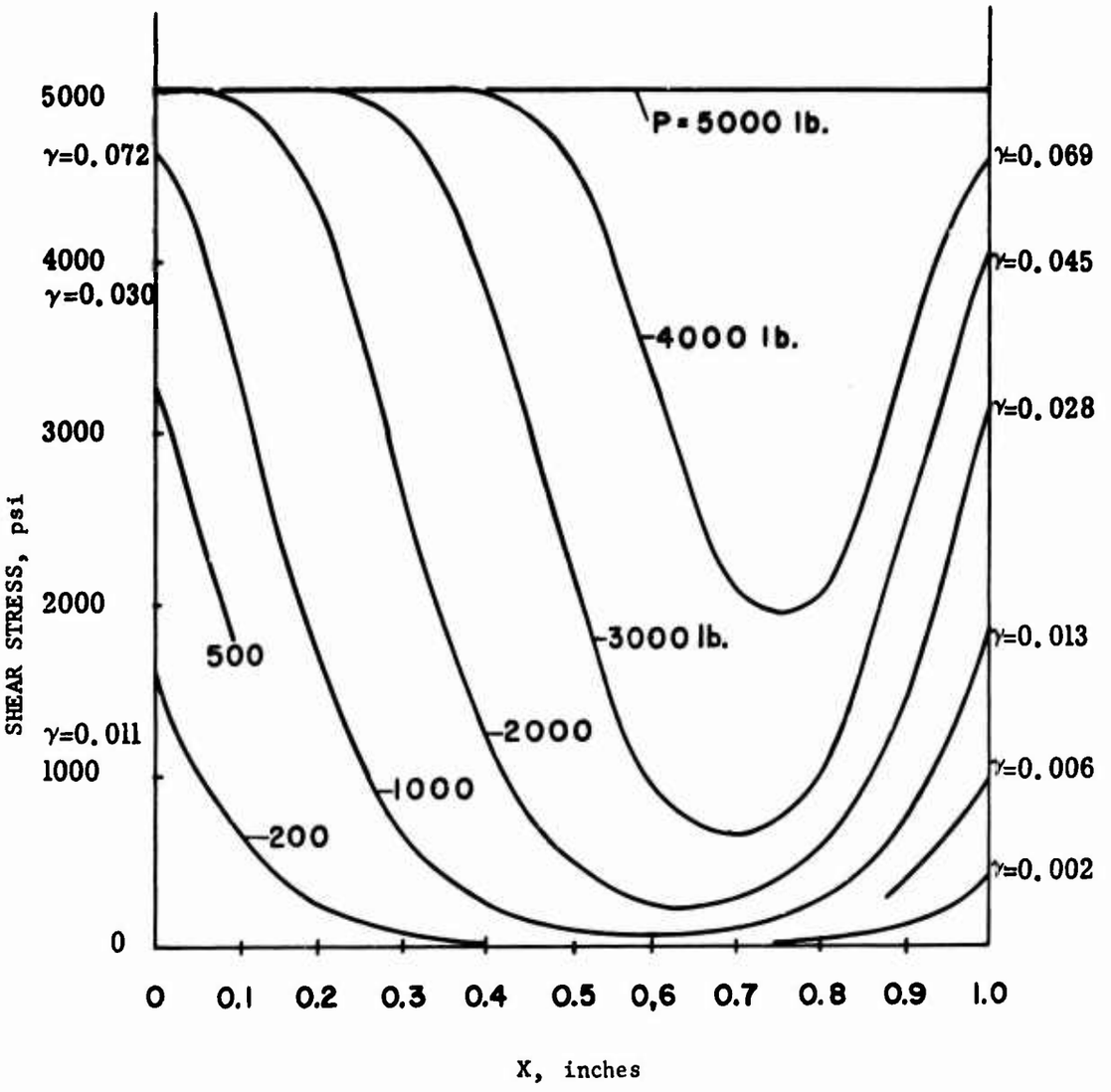

Figure 57. Effect of Doubler Modulus E_1 on Adhesive Shear Stress Distributions, $E_1 = 30 \times 10^6$ psi (Steel) $E_2 = 7 \times 10^6$ psi, $t_1 = t_2 = 0.0625$ inch, $t_a = 0.004$ inch, $\ell = 1.0$ inch, $\tau_\ell = 5{,}000$ psi, k = 36.

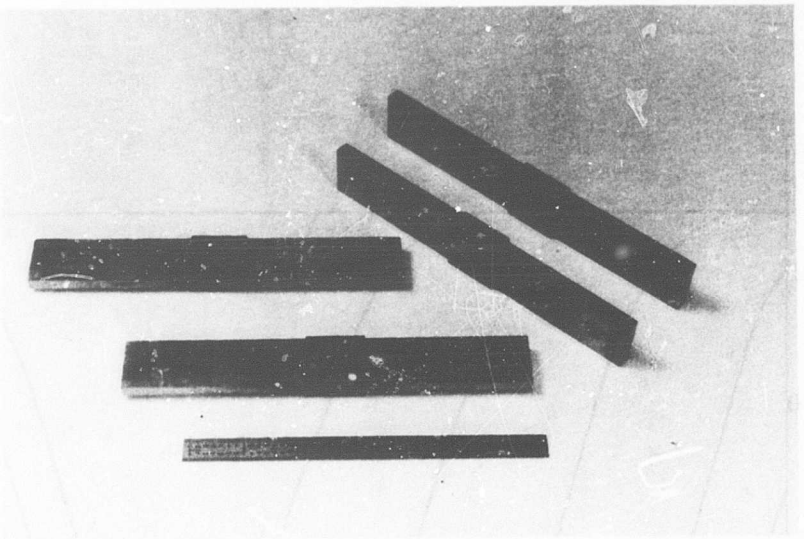

Figure 58. Titanium-Boron/Epoxy Straight-Lap Joints. Configurations Completed.

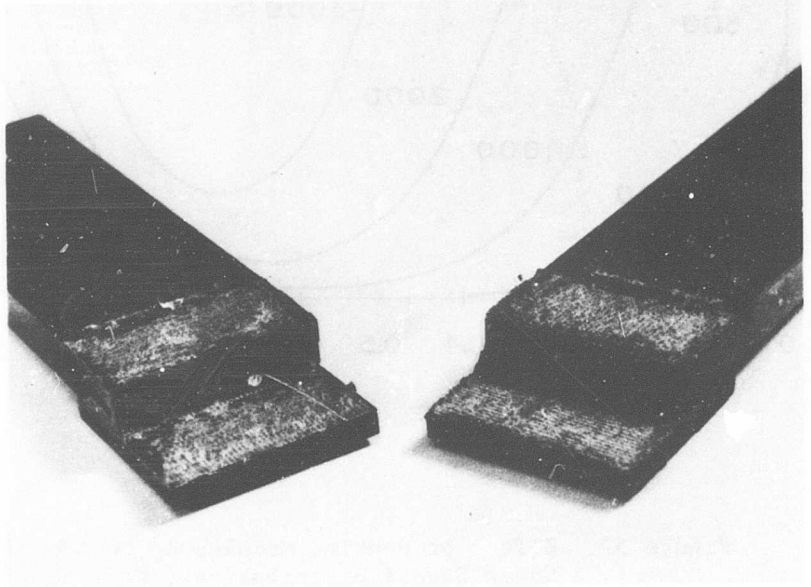

Figure 59. Failure in Straight-Lap Titanium-Titanium Joint.

TABLE II

ADHESIVE LAP-JOINT TEST RESULTS

Specimen	Failure Load (lb)	Average Failure Stress (psi)
1	5010	5010
2	5435	5435
3	5780	5780
4	4095	4095

PHOTOELASTIC TEST RESULTS

In order to evaluate stress concentrations in bolted joints, photoelastic models were prepared and tested. Figures 60a through 60h show the isochromatic lines and the isoclines (0°, 15°, 30°, 45°, 60°, 75°, 90°) obtained in a bolted joint under tension. It can be observed from the position of the isoclines that the polar shear stress $\tau_{r\theta}$ is very small. This result is coincident with that obtained through finite-element analysis.

Figures 61 and 62 show the isochromatic lines in a transparent isotropic model and in the corresponding orthogonal joint made from composite material. In the latter, it is possible to observe the adhesive bond lines.

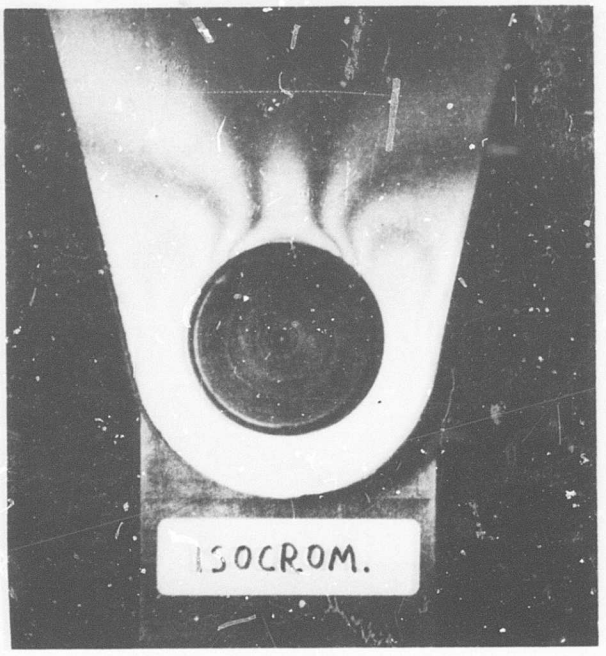

Figure 60a. Photoelastic Model of a Bolted Joint Loaded in Tension; Isochromatics.

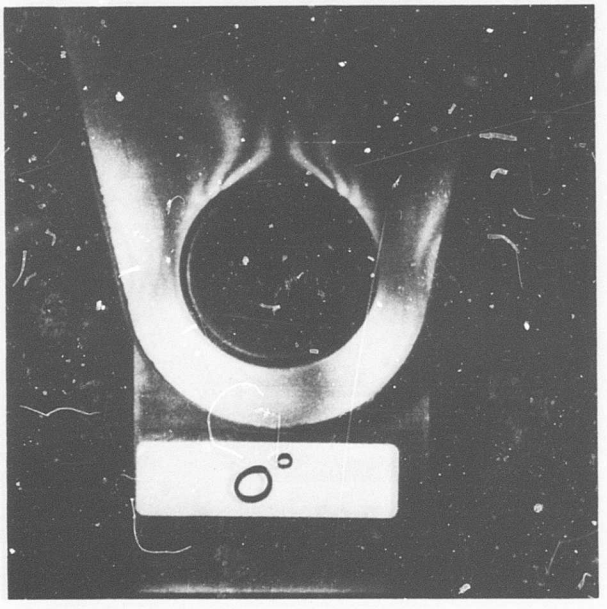

Figure 60b. Photoelastic Model of a Bolted Joint Loaded in Tension; 0° Isoclines.

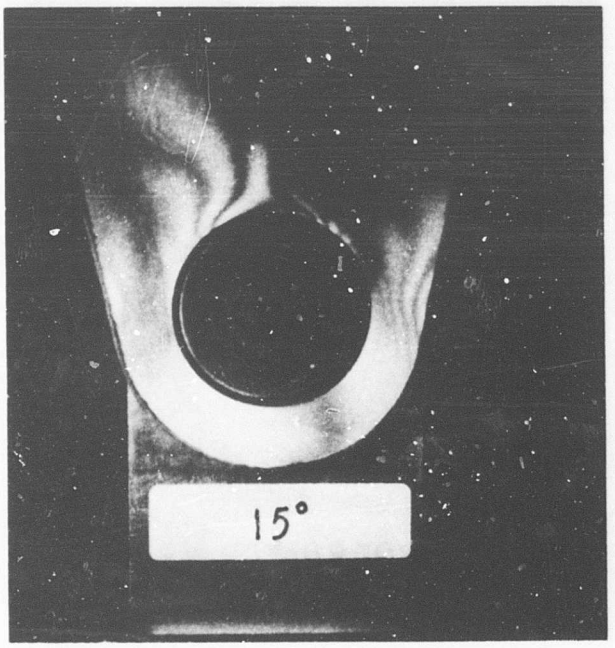

Figure 60c. Photoelastic Model of a Bolted Joint Loaded in Tension; 15° Isoclines.

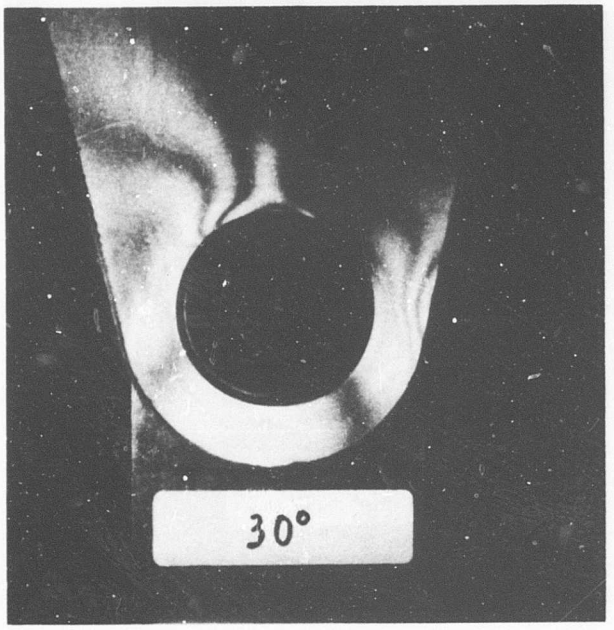

Figure 60d. Photoelastic Model of a Bolted Joint Loaded in Tension; 30° Isoclines.

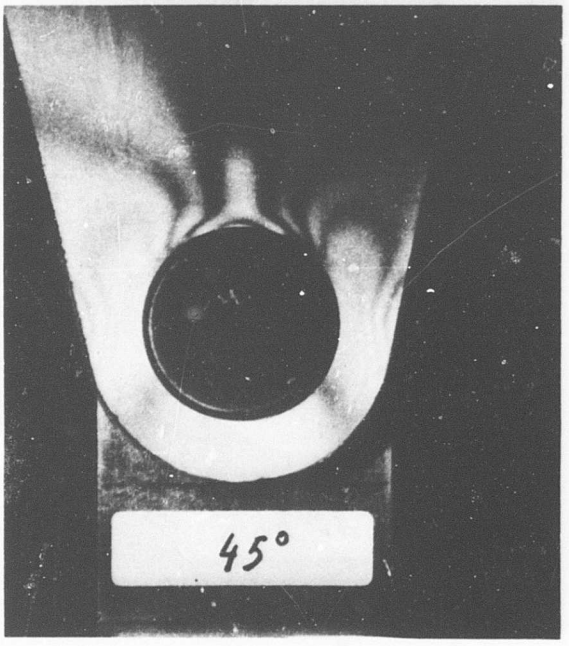

Figure 60e. Photoelastic Model of a Bolted Joint Loaded in Tension; 45° Isoclines.

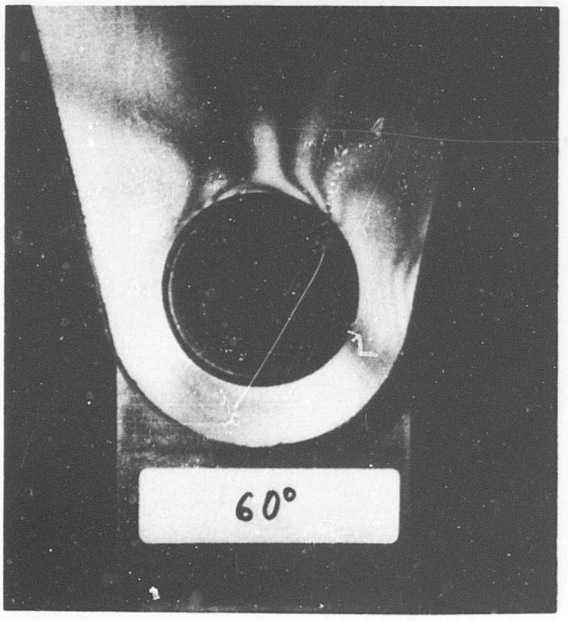

Figure 60f. Photoelastic Model of a Bolted Joint Loaded in Tension; 60° Isoclines.

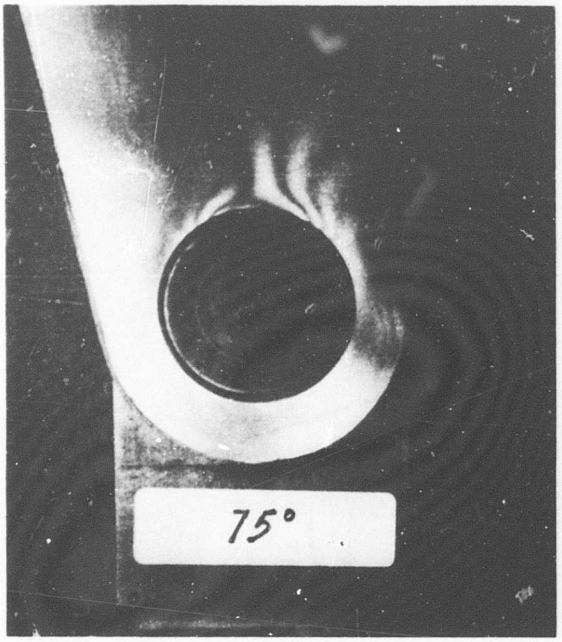

Figure 60g. Photoelastic Model of a Bolted Joint Loaded in Tension; 75° Isoclines.

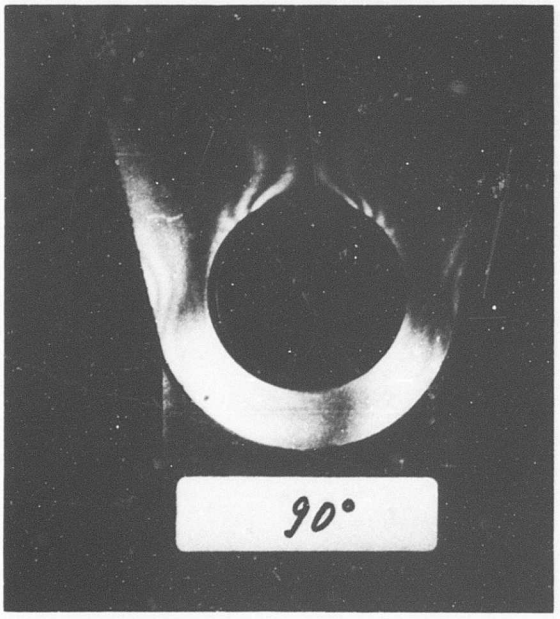

Figure 60h. Photoelastic Model of a Bolted Joint Loaded in Tension; 90° Isoclines.

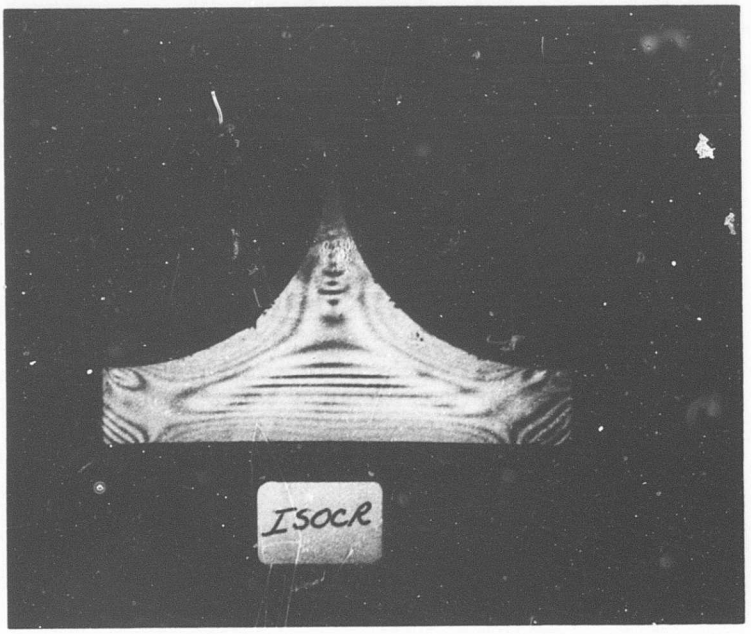

Figure 61. Orthogonal Joint Loaded in Tension; Transparent Model.

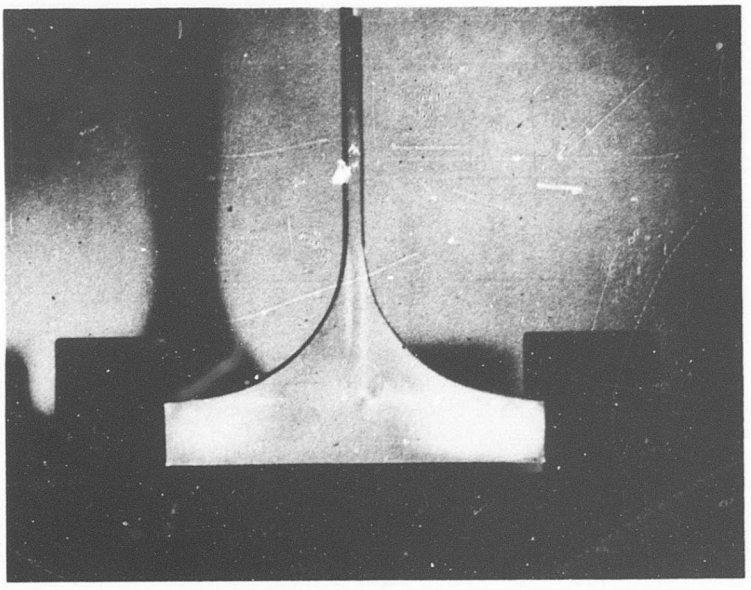

Figure 62. Orthogonal Joint Loaded in Tension; Composite Material (Coated).

FINITE-ELEMENT METHOD FOR STRESS ANALYSIS OF JOINTS IN ANISOTROPIC MATERIALS

In a previous study, a computer program for the stress analysis of anisotropic joints was presented. The displacement field in a triangular element was assumed linear, or, equivalently, the stress field was assumed constant.

In order to improve the accuracy of the results, a new program was developed, based on the assumption of quadratic displacements functions. These functions permit linear variation of stresses along each element. In this way it is possible to calculate the stress at a node of the triangular net simply by averaging the stresses corresponding to each triangle whose vertex is at the node. This operation is performed automatically by the program. The accuracy of the stresses obtained by this averaging process is highly satisfactory, even on the boundaries. Figure 63 represents the basic triangular element referred to the local axis ξ, η.

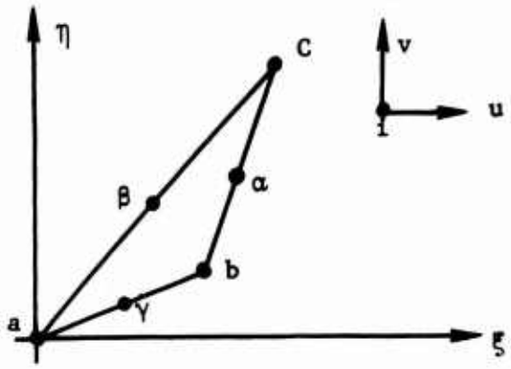

Figure 63. Basic Triangular Element.

The coordinates of the middle points α, β, γ are obtained from

$$\xi_\alpha = \frac{\xi_b + \xi_c}{2} \quad , \quad \eta_\alpha = \frac{\eta_b + \eta_c}{2}$$

$$\xi_\beta = \frac{\xi_c + \xi_a}{2} \quad , \quad \eta_\beta = \frac{\eta_c + \eta_a}{2} \qquad (19)$$

$$\xi_\gamma = \frac{\xi_a + \xi_b}{2} \quad , \quad \eta_\gamma = \frac{\eta_a + \eta_b}{2}$$

Thus, only the vertex coordinates need be introduced as inputs.

The displacement field in the triangular element is assumed to be given by the quadratic functions

$$u = a_1 + a_2\xi + a_3\eta + a_4\xi^2 + a_5\xi\eta + a_6\eta^2$$

$$v = a_7 + a_8\xi + a_9\eta + a_{10}\xi^2 + a_{11}\xi\eta + a_{12}\eta^2 \qquad (20)$$

where a_1 through a_{12} are constants.

Let's introduce the vectors $\{\delta\}$ and $\{a\}$ by the expressions

$$\begin{aligned}\{\delta\} &= \{u_a \;\; u_b \;\; u_c \;\; u_\alpha \;\; u_\beta \;\; u_\gamma \;\; v_a \;\; v_b \;\; v_c \;\; v_\alpha \;\; v_\beta \;\; v_\gamma\} \\ \{a\} &= \{a_1 \;\; a_2 \;\; a_3 \;\; a_4 \;\; a_5 \;\; a_6 \;\; a_7 \;\; a_8 \;\; a_9 \;\; a_{10} \;\; a_{11} \;\; a_{12}\}\end{aligned} \tag{21}$$

Through use of equation (20), a relationship between $\{\delta\}$ and $\{a\}$ can be written:

$$\{\delta\} = [A]\{a\} \tag{22}$$

with

$$[A] = \begin{bmatrix} [A^*] & [0] \\ [0] & [A^*] \end{bmatrix} \; ; \; [A^*] = \begin{bmatrix} 1 & 0 & 0 & 0 & 0 & 0 \\ 1 & \xi_b & \eta_b & \xi_b^2 & \xi_b\eta_b & \eta_b^2 \\ 1 & \xi_c & \eta_c & \xi_c^2 & \xi_c\eta_c & \eta_c^2 \\ 1 & \xi_\alpha & \eta_\alpha & \xi_\alpha^2 & \xi_\alpha\eta_\alpha & \eta_\alpha^2 \\ 1 & \xi_\beta & \eta_\beta & \xi_\beta^2 & \xi_\beta\eta_\beta & \eta_\beta^2 \\ 1 & \xi_\gamma & \eta_\gamma & \xi_\gamma^2 & \xi_\gamma\eta_\gamma & \eta_\gamma^2 \end{bmatrix} \tag{23}$$

From equations (22) and (23), the coefficients a_i are determined immediately:

$$\{a\} = [A]^{-1}\{\delta\} \;\; , \;\; [A]^{-1} = \begin{bmatrix} [A^*]^{-1} & [0] \\ [0] & [A^*] \end{bmatrix} \tag{24}$$

The strains in the element are:

$$\epsilon_x = \frac{\partial u}{\partial \xi} \; , \; \epsilon_y = \frac{\partial v}{\partial \eta} \; , \; \gamma_{xy} = \frac{\partial u}{\partial \eta} + \frac{\partial v}{\partial \xi} \; ,$$

or, taking into account equations (20),

$$\begin{aligned}\epsilon_x &= a_2 + 2\,a_4\xi + a_5\eta \\ \epsilon_y &= a_9 + 2\,a_{11}\xi + a_{12}\eta \\ \gamma_{xy} &= a_3 + a_5\,\xi + 2\,a_6\eta + a_8 + 2\,a_{10}\xi + a_{11}\eta\end{aligned} \tag{25}$$

For an anisotropic material, the stress-strain relationship is expressed as:

$$\sigma_x = C_{11}\epsilon_x + C_{12}\epsilon_y + C_{13}\gamma_{xy}$$

$$\sigma_y = C_{12}\epsilon_x + C_{22}\epsilon_y + C_{23}\gamma_{xy} \qquad (26)$$

$$\tau_{xy} = C_{33}\gamma_{xy} + C_{13}\epsilon_x + C_{23}\epsilon_y$$

The strain energy for the element, using equations (25) and (26), becomes:

$$\begin{aligned} W = \tfrac{1}{2}\iint t \Big\{ & C_{11}\left(a_2^2 + 4a_4^2\xi^2 + a_5^2\eta^2 + 4a_2a_4\xi + 2a_2a_5\eta + 4a_4a_5\xi\eta\right) \\ & + 2C_{12}\left(a_2a_9 + a_2a_{11}\xi + 2a_2a_{12}\eta + 2a_4a_9\xi + 2a_4a_{11}\xi^2\right. \\ & \qquad \left. + 4a_4a_{12}\xi\eta + a_5a_9\eta + a_5a_{11}\xi\eta + 2a_5a_{12}\eta^2\right) \\ & + 2C_{13}\left(a_2a_3 + a_2a_5\xi + 2a_2a_5\eta + a_2a_8 + 2a_2a_{10}\xi + a_2a_{11}\eta\right. \\ & \qquad + 2a_3a_4\xi + 2a_4a_5\xi^2 + 4a_4a_6\xi\eta + a_4a_8\xi + 4a_4a_{10}\xi^2 \\ & \qquad + 2a_4a_{11}\xi\eta + a_3a_5\eta + a_5^2\xi\eta + 2a_5a_6\eta^2 + a_5a_8\eta + 2a_5a_{10}\xi\eta \\ & \qquad \left. + a_5a_{11}\eta^2\right) \\ & + 2C_{22}\left(a_9^2 + a_{11}^2\xi^2 + 4a_{12}^2\eta^2 + 2a_9a_{11}\xi + 4a_9a_{12}\eta + 4a_{11}a_{12}\xi\eta\right) \\ & + 2C_{23}\left(a_3a_9 + a_5a_9\xi + 2a_6a_9\eta + a_8a_9 + 2a_9a_{10}\xi + a_9a_{11}\eta + a_3a_{11}\xi\right. \\ & \qquad + a_5a_{11}\xi^2 + 2a_6a_{11}\xi\eta + a_8a_{11}\xi + 2a_{10}a_{11}\xi^2 + a_{11}^2\xi\eta \\ & \qquad + 2a_3a_{12}\eta + 2a_5a_{12}\xi\eta + 4a_5a_{12}\eta^2 + 2a_8a_{12}\eta + 4a_{10}a_{12}\xi\eta \\ & \qquad \left. + 2a_{11}a_{12}\eta^2\right) \end{aligned} \qquad (27)$$

$$+ C_{33}\Big(a_3^2 + a_5^2\xi^2 + 4a_6^2\eta^2 + a_8^2 + 4a_{10}^2\xi^2 + a_{11}^2\eta^2 + 2a_3a_5\xi$$
$$+ 4a_3a_6\eta + 2a_3a_8 + 4a_3a_{10}\xi + 2a_3a_{11}\eta + 4a_5a_6\xi\eta$$
$$+ 2a_5a_8\xi + 4a_5a_{10}\xi^2 + 2a_5a_{11}\xi\eta + 4a_6a_8\eta + 8a_6a_{10}\xi\eta$$
$$+ 4a_6a_{11}\eta^2 + 4a_8a_{10}\xi + 2a_8a_{11}\eta + 4a_{10}a_{11}\xi\eta\Big)\Big\}\, d\xi d\eta$$

The variation of the thickness t is assumed to be linear in the element. Thus,

$$t = T_1\xi + T_2\eta + T_0 \,, \tag{28}$$

where the constants T_1, T_2 and T_0 can be found from the thicknesses t_a, t_b, t_c at the three vertices:

$$T_1 = -\frac{\Delta_\xi}{\Delta_t} \,, \quad T_2 = -\frac{\Delta_\eta}{\Delta_t} \,, \quad T_0 = \frac{\Delta}{\Delta_t} \tag{29}$$

$$\Delta_\xi = \begin{vmatrix} 0 & t_a & 1 \\ \eta_b & t_b & 1 \\ \eta_c & t_c & 1 \end{vmatrix}, \quad \Delta_\eta = \begin{vmatrix} t_a & 0 & 1 \\ t_b & \xi_b & 1 \\ t_c & \xi_c & 1 \end{vmatrix}, \quad \Delta_t = \begin{vmatrix} 0 & 0 & 1 \\ \xi_b & \eta_b & 1 \\ \xi_c & \eta_c & 1 \end{vmatrix}, \quad \Delta = \begin{vmatrix} 0 & 0 & t_a \\ \xi_b & \eta_b & t_b \\ \xi_c & \eta_c & t_c \end{vmatrix}$$

The equations of the sides of the triangular element depicted in Figure 64 can be written as:

$$R_1): \eta = m_1\xi \;;\; m_1 = \frac{\eta_b}{\xi_b}$$
$$R_2): \eta = m_2\xi \;;\; m_2 = \frac{\eta_c}{\xi_c} \tag{30}$$
$$R_3): \eta = m_3\xi + b_3;\; m_3 = \frac{\eta_c - \eta_b}{\xi_c - \xi_b} \,,\; b_3 = \eta_b - m_3\xi_b$$

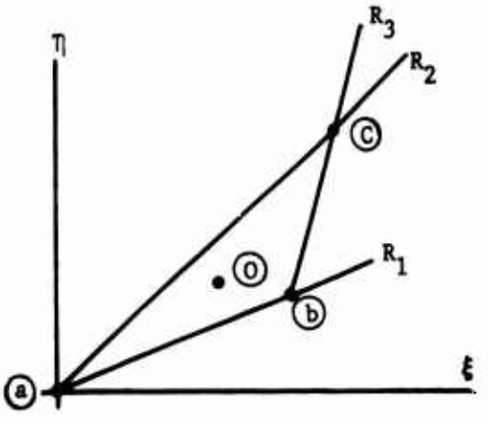

Figure 64. Triangular Element.

Let's define now the following integrals, which will be used to express the strain energy:

$$\gamma_0 = \iint d\xi\, d\eta = \tfrac{1}{2}\left(\xi_b\eta_c - \xi_c\eta_b\right)$$

$$\gamma_1 = \iint \xi\, d\xi\, d\eta = \gamma_0\xi_0$$

$$\gamma_2 = \iint \eta\, d\xi\, d\eta = \gamma_0\eta_0$$

$$\gamma_3 = \iint \xi^2 d\xi\, d\eta = \left(m_2 - m_1\right)\frac{\xi_b^4}{4} + \frac{m_2 - m_3}{4}\left(\xi_c^4 - \xi_b^4\right) - \frac{b_3}{3}\left(\xi_c^3 - \xi_b^3\right)$$

$$\gamma_4 = \iint \eta^2 d\xi\, d\eta = \left(m_2^3 - m_1^3\right)\frac{\xi_c^4}{12} + \frac{m_2^3}{12}\left(\xi_c^4 - \xi_b^4\right) - \frac{1}{12m_3}\left[\left(m_3\xi_c + b_3\right)^4 - \left(m_3\xi_b + b_3\right)^4\right]$$

$$\gamma_5 = \iint \xi\eta\, d\xi\, d\eta = \left(m_2^2 - m_1^2\right)\frac{\xi_b^4}{8} + \frac{m_2^2}{8}\left(\xi_c^4 - \xi_b^4\right) - \frac{1}{8m_3^2}\left[\left(m_3\xi_c + b_3\right)^4 - \left(m_3\xi_b + b_3\right)^4\right] + \frac{b_3}{6m_3^2}\left[\left(m_3\xi_c + b_3\right)^3 - \left(m_3\xi_b + b_3\right)^3\right]$$

$$\gamma_6 = \iint \xi^3 d\xi\, d\eta = \left(m_2 - m_1\right)\frac{\xi_b^5}{5} + \frac{m_2 - m_3}{5}\left(\xi_c^5 - \xi_b^5\right) - \frac{b_3}{4}\left(\xi_c^4 - \xi_b^4\right)$$

$$\gamma_7 = \iint \xi^2\eta\, d\xi\, d\eta = \left(m_2^2 - m_1^2\right)\frac{\xi_b^5}{10} + \frac{m_2^2}{10}\left(\xi_c^5 - \xi_b^5\right) - \frac{1}{2m_3^3}\left\{\frac{1}{5}\left[\left(m_3\xi_c + b_3\right)^5 - \left(m_3\xi_b + b_3\right)^5\right] - \frac{2b_3}{4}\left[\left(m_3\xi_c + b_3\right)^4 - \left(m_3\xi_b + b_3\right)^4\right] + \frac{b_3^2}{3}\left[\left(m_3\xi_c + b_3\right)^3 - \left(m_3\xi_b + b_3\right)^3\right]\right\}$$

$$\gamma_8 = \iint \xi\eta^2 d\xi\, d\eta = \left(m_2^3 - m_1^3\right)\frac{\xi_b^5}{15} + \frac{m_2^3}{15}\left(\xi_c^5 - \xi_b^5\right) - \frac{1}{15m_3^2}\left[\left(m_3\xi_c + b_3\right)^5 - \left(m_3\xi_b + b_3\right)^5\right] + \frac{b_3}{12m_3^2}\left[\left(m_3\xi_c + b_3\right)^4 - \left(m_3\xi_b + b_3\right)^4\right]$$

$$\gamma_9 = \iint \eta^3 d\xi d\eta = \frac{m_2^4 - m_1^4}{20} \xi_b^5 + \frac{m_2^4}{20} \left(\xi_c^5 - \xi_b^5\right) - \frac{1}{20m_3}\left[\left(m_3\xi_c + b_3\right)^5 - \left(m_3\xi_b + b_3\right)^5\right]$$

With equations (28), (29), (30) and the integrals γ_0 through γ_9, the strain energy (27) can be expressed as:

$$W = \tfrac{1}{2} \{a\}^T [B] \{a\} \quad , \tag{31}$$

where the matrix [B] is the one given on the next page. To simplify the writing of [B], the following nomenclature was used:

$$\begin{aligned}
T_{\gamma 1} &= T_1\gamma_1 + T_2\gamma_2 + T_0\gamma_0 \\
T_{\gamma 3} &= T_1\gamma_3 + T_2\gamma_5 + T_0\gamma_1 \\
T_{\gamma 5} &= T_1\gamma_5 + T_2\gamma_4 + T_0\gamma_2 \\
T_{\gamma 6} &= T_1\gamma_6 + T_2\gamma_7 + T_0\gamma_3 \\
T_{\gamma 7} &= T_1\gamma_7 + T_2\gamma_8 + T_0\gamma_5 \\
T_{\gamma 8} &= T_1\gamma_8 + T_2\gamma_9 + T_0\gamma_4
\end{aligned} \tag{32}$$

Introducing equations (24) into equation (31), the strain energy may be expressed as a function of $\{\delta\}$:

	$C_{11}T_{\gamma 1}$	$C_{13}T_{\gamma 1}$	$2C_{11}T_{\gamma 3}$	$C_{11}T_{\gamma 5} + C_{13}T_{\gamma 3}$
		$C_{33}T_{\gamma 1}$	$2C_{13}T_{\gamma 3}$	$C_{13}T_{\gamma 5} + C_{33}T_{\gamma 3}$
			$4C_{11}T_{\gamma 6}$	$2C_{11}T_{\gamma 7} + 2C_{13}T_{\gamma 6}$
				$C_{11}T_{\gamma 8} + 2C_{13}T_{\gamma 7} + C_{33}T_{\gamma 6}$

$2C_{13}T_{\gamma 5}$		$C_{13}T_{\gamma 1}$	$C_{12}T_{\gamma 1}$	$2C_{13}T_{\gamma 3}$	C_{12}
$2C_{33}T_{\gamma 5}$		$C_{33}T_{\gamma 1}$	$C_{23}T_{\gamma 1}$	$2C_{33}T_{\gamma 2}$	C_{33}
$4C_{13}T_{\gamma 7}$		$2C_{13}T_{\gamma 3}$	$2C_{12}T_{\gamma 3}$	$4C_{13}T_{\gamma 6}$	$2C_{1}$
$2C_{13}T_{\gamma 8} + 2C_{33}T_{\gamma 7}$		$C_{13}T_{\gamma 5} + C_{33}T_{\gamma 3}$	$C_{12}T_{\gamma 5} + C_{23}T_{\gamma 3}$	$2C_{13}T_{\gamma 7} + 2C_{33}T_{\gamma 6}$	$(C_{1}$
$4C_{33}T_{\gamma 8}$		$2C_{33}T_{\gamma 5}$	$2C_{23}T_{\gamma 5}$	$4C_{33}T_{\gamma 7}$	$2C_{3}$
		$C_{33}T_{\gamma 1}$	$C_{23}T_{\gamma 1}$	$2C_{33}T_{\gamma 3}$	C_{33}
			$C_{22}T_{\gamma 1}$	$2C_{23}T_{\gamma 3}$	C_{22}
				$4C_{33}T_{\gamma 6}$	$2C_{2}$
					C_{2}

MATRIX [B]

$\gamma_3 + C_{13}T_{\gamma 5}$	$2C_{12}T_{\gamma 5}$
$\gamma_5 + C_{23}T_{\gamma 3}$	$2C_{23}T_{\gamma 5}$
$T_{\gamma 6} + 2C_{13}T_{\gamma 7}$	$4C_{12}T_{\gamma 7}$
$+ C_{33})T_{\gamma 7} + C_{13}T_{\gamma 8} + C_{23}T_{\gamma 6}$	$2C_{12}T_{\gamma 8} + 2C_{23}T_{\gamma 7}$
$T_{\gamma 8} + 2C_{23}T_{\gamma 7}$	$4C_{23}T_{\gamma 8}$
$\gamma_5 + C_{23}T_{\gamma 3}$	$2C_{23}T_{\gamma 5}$
$\gamma_3 + C_{23}T_{\gamma 5}$	$2C_{22}T_{\gamma 5}$
$T_{\gamma 7} + 2C_{23}T_{\gamma 6}$	$4C_{23}T_{\gamma 7}$
$\gamma_6 + C_{33}T_{\gamma 8} + 2C_{23}T_{\gamma 7}$	$2C_{22}T_{\gamma 7} + 2C_{23}T_{\gamma 8}$
	$4C_{22}T_{\gamma 8}$

$$W = \tfrac{1}{2}\{\delta\}^T\left([A]^{-1}\right)^T[B]\ [A]^{-1}\{\delta\}$$

The nodal force vector $\{P\}$ can then be found by using the second theorem of Castigliano:

$$\{P\} = \frac{\partial W}{\partial\{\delta\}} = \left([A]^{-1}\right)^T[B]\ [A]^{-1}\{\delta\},$$

and the 12x12 stiffness matrix [K] of the triangular element is:

$$[K] = \left([A]^{-1}\right)^T[B]\ [A]^{-1} \tag{33}$$

For certain boundary conditions, it is convenient to refer the stiffness matrix to rotated nodal directions. Thus, the new stiffness matrix [K'] is given by:

$$[K'] = [T]^T[K]\ [T] \tag{34}$$

where the transformation matrix [T] is expressed as:

$$[T] = \begin{bmatrix}
\cos\varphi_a & 0 & 0 & 0 & 0 & 0 & -\sin\varphi_a & 0 & 0 & 0 & 0 & 0 \\
0 & \cos\varphi_b & 0 & 0 & 0 & 0 & 0 & -\sin\varphi_b & 0 & 0 & 0 & 0 \\
0 & 0 & \cos\varphi_c & 0 & 0 & 0 & 0 & 0 & -\sin\varphi_c & 0 & 0 & 0 \\
0 & 0 & 0 & \cos\varphi_\alpha & 0 & 0 & 0 & 0 & 0 & -\sin\varphi_\alpha & 0 & 0 \\
0 & 0 & 0 & 0 & \cos\varphi_\beta & 0 & 0 & 0 & 0 & 0 & -\sin\varphi_\beta & 0 \\
0 & 0 & 0 & 0 & 0 & \cos\varphi_\gamma & 0 & 0 & 0 & 0 & 0 & -\sin\varphi_\gamma \\
\sin\varphi_a & 0 & 0 & 0 & 0 & 0 & \cos\varphi_a & 0 & 0 & 0 & 0 & 0 \\
0 & \sin\varphi_b & 0 & 0 & 0 & 0 & 0 & \cos\varphi_b & 0 & 0 & 0 & 0 \\
0 & 0 & \sin\varphi_c & 0 & 0 & 0 & 0 & 0 & \cos\varphi_c & 0 & 0 & 0 \\
0 & 0 & 0 & \sin\varphi_\alpha & 0 & 0 & 0 & 0 & 0 & \cos\varphi_\alpha & 0 & 0 \\
0 & 0 & 0 & 0 & \sin\varphi_\beta & 0 & 0 & 0 & 0 & 0 & \cos\varphi_\beta & 0 \\
0 & 0 & 0 & 0 & 0 & \sin\varphi_\gamma & 0 & 0 & 0 & 0 & 0 & \cos\varphi_\gamma
\end{bmatrix}$$

The angles φ_a through φ_γ are the rotations at the nodes a through γ, respectively.

By adequately combining the matrix [K'] of the elements, a total stiffness

matrix [K*] for the whole structure is obtained. Reference 5 provides details of the procedure to find [K*]. The nodal equilibruim equation for the whole structure can then be written as:

$$\{P^*\} = [K^*]\{\delta^*\} \tag{36}$$

It is convenient to partition this matrix equation in the following form:

$$\begin{Bmatrix} \{P_1^*\} \\ \{P_2^*\} \end{Bmatrix} = \begin{bmatrix} [K_{11}^*] & [K_{12}^*] \\ [K_{21}^*] & [K_{22}^*] \end{bmatrix} \begin{Bmatrix} \{\delta_1^*\} \\ \{\delta_2^*\} \end{Bmatrix} \tag{37}$$

where the symbols have the meaning:

$\{\delta_1^*\}$: vector of unknown displacements

$\{\delta_2^*\}$: vector of known displacements

$\{P_1^*\}$: vector of known forces

$\{P_2^*\}$: vector of unknown forces

From equation (37),

$$[K_{11}^*]\{\delta_1^*\} = \{P_1^*\} - [K_{12}^*]\{\delta_2^*\},$$

which is a system of linear equations that permits solution for $\{\delta_1^*\}$.

Then, also from (37), we obtain:

$$\{P_2^*\} = [K_{21}^*]\{\delta_1^*\} + [K_{22}^*]\{\delta_2^*\}$$

It is convenient to compute this vector $\{P_2^*\}$ for checking purposes, although it is not really necessary for the computation of the stresses.

Once all nodal displacements are known, the vector {a} for each element can be obtained:

$$\{a\} = [A]^{-1}\{\delta\} = [A]^{-1}[T]\{\delta'\} ,$$

where $\{\delta'\}$ are the displacements referred to the rotational directions.

Finally, the stresses are given by:

$$\begin{aligned}
\sigma_x &= C_{11}(a_2 + 2a_4\xi + a_5\eta) + C_{12}(a_9 + a_{11}\xi + 2a_{12}\eta) \\
&\quad + C_{13}(a_3 + a_5\xi + 2a_6\eta + a_9 + 2a_{10}\xi + a_{11}\eta) \\
\sigma_y &= C_{12}(a_2 + 2a_4\xi + a_5\eta) + C_{22}(a_9 + a_{11}\xi + 2a_{12}\eta) \\
&\quad + C_{23}(a_3 + a_5\xi + 2a_6\eta + a_8 + 2a_{10}\xi + a_{11}\eta) \\
\tau_{xy} &= C_{13}(a_2 + 2a_4\xi + a_5\eta) + C_{23}(a_9 + a_{11}\xi + 2a_{12}\eta) \\
&\quad + C_{33}(a_3 + a_5\xi + 2a_6\eta + a_8 + 2a_{10}\xi + a_{11}\eta)
\end{aligned} \tag{38}$$

The value of the stresses at each nodal point of the triangular net is obtained by averaging the values of the stresses at this node from each one of the elements containing the node.

The material constants C_{ij} are obtained by assuming that the material is anisotropic at each triangle and is formed by fibers oriented in one direction in the matrix. The axes x', y' in Figure 65 coincide with the fiber's direction, while x, y are the general axes of reference, parallel to ξ, η.

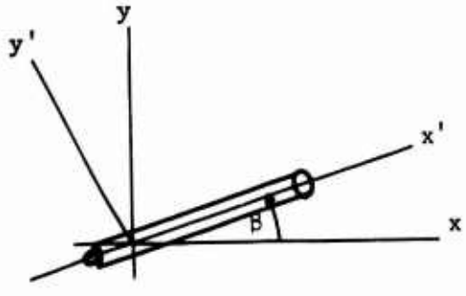

Figure 65. Axes of Reference.

The elastic constants with respect to the x', y' axes are given by;

$$E_{x'} = E_m V_m + E_f V_f \quad , \quad E_{y'} = \frac{E_m E_f}{E_m V_f + E_f V_m}$$

$$\nu_{x'y'} = \nu_m V_m + \nu_f V_f \quad , \quad G_{x'y'} = \frac{G_m G_f}{G_m V_f + G_f V_m}$$

where V_m , V_f are the volumetric fractions of the matrix and fibers, E_m, G_m, ν_m are the elastic constants of the matrix material; and E_f, G_f, ν_f are the elastic constants of the fiber material. From $E_{x'}$, $E_{y'}$, $\nu_{x'y'}$ and $G_{x'y'}$, the following new set of constants is found:

$$b'_{11} = \frac{1}{E_{x'}} \quad , \quad b'_{12} = -\frac{\nu_{x'y'}}{E_{x'}} \quad , \quad b'_{22} = \frac{1}{E_{y'}} \quad , \quad b'_{33} = \frac{1}{G_{x'y'}}$$

The elements of the symmetric matrix [C'] referred to the axes of orthotropy x', y' are:

$$C'_{11} = \frac{b'_{22}}{\Delta} \quad , \quad C'_{12} = -\frac{b'_{12}}{\Delta} \quad , \quad C'_{22} = \frac{b'_{11}}{\Delta} \quad , \quad C'_{33} = \frac{1}{b'_{33}} \quad , \quad C'_{12} = C'_{23} = 0$$

$$\Delta = b'_{11} b'_{22} - b'^{2}_{12}$$

The matrix [G], referred to the axis x and y, is obtained from [C'] by performing the operation

$$[C] = [T_1]^{-1} [C'] [T_2],$$

with

$$[T_1] = \begin{bmatrix} \ell^2 & m^2 & 2\ell m \\ m^2 & \ell^2 & -2\ell m \\ -\ell m & \ell m & \ell^2 - m^2 \end{bmatrix} \quad , \qquad [T_2] = \begin{bmatrix} \ell^2 & m^2 & \ell m \\ m^2 & \ell^2 & -\ell m \\ -2\ell m & 2\ell m & \ell^2 - m^2 \end{bmatrix}$$

$$\ell = \cos\beta$$

$$m = \sin\beta$$

It must be noted that, in general, C_{13} and C_{23} are not zero because x and y are not necessarily axes of orthotropy.

The computer program is contained in the appendix to this report.

LITERATURE CITED

[1] Volkersen, Von Olaf, DIE NIETKRAFTVERTEILUNG IN ZUGBEANSPRUCHTEN NIETVERBINDUNGEN MIT KONSTANTEN LASCHENGUERSCHNITTEN, Luftfahrtforschung, 15, 1938, pp. 41-47.

[2] Goland, M., and Reissner, E., THE STRESSES IN CEMENTED JOINTS, Journal of Applied Mechanics, Vol. 11, 1944, pp. A17-27.

[3] Scherrer, R. E., STRESSES IN A LAP JOINT WITH ELASTIC ADHESIVES, US Forest Products Laboratory, Report No. 1864, September 1957.

[4] Lubkin, J. L., A THEORY OF ADHESIVE SCARF JOINTS, Journal of Applied Mechanics, Vol. 24, 1957, pp. 255-260.

[5] Puppo, A., Haener, J., APPLICATION OF MICROMECHANICS TO JOINTS AND CUTOUTS, USAAVLABS Technical Report 69-25, U. S. Army Aviation Materiel Laboratories, Fort Eustis, Virginia, December 1968.

APPENDIX

COMPUTER PROGRAM FOR FINITE-ELEMENT ANALYSIS OF JOINTS IN ANISOTROPIC MATERIALS

```
      PROGRAM SIXPT
C   FD(I)   - FORCE OR DISPLACEMENT AT NODE I, WHICHEVER IS KNOWN
C
C    ANISOTROPIC
C
C   NO(I,J) - NODE TYPE J AT TRIANGLE I
C   NO(I,1) - A NODE
C   NO(I,2) - GAMMA NODE
C   NO(I,3) - B NODE
C   NO(I,4) - ALPHA NODE
C   NO(I,5) - C NODE
C   NO(I,6) - BETA NODE
C   ETA(I) - ETA AT NODEI)
C   XI(I) - XI AT NODE I
C
C   NT    - NUMBER OF TRIANGLES
C   NV    - NUMBER OF VERTICES
C   NMP   - NUMBER OF MID-POINTS
C   NUD   - NUMBER OF UNKNOWN DISPLACEMENTS
C   NKD   - NUMBER OF KNOWN DISPLACEMENTS
C   NUF   - NUMBER OF UNKNOWN FORCES
C   NKF   - NUMBER OF KNOWN FORCES
C   NN    - TOTAL NUMBER OF NODES
C   NKFD - TOTAL KNOWN FORCES AND DISPLACEMENTS (= 2*NN)
C
C   IDIR(I,1) NUMBER OF X-DISPLACEMENT AT NODE I
C   IDIR(I,2) NUMBER OF Y-DISPLACEMENT AT NODE I
C
C
C   NODF(I,J) - J-TH NODE TOUCHING ITH DIRECTION
C
C
C   NOT(I,J) - J-TH TRIANGLE TOUCHING NODE I (UP TO J=8)
C   NOT(I,9) - NUMBER OF TRIANGLES TOUCHING I-TH NODE
C
C   NOT(I,J)    INCREASES MONOTONICALLY WITH J
C
C   A MAXIMUM OF 80 TRIANGLES
C                250 NODES
C                500 DISPLACEMENTS, KNOWN AND UNKNOWN
C                60 ROWS IN A PARTITIONED SUBMATRIX
C                60 KNOWN DISPLACEMENTS
C                8 TRIANGLES COMMON TO A NODE
C
C      IF TWO VERTICES IN THE SAME TRIANGLE HAVE THE SAME X COORDINATE
C      THEN THEY MUST BE ORDERED TO BE A AND B
C
       COMMON /Z/ NO(80,6), FD(500), NODF(500,2), X(250), Y(250),TH(250),
      1    N, KREM, M, S(60,60,5), IDIR(250,2), ALF(250), T(12,12),
      2    AMX(12,12), BMX(12,12), SP(60,20), EF(80), ER(80), RNU(80),
      3     FNU(80), NOT(250,9), CIJ(6,80),KMX(12,12,80), AS(6,6,80),
      4    G(60), NKD, NUD, NN, NT              ,VF(80),BETA(80)
       REAL KMX
       DIMENSION DUM(13)
       DEG = .0174533
C
```

```
C    ZERO OUT MATRIX T     AND    MATRIX B
       DO 10 I = 1,12
       DO 10 J = 1,12
       BMX(I,J) = 0.
    10 T(I,J) = 0.
C
C     ZERO OUT APPROPRIATE PARTS OF 12X12 A-MATRIX
C
       DO 20 I = 1,6
       DO 20 J = 1,6
       AMX(I+6,J) = 0.
    20 AMX(I,J+6) = 0.
       READ 1000, (DUM(I),I=1,13)
       PRINT 1001, (DUM(I),I=1,13)
       READ 1002, NT, NV, NMP, NUD, NKD
       PRINT 1003, NT, NV, NMP, NUD, NKD
       NN = NV + NMP
       NKF = NUD
       NUF = NKD
       NKFD = NKF + NKD
C
C   ZERO OUT ALL KNOWNS
C
       DO 30 I=1,NKFD
       FD(I) = 0.
    30 CONTINUE
C
C   READ TRIANGLE INFORMATION
C
       DO  40 K = 1,NT
       READ1007,I,(NO(I,J),J=1,6),EF(I),FNU(I),ER(I),RNU(I),VF(I),BETA(I)
    40 CONTINUE
C
C    READ NON-ZERO KNOWNS INTO FD AND PRINT THEM OUT
C
       PRINT 1118
       DO 50 I=1,NKFD
       READ 1115, J,TEMP
       IF (J.EQ.0)  GO TO 60
       FD(J) = TEMP
    50 PRINT 1120 ,J,FD(J)
    60 CONTINUE
C
C   PRINT OUT TRIANGLE DATA
C
       LINE = 4
       PRINT 1030,(J,J=1,6)
       DO 80 I=1,NT
       IF(LINE.LT.54)  GO TO 75
       LINE = 4
       PRINT 1030,(J,J=1,6)
    75 LINE = LINE+2
    80 PRINT 1033,I,(NO(I,J),J=1,6),EF(I),FNU(I),ER(I),RNU(I),
      1     VF(I), BETA(I)
C
C   PRINT FD
C
C
C   READ IN VERTEX INFORMATION
C
       DO 100 K=1,NV
       READ 1005,  I, IDIR(I,1), IDIR(I,2),ALF(I), X(I), Y(I), TH(I)
       ALF(I) = ALF(I) * DEG
   100 CONTINUE
```

```
C
C  READ IN MID-POINT INFORMATION
C
      DO 135 K = 1,NMP
      READ 1006,  I, IDIR(I,1), IDIR(I,2),ALF(I)
      ALF(I) = ALF(I) * DEG
C
C FIND X,Y FOR MID POINT
C
      DO 105 L = 1,NT
      DO 105 J = 1,6
      IF(I.EQ.NO(L,J)) GO TO 110
  105 CONTINUE
      PRINT 1050 ,I
      STOP
  110 NOL1 = NO(L,1)
      IF(J.EQ.6)       GO TO 115
      NOLJP1 = NO(L,J+1)
      GO TO 120
  115 NOLJP1 = NO(L,1)
  120 NOLJM1 = NO(L,J-1)
  130 Y(I) = (Y(NOLJM1)+Y(NOLJP1))/2.
      X(I) = (X(NOLJM1)+X(NOLJP1))/2.
      TH(I) = (TH(NOLJP1)+TH(NOLJM1))/2.
  135 CONTINUE
C
C  PRINT OUT NODE INFORMATION
C
      I = 1
  140 CONTINUE
      LINE = 4
      PRINT 1020
  145 CONTINUE
      BLD = ALF(I)/DEG
      PRINT 1021, I, IDIR(I,1),IDIR(I,2),X(I),Y(I),TH(I),BLD
      I = I+1
      IF(I.GT.NN) GO TO 160
      LINE = LINE + 2
      IF(LINE.GT.53) GO TO 140
      GO TO 145
  160 CONTINUE
C
C  READ IN PARTITIONING INFORMATION
C
      READ 1016, MSIZE , KREM , N
      M = MSIZE / N
      IF(KREM.NE.N)  M = M+1
C
C
C   GENERATE TABLE OF TRIANGLES VS NODES
C
      DO 200 I= 1,NN
      NOT(I,9) = 0.
  200 CONTINUE

      DO 300 I=1,NT
      DO 300 J = 1,6
      K = NO(I,J)
      NOT(K,9) = NOT(K,9) + 1
      L = NOT(K,9)
      NOT(K,L) = I
  300 CONTINUE

C
```

```
C  GENERATE TABLE OF NODES VS DIRECTIONS
C
      DO 350 I=1,NN
      DO 350 J=1,2
      K = IDIR(I,J)
      NODE(K,2) = J
  350 NODE(K,1) = I
C  GENERATE SMALL K-MATRICES AND ALL A-STAR MATRICES
C
C
      DO 400 I=1,NT
      BETA(I) = BETA(I)*DEG
      CALL SMALLK(I)
  400 CONTINUE

      CALL SOLVIT
 1000 FORMAT(13A6)
 1001 FORMAT(1H1,13A6////)
 1002 FORMAT(5I3)
 1003 FORMAT(1X, 6X,9HTRIANGLES,7X,8HVERTICES,5X,10HMID-POINTS,
     1   5X,13HUNKNOWN DISPS,5X,11HKNOWN DISPS/1X3(12X,I3),15X,I3,13X,
     2      I3)
 1005 FORMAT(3I3,4E6.3)
 1006 FORMAT(3I3,F6.3)
 1007 FORMAT(7I3,6E9.3)
 1016 FORMAT(3I3)
 1020 FORMAT(5H1NODE,3X,5HDIR 1,3X,5HDIR 2,9X,1HX,9X,1HY,4X,9HTHICKNESS,
     1    5X,5HANGLE/)
 1021 FORMAT(2X,I3,2(5X,I3),4F10.3/)
 1030 FORMAT(9H1TRIANGLE,6(2X,3HPT ,I1),10X,2HEE,8X,4HNU E,10X,2HER,
     1     8X,4HNU R,10X,2HVF,8X,4HBETA/)
 1033 FORMAT(6X,I3,6(3X,I3),6(E12.5)/)
 1050 FORMAT(5H1NODE,I3,21HNOT IN TRIANGLE INPUT)

 1115 FORMAT(I3,E15.6)
 1118 FORMAT(1H1,10X,28HNON-ZERO BOUNDARY CONDITIONS  //)
 1120 FORMAT(7H KNOWN(,I3,3H) =,E15.8)
      STOP
      END
```

```
      SUBROUTINE LARGEK(ICYCLE,A,B,C,CS,Q,SK12,I1,I2,I3,I4,I5)
C
C   ANISOTROPIC
C

C   THIS SUBROUTINE IS CALLED BY SUBROUTINE SOLVIT TO GENERATE A ROW OF
C   SUBMATRICES FROM THE MATRIX K-STAR. THE SMALL (12X12) K-MATRICES
C   GENERATED ON THE PREVIOUS PASS WILL BE SAVED ON THIS PASS, AND THE
C   REQUIRED SMALL K-MATRICES NOT ON HAND WILL BE GENERATED. THE MATRIX
C   ASTAR-INVERSE WILL BE SAVED FOR THE CALCULATION OF STRESSES, AS WILL
C   C11,C12,C22,C33 FOR EACH NEW TRIANGLE.
C
C
C  A CORRESPONDS TO A(I,I-1) IN THE PARTITIONED MATRIX
C  B CORRESPONDS TO A(I,I  ) IN THE PARTITIONED MATRIX
C  C CORRESPONDS TO A(I,I+1) IN THE PARTITIONED MATRIX
C  THEREFORE, A(I) IS THE TRANSPOSE OF C(I-1), I.GT.1
C
C
C      ON THE M-TH PASS, K22 STAR(NKD X NKD) IS RETURNED IN C
C
      COMMON /Z/ NO(80,6), FD(500), NODF(500,2), X(250), Y(250),TH(250),
     1   N, KREM, M, S(60,60,5), IDIR(250,2), ALF(250), T(12,12),
     2   AMX(12,12), BMX(12,12), SP(60,20), EF(80), ER(80), RNU(80),
     3    FNU(80), NOT(250,9), CIJ(6,80),KMX(12,12,80), AS(6,6,80),
     4   G(60), NKD, NUD, NN, NT                 ,VF(80),BETA(80)
      REAL KMX
      DIMENSION A(I1,I2) , B(I1,I1), C(I1,I3) , SK12(I1,I4)
      DIMENSION  CS(I5,I1), Q(I4,I4)
C
      DIMENSION  RK12(3600)
      EQUIVALENCE  (S(7201),RK12)
      DIMENSION  NDIR(6,2)  , R(80)
      DATA  NDIR / 1, 6, 2, 4, 3, 5, 7, 12, 8, 10, 9, 11/
C
C  NDIR(I,J)  -  POSITION IN GENERIC TRIANGLE OF DIRECTION J AT NODE I
C
C  (J=1,2)  ,  (I=1,6)
C
      IG = I1
      IABC2 = 4
      IF(ICYCLE.GT.1)  GO TO 10
      REWIND 15
      IABC1 = 2
      IS = 0
      JS = -I2
      GO TO 22
   10 CONTINUE
      IF(ICYCLE.GT.2)  GO TO 15
      JS = 0
      K2 = KREM
      GO TO 20
   15 JS = KREM + (ICYCLE-3)*N
   20 IS = KREM + (ICYCLE-2)*N
C
C  IS  -  BIAS FOR ROWS
C  JS  -  BIAS FOR COLUMNS
C
      IABC1 = 1
      IF(ICYCLE.EQ.M) IABC2 = 5
   22 JSA = JS
      JSB = JSA + I2
```

```
      ISC = JSB + I1
      IROW1 = 1 + IS
      IROW2 = I1 + IROW1 -1
      DO 150 IABC = IABC1,IABC2
      GO TO (25,35,40,41,49),IABC
   25 REWIND 11
      READ(11) ((A(I,J),I=1,I1),J=1,I2)
      GO TO 150
   35 ICOL1 = JSB + 1
      ICOL2 = ICOL1 + I1 - 1
      GO TO 45
   40 IF(ICYCLE.EQ.M) GO TO 150
      ICOL1 = JSC + 1
      ICOL2 = ICOL1 + I3 -1
      GO TO 45
   41 ICOL1 = NUD + 1
      ICOL2 = NUD + NKD
      GO TO 45
   49 ICOL1 = NUD+1
      ICOL2 = ICOL1 + NKD - 1
      IROW1 = ICOL1
      IROW2 = ICOL2
   45 CONTINUE
      DO 100 I=IROW1,IROW2
      NOI = NODE(I,1)
C
C  NOI - NODE WHERE DIRECTION I IS LOCATED
C
      DO 100 J=ICOL1,ICOL2
      NOJ = NODE(J,1)
C
C  NOJ - NODE WHERE DIRECTION J IS LOCATED
C
      TEMP = 0.
      NOTI9 = NOT(NOI,9)
      NOTJ9 = NOT(NOJ,9)
C
C IMAX - NO OF TRIANGLES AT NODE
C
      DO 64 K=1,NOTI9
      NOTI = NOT(NOI,K)
      DO 64 KK=1,NOTJ9
C
C  NOTI - KTH TRIANGLE TOUCHING NODE NOI
C
      IF(NOTI.NE.NOT(NOJ,KK)) GO TO 64
      DO 60 L=1,6
      IF(NOI.EQ.NO(NOTI,L)) IK = L
      IF(NOJ.EQ.NO(NOTI,L)) JK = L
   60 CONTINUE
      IM = NODE(I,2)
C
C  IM -  DIRECTION 1 OR 2, NODE NOI

   62 NDIRI = NDIR(IK,IM)
      JM = NODE(J,2)
C
C  JM -  DIRECTION 1 OR 2, NODE NOJ
C
      NDIRJ = NDIR(JK,JM)
      TEMP = TEMP+KMX(NDIRI,NDIRJ,NOTI)
   64 CONTINUE
```

```
   65 GO TO (70,70,80,82,85),IABC
   70 B(I-IS,J-JSB) = TEMP
      GO TO 90
   80 CONTINUE
      C(I-IS,J-JSC)= TEMP
      CS  (J-JSC,I-IS) = TEMP
C
C  CS IS THE TRANSPOSE OF C, SAVED FOR USE AS A IN THE FOLLOWING CYCLE
C
      GO TO 90
   82 SK12(I-IS,J-NUD) = TEMP
      GO TO 90
   85 Q(I-NUD,J-NUD) = TEMP
   90 CONTINUE
C
C  K22-STAR (NKD X NKD)  LEFT IN (S4 = Q) AFTER M-TH PASS
C
  100 CONTINUE
      IF(IABC.NE.3)  GO TO 110
      REWIND 11
      WRITE (11) ((CS(J,I),J=1,I5),I=1,I1)
  110 CONTINUE
      IF(IABC.NE.4)  GO TO 150
C
C  CALCULATE INDEPENDENT VECTOR SEGMENT G
C
      DO 130 L=1,IG
      G(L) = FD(L+IS)
  130 CONTINUE
      CALL MXMULT(S(1,1,3),FD(NUD+1),R,I1,NKD,1)
      DO 140 L=1,IG
      G(L) = G(L) - R(L)
  140 CONTINUE
  150 CONTINUE
      K21DIM = I1*NKD
      WRITE  (10)  (RK12(JJJ),JJJ=1,K21DIM)
C
C
      RETURN
      END
```

```
      SUBROUTINE SOLVIT
C
C    ANISOTROPIC
C
C
C  THIS ROUTINE SOLVES  SU=G , WHERE S IS A TRI-DIAGONAL MATRIX IN
C  SUBMATRICES, WITH ELEMENTS OF ORDER N.
C  S IS KNOWN
C  SP IS A VECTOR OF DIMENSION (NXM) WHERE M IS THE NUMBER OF DIVISIONS OF S
C  C IS WRITTEN ONTO TAPE AFTER DERIVATION ON THE FORWARD PASS,
C  AND READ BACK IN ON THE BACKSWEEP
C  S(1,1,1)   INITIALLY CONTAINS  S(I,I-1)
C  S(1,1,2)   INITIALLY CONTAINS  S(I,I  )
C  S(1,1,4)   INITIALLY CONTAINS  S(I,I+1)
C  SP CORRESPONDS TO P IN THE WRITEUP BY GATEWOOD ON THE FORWARD PASS.
C  ON THE BACKSWEEP, IT CORRESPONDS TO U.
      COMMON /Z/ NO(80,6), FD(500), NODE(500,2), X(250), Y(250),TH(250),
     1    N, KREM, M, S(60,60,5), IDIR(250,2), ALF(250), T(12,12),
     2    AMX(12,12), BMX(12,12), SP(60,20), EF(80), ER(80), RNU(80),
     3     FNU(80), NOT(250,9), CIJ(6,80),KMX(12,12,80), AS(6,6,80),
     4    G(60), NKD, NUD, NN, NT                ,VF(80),BETA(80)
      REAL KMX
      EQUIVALENCE  (S(14401),C)
      DIMENSION C(3600)
      DATA  XLIMIT /1.E-8/
      REWIND 9
      N2 = 2*N
      KREM2 = 2*KREM
      DO 30 ICYCLE =1,M
      IF(ICYCLE-2) 1,2,3
    1 K1 = KREM
      K2 = KREM
      K3 = KREM2
      GO TO 4
    2 K1 = N
      K2 = KREM
      K3 = N2
      GO TO 4
    3 K1 =N
      K2 =N
      K3 =N2
    4 CONTINUE
      K4 = N
      IF(ICYCLE.EQ.M)  K4 = NKD
      CALL LARGEK(ICYCLE,S,S(1,1,2),S(1,1,4),S(1,1,3),S(1,1,4),S(1,1,3),
     1      K1,K2,K4,NKD,N)
      IF(ICYCLE.EQ.1) GO TO 10
      CALL MXMULT(S(1,1,1) , S(1,1,5) , S(1,1,3) ,K1,K2,K1)
C
C  S(1,1,5) CONTAINS C FROM LAST CYCLE
C
      CALL MXSUB(S(1,1,2) , S(1,1,3) , S(1,1,2) ,K1,K1)
   10 CONTINUE
C
C  B(I,I)  NOW IN S(1,1,2)
C
      CALL INVERT(S(1,1,2) , K1   K3, XLIMIT , FLAG)
      IF (FLAG.NE.0.0) GO TO 500
C
C  INVERSE OF B(I,I) NOW IN  S(1,1,2)
C
      IF (ICYCLE.EQ.1) GO TO 2
```

```
      CALL MXMULT(S(1,1,1) ,SP(1,ICYCLE-1) , S(1,1,3) , N, K2 , 1)
      CALL MXSUB (G  ,  S(1,1,3), G, N, 1)
   20 CONTINUE
      CALL MXMULT(S(1,1,2) , G ,SP(1, ICYCLE  ) , K1 , K1 ,  1)
      IF (ICYCLE.GE.M) GO TO 35
      CALL MXMULT (S(1,1,2) , S(1,1,4) , S(1,1,5), K1 , K1 , N)
      NSQ = K1*N
      WRITE (9)  (C(JJJ),JJJ=1,NSQ)
   30 CONTINUE
   35 CONTINUE
C
C  NOW IN BACKSWEEP, SOLVING FOR U
C
      DO 60 I = 2,M
      JCYCLE = M-I+1
      IF(JCYCLE.GT.1)  GO TO 36
      K1 = KREM
      GO TO 37
   36 K1 = N
   37 CONTINUE
      NSQ = K1*N
      IF (JCYCLE.EQ.M-1)  GO TO 41
      BACKSPACE 9
   41 CONTINUE
      BACKSPACE 9
      READ  (9)  (C(JJJ),JJJ=1,NSQ)
C
C  U(M)=SP(M) , CONSIDER FIRST (M-1)TH CYCLE
C
      CALL MXMULT(S(1,1,5) ,SP(1,JCYCLE+1),S(1,1,1),K1,N, 1)
      CALL MXSUB(SP(1,JCYCLE), S(1,1,1) ,SP(1,JCYCLE), K1 ,  1)
   60 CONTINUE
C
C  U(NS,1) NOW STORED IN SP(N,I) , I=1,M
C
      CALL ENDIT
      RETURN
  500 CONTINUE
      PRINT 1000 , ICYCLE
      STOP
 1000 FORMAT (31H1COULD NOT INVERT MATRIX IN ROW,I2)
      END
```

```
      SUBROUTINE FNDIT
C
C  THIS SUPROUTINE CALCULATES THE STRESSES SIGMAX, SIGMAY, AND TAUXY
C  AT EACH NODE, FOR EACH TRIANGLE.   THEN FOR EACH NODE, AN AVERAGE
C  VALUE IS DERIVED BY SUMMING THE  VALUES ARRIVED AT IN EACH
C  CONTIGUOUS TRIANGLE, AND DIVIDING BY THE NUMBER OF TRIANGLES9
C
C
C  SHIFT THE DELS TO REMOVE THE GAPS
C
      EQUIVALENCE (S,SMALLA) , (S(3601),PSTR) , (S(10801),Q)
      DIMENSION  SMALLA(12, 80) , DX(12) , SX(3,250)
      DIMENSION  PSTR(3,250)  , Q(3600)
      EQUIVALENCE  (S(7201),SX) , (S(8001),DEL)
      COMMON /Z/ NO(80,6), FD(500), NODE(500,2), X(250), Y(250),TH(250),
     1   N, KREM, M, S(60,60,5), IDIR(250,2), ALF(250), T(12,12),
     2   AMX(12,12), BMX(12,12), SP(60,20), EE(80), ER(80), RNU(80),
     3    ENU(80), NOT(250,9), CIJ(6,80),KMX(12,12,80), AS(6,6,80),
     4   G(60), NKD, NUD, NN, NT              ,VF(80),BETA(80)
      REAL KMX
      DIMENSION DEL(500) , PS2(60) , NTRI(6) ,DXP(12),NOD(6)
      DATA NTRI/1,3,5,4,6,2/
      MSIZE = NKD+NUD
      PI = 3.1415927
      DO 10 J=1,KREM
      DEL(J) = SP(J,1)
   10 CONTINUE
      KLOC = KREM -N
      DO 20 I=2,M
      KLOC = KLOC + N
      DO 20 J=1,N
      DEL(KLOC+J) = SP(J,I)
   20 CONTINUE
      DO 22 I=1,NKD
   22 DEL(NUD+I) = FD(NUD+I)
      PRINT 1010
      NDEL = (NUD+NKD) / 7
      JCNT = 0
      DO 30 J=1,NDEL
      JCNT = JCNT + 1
      IF(JCNT.LE.17)  GO TO 25
      PRINT 1010
      JCNT = 1
   25 JFIR = 7*(J-1) + 1
      JLAST =  JFIR + 6
      PRINT 1011 , (K,K=JFIR,JLAST)
      PRINT 1012, (DEL(K),K=JFIR,JLAST)
   30 CONTINUE
      LOC1 = 7*NDEL+1
      LOC2 = NUD + NKD
      IF(LOC1.GT.LOC2)  GO TO 40
      PRINT 1011,(K,K=LOC1,LOC2)
      PRINT 1012, (DEL(K),K=LOC1,LOC2)
   40 CONTINUE
C
C  CALCULATE STRESSES
C
      DO 100 I=1,NT
C
      DO 60 J=1,6
      NTRIJ = NTRI(J)
      NOD(J) = NO(I,NTRIJ)
```

```
      NOE = NOD(J)
      IDIR1 = IDIR(NOE,1)
      IDIR2 = IDIR(NOE,2)
      DXP(J) = DEL(IDIR1)
   60 DXP(J+6) = DEL(IDIR2)
C
C    CALCULATE DELTA BY ROTATING DXP
C
      DO 80 J=1,6
      NOE = NOD(J)
      CALP = COS(ALF(NOE))
      SALP = SIN(ALF(NOE))
      DX(J) = CALP*DXP(J)-SALP*DXP(J+6)
   80 DX(J+6) = SALP*DXP(J) + CALP*DXP(J+6)
      CALL MXMULT(AS(1,1,I),DX(1),SMALLA(1,I),6,6,1)
      CALL MXMULT(AS(1,1,I),DX(7),SMALLA(7,I),6,6,1)
  100 CONTINUE
C
C   HAVE VECTOR SMALL A FOR EACH TRIANGLE
C
C   FIND SIGMAX,SIGMAY,TAUXY FOR EACH NODE, THEN AVERAGE AMONG TRIANGLES
C
      DO 200 I = 1,NN
      NOT9 = NOT(I,9)
      DO 110 J=1,3
      SX(J,I) = 0.
  110 CONTINUE
      DO 120 J=1,NOT9
      L = NOT(I,J)
      NOL1 = NO(L,1)
      XI = X(I) - X(NOL1)
      ETA = Y(I) - Y(NOL1)
      C11 = CIJ(1,L)
      C12 = CIJ(2,L)
      C13 = CIJ(3,L)
      C22 = CIJ(4,L)
      C23 = CIJ(5,L)
      C33 = CIJ(6,L)
      A2ETC = SMALLA(2,L)+2.*SMALLA(4,L)*XI    +SMALLA(5,L)*ETA
      A9ETC = SMALLA(9,L)+SMALLA(11,L)*XI    +2.*SMALLA(12,L)*ETA
      A3ETC = SMALLA(3,L)+SMALLA(8,L)+XI *(SMALLA(5,L)+SMALLA(10,L)*2.)
     1                                 +ETA*(2.* SMALLA(6,L)+SMALLA(11,L))
      SX(1,I) = SX(1,I) + C11*A2ETC + C12*A9ETC+C13*A3ETC
      SX(3,I) = SX(3,I) + C33*A3ETC +C13*A2ETC+C23*A9ETC
  120 SX(2,I) = SX(2,I) + C12*A2ETC + C22*A9ETC    +C23*A3ETC
      DO 130 J = 1,3
  130 SX(J,I) = SX(J,I) / NOT9
C
C    FIND PRINCIPAL STRESSES PSTR
C


      RHS = SQRT( ( SX(1,I)- SX(2,I))**2  /4. +  SX(3,I)**2)
      PSTR(1,I) = ( SX(1,I) +  SX(2,I)) / 2.  + RHS
      PSTR(2,I) = ( SX(1,I) +  SX(2,I)) / 2.  - RHS
      PSTR(3,I)=90.*  ATAN(2.* SX(3,I)/(SX (1,I)-SX (2,I)))/PI
  200 CONTINUE
C
C    DERIVE P STAR 2
C
C   KS22(NKD X NKD) IS IN S(1,1,4)
C    K12 (NUD X NKD) IS ON TAPE 10
C    K21 IS THE TRANSPOSE OF K12
C
```

```
      NK22 =    NKD*NKD
      CALL MXMULT(S(1,1,4),FD(NUD+1),PS2,NKD,NKD,1)
      REWIND 10
      DO 290 I=1,M
      IF(I.GT.1) GO TO 230
      LOCFD = 1
      K21DIM = KREM*NKD
      I1 = KREM
      GO TO 240
  230 I1 = N
      K21DIM = N*NKD
      LOCFD = KREM+(I-2)*N+1
  240 CONTINUE
      READ (10) (Q(JJJ),JJJ=1,K21DIM)
      CALL TMXMUL(Q,DEL(LOCFD),PS2,I1,NKD,1)
  290 CONTINUE
C
C   PRINT P-STAR 2
C
      NPSTR = NKD/7
      IF(NKD.GT.NPSTR*7)  NPSTR = NPSTR+1
      DO 350 I=1,NPSTR
      I1 = 7*(I-1)+1
      II1 = I1 + NUD
      I2 = MIN0(I1+6,NKD)
      II2 = I2 + NUD
      PRINT 1030,(K, K=II1,II2)
      PRINT 1012,(PS2(K),K=I1,I2)
  350 CONTINUE
C
C    PRINT OUT STRESSES
C
      I = 1
  870 CONTINUE
      PRINT 1000
      LINE = 3
  871 CONTINUE
      DO  880  J=1,3
      IF(J-2)  873,874,875
  873 PRINT 1001, I,  X(I),  SX(J,I) , PSTR(J,I)
      GO TO 876
  874 PRINT 1002,      Y(I),  SX(J,I) , PSTR(J,I)
      GO TO 876
  875 PRINT 1003,             SX(J,I) , PSTR(J,I)
  876 CONTINUE
  880 CONTINUE
      LINE = LINE + 5
      I = I+1
      PRINT 1004
      IF (I.GT.NN)  GO TO 890
      IF (LINE.GT.50) GO TO 870
      GO TO 871
  890 CONTINUE
      RETURN
 1000 FORMAT(1H1,8H    NODE,6X,8HPOSITION,9X,13HVECTOR  SIGMA,5X,
     1        18HPRINCIPAL STRESSES/)
 1001 FORMAT(1H ,3X,I3,6X,E12.5,2(6XE15.8))
 1002 FORMAT(1H ,3X,3X,6X,E12.5,2(6XE15.8))
 1003 FORMAT(1H ,3X,3X,6X,12X  ,2(6XE15.8))
 1004 FORMAT(/)
 1010 FORMAT(1H1,50X,13HDISPLACEMENTS,/)
 1011 FORMAT(1H ,7(8X,4HDEL(,I3,1H) ))
 1012 FORMAT(1H ,7(2X,E14.7)/)
 1030 FORMAT(1H 7(8X,4HPS2(,I3,1H)))
      END
```

```
      SUBROUTINE SMALLK(I)
C
C   ANISOTROPIC
C
C
C  THIS SUBROUTINE DERIVES THE MATRIX SMALL K FOR THE TRIANGLE I
C
C  ALSO CALCULATED AND STORED FOR THE STRESS ROUTINE ARE THE A-STARS
C
      COMMON /Z/ NO(80,6), ED(500), NODE(500,2), X(250), Y(250),TH(250),
     1   N, KREM, M, S(60,60,5), IDIR(250,3), AREF(250), T(12,12),
     2   AMX(12,12), BMX(12,12), SP(60,20), EE(80), ER(80), RNU(80),
     3    FNU(80), NOT(250,9), CIJ(6,80),KMX(12,12,80), AS(6,6,80),
     4   G(60), NKD, NUD, NN, NT                 ,VF(80),BETA(80)
      REAL KMX
      DIMENSION  C(3,3) , CP(3,3) , CD(3,3) , T1(3,3)
      DATA   XLIMIT / .8E-8/
      IA = NO(I,1)
      IB = NO(I,3)
      IC = NO(I,5)
C
      IAG = NO(I,4)
      IBG = NO(I,6)
      ICG = NO(I,2)
      XIA = X(IA)
      XIB = X(IB) - XIA
      XIC = X(IC) - XIA
      YIA = Y(IA)
      ETAB = Y(IB) - YIA
      ETAC = Y(IC) - YIA
      XIO  = (XIB+XIC)/3.
      ETAO = (ETAB+ETAC) /3.
      DELT = XIB*ETAC - XIC*ETAB
      T11= -(TH(IA)*(ETAC-ETAB) - TH(IB)*ETAC + TH(IC)*ETAB ) / DELT
      T2 = -(TH(IA)*(XIB - XIC) + TH(IB)*XIC  - TH(IC)*XIB  ) / DELT
      TO = TH(IA)
      EM2 = ETAC / XIC
      IF(XIB.NE.0.)  GO TO 15
      EM1 = EM2
      GO TO 17
   15 EM1 = ETAB / XIB
   17 EM3 = (ETAC - ETAB) / (XIC - XIB)
      B3 = ETAB - EM3 * XIB
      B32 = B3**2
      B33 = B32*B3
      B34 = B33*B3
      EM211 = EM2 - EM1
      EM212 = (EM2+EM1) * EM211
      EM213 = EM2**3 - EM1**3
      EM231 = EM2 - EM3
      EM214 = EM2**4 - EM1**4
      XIC3 = XIC ** 3
      XIC4 = XIC * XIC3
      XIC5 = XIC * XIC4
      XIB3 = XIB ** 3
      XIB4 = XIB * XIB3
      XIB5 = XIB * XIB4
      EMEC1= EM3*XIC +B3
      EMEB1= EM3*XIB +B3
      EMECB3 = EMEC1**3
      EMECB4 = EMEC1 * EMECB3
      EMECB5 = EMEC1 * EMECB4
```

```
      EMEBB3 = EMEB1**3
      EMEBB4 = EMEB1 * EMEBB3
      EMEBB5 = EMEB1 * EMEBB4
      ECB1 = XIC-XIB
      ECB2 = XIC**2 - XIB**2
      ECB3 = XIC**3 - XIB**3
      ECB4 = XIC**4 - XIB**4
      ECB5 = XIC**5 - XIB**5
      EM32 = EM3 * EM3
      EM33 = EM3 * EM32
      EM22 = EM2 * EM2
      EM23 = EM2 * EM22
      EM24 = EM2 * EM23
C
C CALCULATE THE GAMMAS
C
      G0 = DELT / 2.
      G1 = G0 * XIC
      G2 = G0 * ETA0
      G3 = EM211 * XIB4/4. + EM231/4.*ECB4-B3/3. * ECB3
      G6 = EM211 * XIB5/5. + EM231/5.*ECB5 - B3/4. * ECB4
C
      IF(EM3.NE.0.) GO TO 18
      G4 = EM213 * XIB4/12.+ EM23/12.*ECB4-B33*ECB1/3.
C
      G5 = EM212 * XIB4/8. + EM22/8. *ECB4-B32*ECB2/4.
C
      G7 = EM212 * XIB5/10.+ EM22/10.*ECB5-B32*ECB3/6.
C
      G8 = EM213 * XIB5/15.+ EM23/15.*ECB5-B32*ECB2/6.
C
      G9 =(EM214*XIB5    +EM24*ECB5)/20. -B34*ECB1/4.
C
      GO TO 19
C
   18 G4 = EM213 * XIB4/12.+ EM23/12.*ECB4-(EMECB4-EMEBB4)/(12.*EM3)
      G5 = EM212 * XIB4/8. + EM22/8. *ECB4-(EMECB4-EMEBB4)/(8.*EM32)
     1           + B3/(6.*EM32) * (EMECB3 - EMEBB3)
C
C
      G7 = EM212 * XIB5/10.+ EM22/10.*ECB5-((EMECB5-EMEBB5)/10.
     1           - (EMECB4-EMEBB4)*B3/4. + B32*(EMECB3-EMEBB3)/6.)/EM33
C
      G8 = EM213 * XIB5/15.+ EM23/15.*ECB5- (EMECB5-EMEBB5)/(15.*EM32)
     1           + B3/(12.*EM32) * (EMECB4-EMEBB4)
C
      G9 =(EM214*XIB5    +EM24*ECB5 - (EMECB5-EMEBB5)/EM3) / 20.
C
C
   19 T(1,1) = COS(ALF(IA))
      T(2,2) = COS(ALF(IB))
      T(3,3) = COS(ALF(IC))
      T(4,4) = COS(ALF(IAG) )
      T(5,5) = COS(ALF(IBG))
      T(6,6) = COS(ALF(ICG))
      T(7,7) = T(1,1)
      T(8,8) = T(2,2)
      T(9,9) = T(3,3)
      T(10,10) = T(4,4)
      T(11,11) = T(5,5)
      T(12,12) = T(6,6)
      T(1,7)  = -SIN(ALF(IA ) )
```

```
      T(2,8)   = -SIN(ALF(IB ) )
      T(3,9)   = -SIN(ALF(IC ) )
      T(4,10)  = -SIN(ALF(IAG) )
      T(5,11)  = -SIN(ALF(IBG) )
      T(6,12)  = -SIN(ALF(ICG) )
C
      T(7,1)   = - T(1,7)
      T(8,2)   = - T(2,8)
      T(9,3)  = - T(3,9)
      T(10,4)  = - T(4,10)
      T(11,5)  = - T(5,11)
      T(12,6)  = - T(6,12)
C
      VR = 1. - VF(I)
      GR = FR(I)/(2.*(1.+RNU(I)) )
      GF = EF(I)/(2.*(1.+FNU(I)) )
      EXP = ER(I)*VR+EF(I)*VF(I)
      EYP = ER(I)*EF(I)/(ER(I)*VF(I)+EF(I)*VR)
      XYNUP = RNU(I)*VR + FNU(I)*VF(I)
      GXYP = GR*GF / (GR*VF(I) + GF*VR)
      B11P = 1./EXP
      B12P = -XYNUP*B11P
      B22P = 1./FYP
      B33P = 1./GXYP
      DELTA = B11P*B22P-B12P*B12P
      CP(1,1)    = B22P/ DELTA
      CP(2,1)    = - B12P/ DELTA
      CP(3,1)    =  0.
      CP(1,2) = CP(2,1)
      CP(2,2)    = B11P/DELTA
      CP(3,2)    =  0.
      CP(1,3)    =  0.
      CP(2,3)    =  0.
      CP(3,3) = 1./B33P
      EL = COS(BETA(I))
      EM = SIN(BETA(I))
      T1(1,1) = EL**2
      T1(1,2) = EM**2
      T1(1,3) = EL * EM
      T1(2,1) = T1(1,2)
      T1(2,2) = T1(1,1)
      T1(2,3) = -T1(1,3)
      T1(3,1) = 2.*T1(2,3)
      T1(3,2) = -T1(3,1)
      T1(3,3) = T1(1,1) - T1(1,2)
C
C   T2 NOW IN T1
C
      CALL MXMULT(CP,T1,CD,3,3,3)
      T1(3,2) = T1(2,3)
      T1(3,1) = T1(1,3)
      T1(1,3) = 2.*T1(3,2)
      T1(2,3) = 2.*T1(3,1)
C
C   T1 INVERSE NOW IN T1
C
      CALL MXMULT(T1,CD,C,3,3,3)
C
C   NOW HAVE C MATRIX IN C
C
C
      CIJ(1,I) = C(1,1)
```

```
      CIJ(2,I) = C(1,2)
      CIJ(3,I) = C(1,3)
      CIJ(4,I) = C(2,2)
      CIJ(5,I) = C(2,3)
      CIJ(6,I) = C(3,3)
C
C     CALCULATE A-STAR MATRIX
      AS(1,2,I) = 0.
      AS(1,3,I) = 0.
      AS(2,2,I) = XIB
      AS(3,2,I) = XIC
      AS(4,2,I) = X(IAG) - XIA
      AS(5,2,I) = X(IBG) - XIA
      AS(6,2,I) = X(ICG) - XIA
      AS(2,3,I) = ETAB
      AS(3,3,I) = ETAC
      AS(4,3,I) = Y(IAG) - YIA
      AS(5,3,I) = Y(IBG) - YIA
      AS(6,3,I) = Y(ICG) - YIA
      DO 20  J = 1,6
      AS(J,1,I) = 1.
      AS(J,4,I) = AS(J,2,I)**2
      AS(J,5,I) = AS(J,2,I) * AS(J,3,I)
   20 AS(J,6,I) = AS(J,3,I)**2
C
      CALL INVERT(AS(1,1,I),6,12,XLIMIT,FLAG)
      IF(FLAG.NE.0.)GO TO 500
C
C    NOW HAVE A-STAR-INVERSE, GET A-MATRIX
C
      DO 25 J=1,6
      DO 25  K=1,6
      AMX(J+6,K+6) = AS(J,K,I)
   25 AMX(J  ,K  ) = AS(J,K,I)
      TG1 =T11* G1+T2*G2+T0*G0
      TG3 =T11* G3+T2*G5+T0*G1
      TG5 =T11* G5+T2*G4+T0*G2
      TG6 =T11* G6+T2*G7+T0*G3
      TG7 =T11* G7+T2*G8+T0*G5
      TG8 =T11* G8+T2*G9+T0*G4
      BMX(2,2) = C(1,1) * TG1
      BMX(3,2) = C(1,3)*TG1
      BMX(4,2) = 2.* C(1,1) * TG3
      BMX(5,2) = C(1,1) * TG5  + C(1,3)*TG3
      BMX(6,2) = 2.*C(1,3)*TG5
      BMX(8,2) = BMX(3,2)
      BMX(9,2) = C(1,2) * TG1
      BMX(10,2) = 2. * C(1,3) * TG3
      BMX(11,2)= C(1,2) * TG3 +C(1,3) * TG5
      BMX(12,2)= 2.* C(1,2) * TG5
      BMX(3,3) = C(3,3) * TG1
      BMX(4,3) = BMX(10,2)
      BMX(5,3) = C(3,3) * TG3 +C(1,3) * TG5
      BMX(6,3) = 2.* C(3,3)*TG5
      BMX(8,3) = BMX(3,3)
      BMX(9,3) = C(2,3)*TG1
      BMX(10,3) = 2.*C(3,3)*TG3
      BMX(11,3)= C(3,3) * TG5 + C(2,3) * TG3
      BMX(12,3) = 2.*C(2,3)*TG5
      BMX( 4, 4) = 4.* C(1,1) * TG6
      BMX( 5, 4) = 2.* C(1,1) * TG7 +2.*C(1,3)*TG6
      BMX(6,4) = 4.*C(1,3)*TG7
      BMX(8,4) = BMX(10,2)
      BMX( 9, 4) = 2.* C(1,2) * TG3
      BMX(10,4) = 4.*C(1,3)*TG6
      BMX(11, 4) = 2.* C(1,2) * TG6 + 2.*C(1,3)*TG7
```

```
      BMX(12, 4) = 4.* C(1,2) * TG7
      BMX( 5, 5) = C(1,1)*TG8 + C(3,3) * TG6 + 2.* C(1,3) * TG7
      BMX( 6, 5) = 2.* C(3,3)*TG7  + 2.*C(1,3) * TG8
      BMX( 8, 5) = BMX(5,3)
      BMX( 9, 5) = C(1,2)*TG5  + C(2,3) * TG3
      BMX(10, 5) = 2.* C(3,3) * TG6 + 2.*C(1,3)*TG7
      BMX(11, 5) =     (C(1,2)+C(3,3))*TG7 +C(1,3)*TG8+C(2,3)*TG6
      BMX(12, 5) = 2.* C(1,2)* TG8 +2.*C(2,3)*TG7
      BMX(6,6) = 4.*C(3,3)*TG8
      BMX( 8, 6) = BMX(6,3)
      BMX(9,6) = BMX(12,3)
      BMX(10,6) = 4.*C(3,3)*TG7
      BMX(11, 6) = 2.* C(3,3)* TG8  +2.*C(2,3)*TG7
      BMX(12,6) = 4.*C(2,3)*TG8
      BMX( 8, 8) = BMX(8,3)
      BMX(9,8) = BMX(9,3)
      BMX(10, 8) = BMX(10,3)
      BMX(11, 8) = BMX(11,3)
      BMX(12,8) = BMX(12,3)
      BMX( 9, 9) = C(2,2)*TG1
      BMX(10,9 ) = 2.*C(2,3)*TG3
      BMX(11, 9) = C(2,2)*TG3 + C(2,3)*TG5
      BMX(11,10) = 2.*C(3,3)*TG7 + 2.*C(2,3)*TG6
      BMX(12,9) = C(2,2)*TG5 *2.
      BMX( 11, 11) =  C(2,2) * TG6 + C(3,3) * TG8+2.*C(2,3)*TG7
      BMX(10,10) = 4.*C(3,3)*TG6
      BMX(12,10) = 4.*C(2,3)*TG7
      BMX( 12, 11) = 2.* C(2,2) * TG7 + 2.*C(2,3)*TG8
      BMX( 12, 12) = 4.* C(2,2) * TG8
C
C  APPLY SYMMETRY HERE
C
      DO 200 J=3,12
      J1 = J-1
      DO 200 L=2,J1
  200 BMX(L,J) = BMX(J,L)
C
      CALL MXMULT(BMX,AMX,KMX(1,1,I+1) ,12,12 , 12)
      CALL MXMULT(KMX(1,1,I+1),T,KMX(1,1,I),12,12,12)
      DO 250 J=1,6
      DO 250 K=1,6
  250 AMX(J,K) = AMX(K+6,J+6)
      DO 260 J=1,6
      DO 260 K=1,6
      AS(K,J,I) = AMX(J,K)
  260 AMX(J+6,K+6) = AMX(J,K)
C
C  TRANSPOSE OF INVERSE OF A NOW IN AMX, INVERSE OF A-STAR NOW IN AS
C
      DO 270 J = 1,6
      T(J,J+6) = -T(J,J+6)
  270 T(J+6,J) = -T(J+6,J)
C
C  INVERSE OF T NOW IN T
C
      CALL MXMULT(AMX,KMX(1,1,I  ),KMX(1,1,I+1),12,12,12)
      CALL MXMULT(T,KMX(1,1,I+1), KMX(1,1,I),12,12,12)
C
C  K-PRIME MATRIX NOW IN KMX(1,1,I)
C
      RETURN
  500 PRINT 1000,I
 1000 FORMAT(44H1  COULD NOT INVERT A-STAR MATRIX, TRIANGLE ,I3)
      STOP
      END
```

```
      SUBROUTINE INVERT(B,K,K2,XMIN,FLAG)

C  THIS SUBROUTINE SETS UP A UNIT MATRIX ADJACENT TO B(K,K)
C  ELEMENTARY ROW OPERATIONS ARE THEN PERFORMED ON THE NEW K X 2K MATRIX
C  TO REDUCE B(K,K) TO A UNIT MATRIX.  THIS WILL PLACE THE INVERSE OF
C  THE MATRIX B(K,K) IN THE RIGHT HALF OF B(K,2K)
C  ON EXIT, THE INVERSE OF B REPLACES B
C   09+S N ARRAY OF 2*K**2 LOCATIONS CONTAINING THE MATRIX
C  K IS THE DIMENSION OF THE SQUARE MATRIX B
C  K2 IS 2*K
C  XMIN IS THE SMALLEST ALLOWABLE MAGNITUDE OF THE PIVOT
C  FLAG WILL BE RETURNED AS 0. IF THE INVERSION WENT OFF OK
C  FLAG WILL BE RETURNED AS 10. IF A PIVOT ELEMENT WAS TOO SMALL
C  FLAG SHOULD BE TESTED AFTER EACH CALL TO THIS ROUTINE
C
      DIMENSION B(K,K2)
C
      FLAG = 0.
C
C  SET UP UNIT MATRIX
C
      IF(K.GT.1)  GO TO 20
      IF(ABS(B(1,1)).LT.XMIN)  GO TO 10
      B(1,1) = 1./B(1,1)
      RETURN
   20 CONTINUE
      DO 1  I=1,K
      DO 1  J=1,K
      B(I,K+J) = 0.
      IF(I.EQ.J)  B(I,K+J) = 1.
    1 CONTINUE
C
C  FIND LEADING ELEMENT WITH GREATEST MAGNITUDE
C
      DO 6  J=1,K
      M = J
      N = J+1
      IF(J.EQ.K) GO TO 21
      DO 2  L=N,K
      IF (ABS(B(M,J)).LT.ABS(B(L,J)))  M=L
    2 CONTINUE
   21 CONTINUE
      IF (ABS(B(M,J)).LT.XMIN)  GO TO 10
      IF(J.EQ.K) GO TO 31
C
C  INTERCHANGE JTH AND MTH ROWS
C
      DO 3  L=J,K2
      D = B(J,L)
      B(J,L) = B(M,L)
      B(M,L) = D
    3 CONTINUE
   31 CONTINUE
C
C  ZERO OUT PIVOTAL JTH COLUMN,  SKIPPING PIVOTAL JTH ELEMENT
C
C  DIVIDE JTH ROW BY PIVOT
C
      DO  4  M=N,K2
      B(J,M) = B(J,M) / B(J,J)
    4 CONTINUE
      DO 6  M=1,K
```

```
C
C   M DETERMINES ROW BEING MODIFIED, ONE WHOLE ROW AT A TIME
C
      IF ( M.EQ.J )   GO TO 6
      DO 5  L=M,K2
C
C   L DETERMINES ELEMENT IN THE MTH ROW
C
      B(M,L) = B(M,L) - B(M,J) * B(J,L)
    5 CONTINUE
    6 CONTINUE
C
C   INVERSE OF B IS NOW IN RIGHT HALF OF B(K,K2)
C   NOW MOVE B INVERSE TO WHERE B WAS
      DO 7  I=1,K
      DO 7  J=1,K
      B(I,J) = B(I,J+K)
    7 CONTINUE
      RETURN
   10 FLAG = 10.
      RETURN
      END


      SUBROUTINE MXCON(A,B,X,M,N)
C
C   THIS SUBROUTINE MULTIPLIES MATRIX A (MXN) BY CONSTANT X, RESULT IN B
C   A MAY BE SAME AS B.
C   THIS SUBROUTINE MULTIPLIES MATRIX A (MXN) BY CONSTANT X, RESULT IN B
C   A MAY BE SAME AS B.
      DIMENSION  A(M,N) , B(M,N)
      DO 1 I=1,M
      DO 1 J=1,N
      B(I,J)= X*A(I,J)
    1 CONTINUE
      RETURN
      END


      SUBROUTINE MXSUB(A,B,C,M,N)
C
C   THIS SUBROUTINE SUBTRACTS MATRIX B FROM MATRIX A,STORES RESULT IN C
C
C   A, B, AND C ARE (M X N)        (C CAN BE THE SAME AS A OR B)
C
      DIMENSION   A(M,N) , B(M,N) ,C(M,N)
C
      DO 1  I=1,M
      DO 1  J=1,N
      C(I,J) = A(I,J) - B(I,J)
    1 CONTINUE
      RETURN
      END
```

```
      SUBROUTINE MXMULT(A,B,C,M,N,K)
C
C   THIS SUBROUTINE MULTIPLIES MATRIX A BY MATRIX B  AND STORES THE
C   PRODUCT IN C.    (C CANNOT BE THE SAME AS A OR B.)
C
C   A IS (M X N)
C   B IS (N X K)
C   C IS (M X K)
C
      DIMENSION  A(M,N) , B(N,K) , C(M,K)
C
      DO 1  I=1,M
      DO 1  L=1,K
      C(I,L) = 0.
      DO 1  J=1,N
      C(I,L) = C(I,L) + A(I,J) * B(J,L)
    1 CONTINUE
      RETURN
      END

      SUBROUTINE TMXMUL(A,B,C,N,M,K)
C
C   THIS SUBROUTINE MULTIPLIES MATRIX B BY THE TRANSPOSE OF MATRIX A
C   THE PRODUCT IS ADDED TO C
C
C     A IS (N X M)
C   B IS (N X K)
C   C IS (M X K)
C
      DIMENSION  A(N,M) , B(N,K) , C(M,K)
      DO 1  I=1,M
      DO 1  L=1,K
C     C(I,L) = 0.
      DO 1  J=1,N
      C(I,L) = C(I,L) + A(J,I) * B(J,L)
    1 CONTINUE
      RETURN
      END
```

UNCLASSIFIED

Security Classification

DOCUMENT CONTROL DATA - R & D

(Security classification of title, body of abstract and indexing annotation must be entered when the overall report is classified)

1. ORIGINATING ACTIVITY (Corporate author) Whittaker Corporation Research & Development Division San Diego, California	2a. REPORT SECURITY CLASSIFICATION Unclassified 2b. GROUP

3. REPORT TITLE

CALCULATION AND DESIGN OF JOINTS MADE FROM COMPOSITE MATERIALS

4. DESCRIPTIVE NOTES (Type of report and inclusive dates)

FINAL REPORT

5. AUTHOR(S) (First name, middle initial, last name)

Alberto H. Puppo
Harold Evensen

6. REPORT DATE	7a. TOTAL NO. OF PAGES	7b. NO. OF REFS
May 1970	108	5

8a. CONTRACT OR GRANT NO. DAAJ02-69-C-0034 b. PROJECT NO. Task 1F162204A17001 c. d.	9a. ORIGINATOR'S REPORT NUMBER(S) USAAVLABS Technical Report 70-27 9b. OTHER REPORT NO(S) (Any other numbers that may be assigned this report) Whittaker MJO-3870

10. DISTRIBUTION STATEMENT

This document is subject to special export controls, and each transmittal to foreign governments or foreign nationals may be made only with prior approval of U. S. Army Aviation Materiel Laboratories, Fort Eustis, Virginia 23604.

11. SUPPLEMENTARY NOTES	12. SPONSORING MILITARY ACTIVITY
	U.S. Army Aviation Materiel Laboratories Fort Eustis, Virginia

13. ABSTRACT

This report contains a study of joints made from fiber composite materials. Several types of joints are considered, such as bolted and adhesive joints.

Elements for a rational joint design are presented, as well as test results. A finite-element computer program, used to obtain stress distributions in composite joints, is included.

DD FORM 1 NOV 68 1473 REPLACES DD FORM 1473, 1 JAN 64, WHICH IS OBSOLETE FOR ARMY USE.

UNCLASSIFIED

Security Classification

14 KEY WORDS	LINK A		LINK B		LINK C	
	ROLE	WT	ROLE	WT	ROLE	WT
Joints in Composite Materials Bolted Bonded						
Joint Design and Fabrication						
Joint Analysis and Testing						
Nonlinear Analysis						
Finite-Element Analysis						